CMC2026

5th Croatian Microscopy Congress

with international participation



BOOK OF ABSTRACTS

16-18 SEPTEMBER 2026

Osijek, Croatia

ORGANISED BY

CMC2026

5th Croatian Microscopy Congress

with international participation

BOOK OF ABSTRACTS

16-18 September 2026
Faculty of Agrobiotechnical Sciences Osijek
Vladimira Preloga 1, 31000 Osijek, Croatia

Edited by: Petra Peharec Štefanić and Maja Herak Bosnar
Published by: Croatian Microscopy Society
Zagreb, 2026

ORGANISING INSTITUTIONS

Croatian Microscopy Society

Faculty of Agrobiotechnical Sciences Osijek

Faculty of Medicine Osijek

COMMITTEES

Scientific guidance and congress organisation

SCIENTIFIC COMMITTEE

- Petra Peharec Štefanić
- Andreja Gajović
- Davor Kovačević
- Goran Kovačević
- Igor Weber
- Jelena Macan
- Maja Herak Bosnar
- Suzana Šegota
- Tatjana Belovari

ORGANISING COMMITTEE

- Bruno Komazec
- Nikola Bjelić
- Damir Sirovina
- Danijel Jug
- Edi Rođak
- Nika Srb
- Ante Krstanović

IMPRESSUM

Publication details

TITLE	**5th Croatian Microscopy Congress with international participation: Book of Abstracts**
CONGRESS	16-18 September 2026 · Osijek, Croatia
EDITORS	Petra Peharec Štefanić Maja Herak Bosnar
TECHNICAL EDITOR	Bruno Komazec
PUBLISHER	Hrvatsko mikroskopijsko društvo (Croatian Microscopy Society) Bijenička cesta 54 10000 Zagreb, Croatia
PLACE AND YEAR OF PUBLICATION	Zagreb, 2026
ISBN	978-953-57138-2-1

The abstracts are published in the form submitted by the authors. Copyright © 2026 Hrvatsko mikroskopijsko društvo (Croatian Microscopy Society).



THANK YOU

CMC2026 gratefully acknowledges the support of our sponsors and exhibitors

GOLD SPONSOR

ITRLAB JUST FOCUS

ThermoFisher SCIENTIFIC

SILVER SPONSORS

SCAN

JEOL Solutions for Innovation

SpeciOn

BRONZE SPONSORS

ANSAR-ANALITIKA ANALYTICAL EQUIPMENT

biosistemi YOUR TRUSTED PARTNER IN CREATING THE FUTURE

nanosurf lach:ner

ZEISS

AstraFokus FOKUSIRANI NA MIKROSKOPIJU

EXHIBITORS

Ru-Ve tvoj lab partner

KERN

Mikrolux www.mikrolux.hr

Tescan

KEFO 75

Labena

Unlock the power of precision with our advance electron microscopy services.

Explore the microscopic world like never before. Our cutting edge electron microscopes deliver unmatched resolution and clarity for research needs.

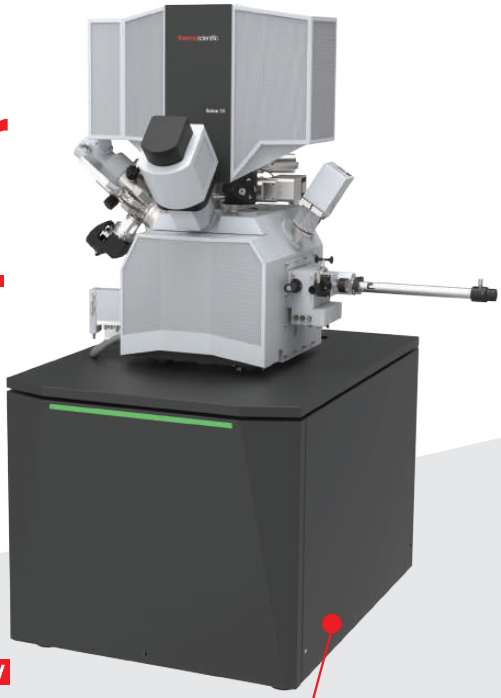

ELECTRON MICROSCOPY



NEW

Thermo Scientific SCIOS 3 FIB-SEM

Thermo Scientific Scios 3 FIB-SEM builds on well-known AutoTEM and Auto Slice & View with the new **Auto Cross Section (AXS)** software, enabling automated FIB cross-sectioning and multi-scale SEM imaging for fast, precise, and reliable materials analysis.

ThermoFisher SCIENTIFIC



ILIAD Ultra

Thermo Scientific ILIAD Ultra (S)TEM is an advanced, fully integrated system featuring a new EELS spectrometer, energy filter, and dedicated camera. It offers high stability, seamless integration, and improved serviceability, with user-friendly Velox software and Python-based Autoscript enabling flexible, AI-supported data collection workflows.

WWW.ITR-LAB.SI

Phenom XL G3 Desktop SEM

Discover the new **Thermo Scientific™ Phenom™ XL G3 Desktop SEM,** the longer-lasting CeB6 electron source reduces downtime and costs, while the improved backscatter electron detector delivers higher contrast, better compositional analysis, and superior signal-to-noise ratio—ideal for both industry and academia.

ALL YOU NEED FOR MICROSCOPY

ULTIMATE EQUIPMENT SOLUTIONS ▪ CUSTOM SERVICE ▪ HIGH QUALITY FOR OUR CUSTOMERS
PERSONAL PROFESSIONAL APPROACH ▪ COMMITMENT TO YOUR SUCCESS

ITRLAB

TABLE OF CONTENTS

Abstracts arranged by presentation type and research field

PLENARY LECTURES · LIFE SCIENCE 1

Iva Tolić — Mechanobiology of Mitosis: Visualizing, Manipulating, and Scaling the Mitotic Spindle 2

Marie Vancová — Volume Electron Microscopy: What It Can Reveal and What It Takes 4

PLENARY LECTURES · MATERIAL SCIENCE 5

Sandra Bischof — SEM in Textile Science: Advances in Topological, Morphological and Chemical Characterization 6

Sašo Šturm — Transmission Electron Microscopy of Nanoparticle Nucleation, Growth and Dissolution: From Stardust to Nanoconfined Electrochemistry 8

INVITED LECTURES · LIFE SCIENCE 10

Ágnes Kittel — Changing Significance of Electron Microscopy in the Investigation of Extracellular Vesicles 11

Ivana Restović — Ultrastructural and Biochemical Characterisation of the Renal Parenchyma in Rainbow Trout (*Oncorhynchus mykiss*) under Intensive Cage-Farming Conditions 13

Edi Rođak — Inflammation Expands a Previously Unrecognized Osteoclast Progenitor Population 15

Krunoslav Vinicki — Computational Imaging for Routine Pathology and Cytology: Aberration Calibration, Real-Time Sparse Deconvolution and Deep Learning-Assisted Acquisition 16

INVITED LECTURES · MATERIAL SCIENCE 17

Nina Daneu — Atomic Scale Insights into the Formation Mechanism and Photocatalytic Properties of $SrTiO_3/Bi_4Ti_3O_{12}$ Nanoplatelets 18

Marin Petrović — Spectromicroscopy of Epitaxial Borophene: Synthesis, Functionalization and Heterostructures 20

Tin Klačić — Atomic Force Microscopy: A Powerful Tool for Studying Polyelectrolyte Multilayers 22

Helena Otmačić Ćurković — Corrosion of Archaeological and Art Objects – Combined Electrochemical, Microscopic and Spectroscopic Studies 23

TABLE OF CONTENTS

Abstracts arranged by presentation type and research field

SELECTED ORAL PRESENTATIONS · LIFE SCIENCE 26

Lea Vrbančić — Defining the Sequence Signals Governing NME6 Mitochondrial Targeting 27

Dunja Igrec — Establishment and Microscopic Characterisation of an *In Vitro* Adipogenesis Model in 3T3-L1 Cells 28

Lovro Mihajlović — Confocal Microscopy Reveals F-Actin Remodelling Associated with Hepatic Lipid Accumulation Following Gonadectomy and Aging 29

Ivana Ilić — Dermoscopy as an Important Tool in Everyday Clinical Practice and in the Diagnosis of Various Dermatological Entities 31

Igor Weber — Insight into the Intracellular Dynamics of Rac1 GTPases by Confocal Microscopy and Mathematical Modelling 32

Danijela Poljuha — Cytotoxic and Genotoxic Activity of Invasive Alien Plant Extracts Reveals Their Selective Antitumor Potential in Human Cell Lines 33

SELECTED ORAL PRESENTATIONS · MATERIAL SCIENCE 35

Vedran Kojić — Morphology of Lead Halide Perovskite Thin Films via Spin Coating and Slot Die Coating 36

Andreja Gajović — The Atomic Resolution Electron Microscopy Study of the WTaVCr Intended for Fusion Application 37

Suzana Inkret — Designing Infection-Resistant Surfaces: Physico-Chemical and Antibacterial Characterization of Calcium Phosphates/Silver Nanoparticles Composite Coatings for Titanium Implants 39

Tihana Čižmar — Synthesis of Multicomponent Transition-Metal Alloys and Oxides for Dual Photocatalytic and Antibacterial Applications 40

Jelena Macan — Light and Electron Microscopy in Research of Historical Papers 42

Monika Vyšanská — Advanced Light Microscopy and Digital Image Analysis in Textile Structure Characterization 44

TABLE OF CONTENTS

Abstracts arranged by presentation type and research field

POSTER PRESENTATIONS · LIFE SCIENCE **47**

Elma Vuko — Leaf Anatomy and Ultrastructural Characteristics of the Endemic *Seseli tomentosum* Vis.: Insights into Species-Specific Adaptations 48

Sara Cerovski — Dark-Field Microscopy-Based Tracking of *Dictyostelium discoideum* Cells Lacking the Small GTPase Rac1 Isoforms 49

Mateja Jagić — Possible Alternative BPM2 Isoforms Influence the Subcellular Localization of Target Proteins 51

Magdalena Knapp — Towards Ultra-rapid TEM Sample Processing 53

Robert Mujkić — Incidental Bile Duct Hamartoma (Von Meyenburg Complex) Identified During Forensic Autopsy 54

Nives Novosel Vlašić — Combined Effects of Nanoplastic Exposure and Salinity Stress on Marine Microalgal Physiology and Cell Surface Properties 55

Tatjana Prebeg — Variation in Petal Epidermal Cell Morphology in *Primula elatior* Cultivars with Different Flower Colours 56

Vedran Rušec — Potential of Dutch Elm Disease Fungus *Ophiostoma novo-ulmi* for Biosynthesis of Selenium Nanoparticles 57

Magdalena Knapp — From Ultrastructure to Volume EM: 3D Electron Microscopy Approaches in Invertebrate Systems 59

Nika Srb — Hepatic Collagen Deposition, Oxidative Status, and Lipid Metabolism Following Alendronate and Standardized Hop Extract Treatment in Ovariectomized Rats 60

Dona Vuković — Microplastics Modulate the Toxicity of CTAB-Coated Silver Nanoparticles in *Chlorella vulgaris*: Evidence from Oxidative Stress and Ultrastructural Changes 62

Bruno Komazec — Microplastics Modulate Silver Nanoparticle-Induced Oxidative Stress in *Chlorella vulgaris*: TEM Insights into Particle-Cell Interactions 64

POSTER PRESENTATIONS · MATERIAL SCIENCE **66**

Irena Ivanišević — Development of Hybrid TiO_2 Nanoplates-Based Antimicrobial Coatings for Stainless Steel Surfaces 67

Katarina Jerin — From Silica to Apple Skin: AFM Insights into Roughness and Smoothing Effect of Polyelectrolyte Multilayer 69

Lucija Klobučar — Morphology and Charge Transport of TiO_2 Electron Transport Bilayers Modified with Transition Metal Dichalcogenide Nanotubes 71

Sergej Ražnjević — Correlating Microstructure and Magnetic Domain Evolution in NdFeB Micromagnets Using Lorentz TEM 73

Amra Salčinović Fetić — SEM–EDS Characterization of Ottoman Gold Coins 75

Karlo Vojtkuf — Bio-Based Tannic Acid and Phytic Acid Coatings for Multifunctional Textiles 77

Sponsor advertisements 9, 25, 46, 78–79

Author index 80

PLENARY LECTURES

LIFE SCIENCE

Mechanobiology of Mitosis: Visualizing, Manipulating, and Scaling the Mitotic Spindle

Tolić Iva

Ruđer Bošković Institute, Bijenička cesta 54, 10000 Zagreb, Croatia

Corresponding author: tolic@irb.hr

Accurate chromosome segregation during mitosis is essential for genomic stability, whereas errors lead to aneuploidy, a hallmark of cancer and severe developmental disorders. Rather than being governed only by pulling forces, the mitotic spindle is a dynamic three-dimensional mechanochemical network in which pushing, pulling and rotational forces cooperate to align and segregate chromosomes. Our laboratory combines advanced imaging, laser ablation, optogenetics and theoretical modelling to uncover the biophysical principles and scaling laws that govern this system. We identified bridging fibres, a previously unrecognized class of microtubules that contributes to chromosome segregation. STED nanoscopy and expansion microscopy enabled visualization of these densely packed sub-diffraction structures (Figure 1), while laser ablation and photoactivation showed that bridging fibres are mechanically linked to kinetochore fibres and that their microtubules slide apart during segregation. To investigate their function in real time, we developed an optogenetic knocksideways approach that acutely and reversibly relocates microtubule crosslinkers from the spindle to the plasma membrane. These experiments demonstrated that bridging fibres promote chromosome alignment at the spindle midplane. The resulting Flux-Driven Centering Model predicts that longer kinetochore fibres slide faster than shorter ones and thereby return misaligned chromosomes towards the spindle centre. High-resolution fluorescent speckle microscopy confirmed differential poleward flux rates, and experimentally slowing flux improved chromosome alignment and reduced segregation errors in non-transformed and cancer cells. Our latest work revealed a universal power-law scaling of mitotic spindles across eukaryotes [1]. By combining confocal and lattice light-sheet microscopy, cell compression, genetic and biochemical perturbations, organoids and theoretical modelling, we found that chromosome crowding generates an outward mechanical force that links spindle architecture to genome size. This physical scaling rule provides insight into open mitosis, mitotic cell rounding and tolerance to polyploidy in tumours and during speciation.

References

1. L. Gudlin et al., Nat. Cell Biol. (2026) in press.

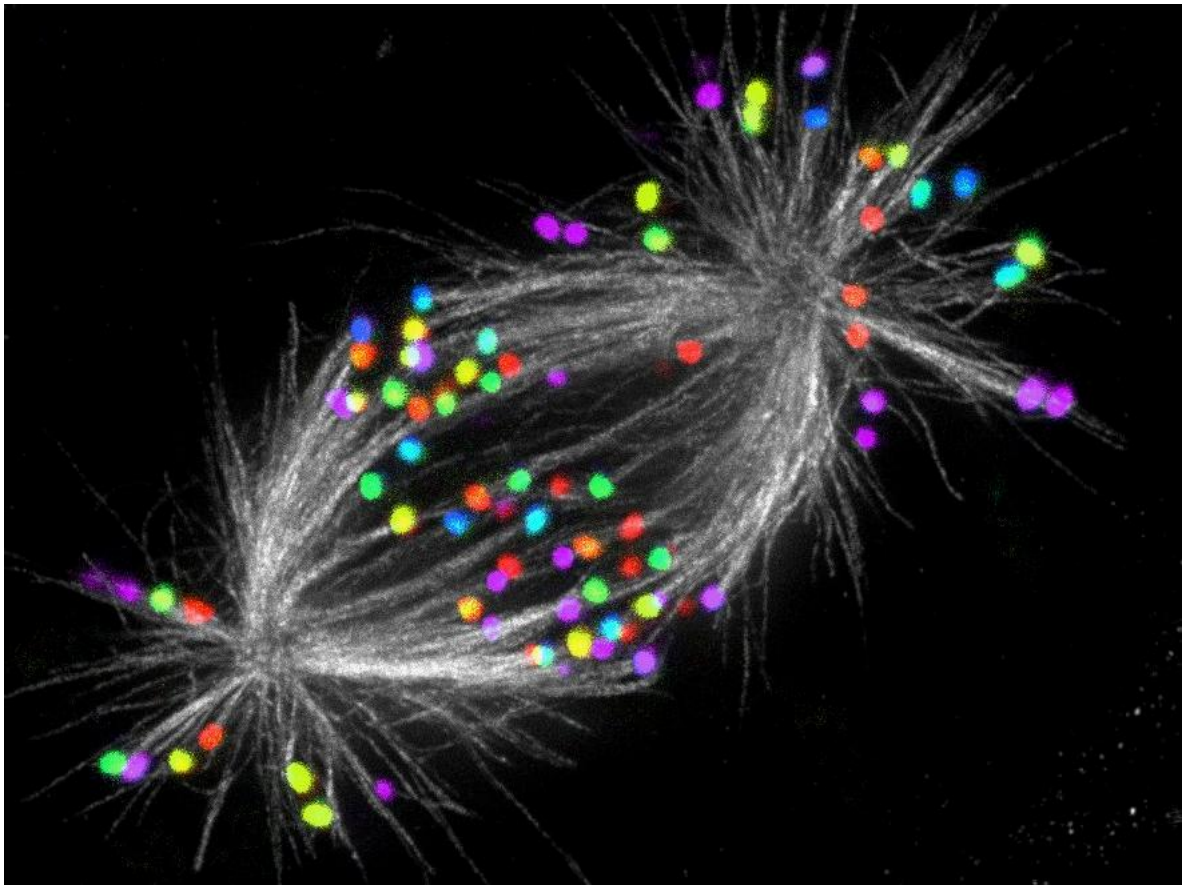

Figure 1. Mitotic spindle. STED super-resolution image of microtubules (white) together with a confocal image of kinetochores colored for depth.

Volume Electron Microscopy: What It Can Reveal and What It Takes

Vancová Marie[a,b], Týč Jiří[a], Kitzberger František[a], Strnad Martin[a]

[a]*Laboratory of Electron Microscopy, Biology Centre CAS, Branišovská 31, 370 05 České Budějovice, Czech Republic*
[b]*Faculty of Science, University of South Bohemia, Branišovská 31, 370 05 České Budějovice, Czech Republic*

Corresponding author: vancova@paru.cas.cz

Volume electron microscopy (vEM) has become a valuable tool in cell and tissue biology for studying complex cellular architecture, tissue organisation, cell–cell and host–pathogen interactions, and rare biological events. A broad range of approaches is now available, enabling three-dimensional imaging across scales ranging from subcellular structures to large regions of cells and tissues. These techniques include serial block-face scanning electron microscopy, focused ion beam scanning electron microscopy, array tomography, serial-section electron microscopy, and electron tomography. This lecture will present selected applications and show how the choice of imaging method, sample preparation protocol, acquisition volume, spatial resolution, and imaging strategy can be tailored to specific biological questions that cannot be reliably addressed using conventional two-dimensional imaging alone. Sample preparation is a critical factor, as it determines image contrast, ultrastructural preservation, achievable resolution, and whether a specimen is suitable for a given vEM technique. The lecture will also consider the limitations and practical challenges of vEM. Large datasets, demanding sample preparation, anisotropic resolution, restricted imaging volumes, destructive acquisition, and time-consuming image analysis may limit its usefulness or make alternative imaging and quantitative approaches more appropriate. Finally, future perspectives will be discussed, including multimodal and correlative imaging, automated data acquisition, machine-learning-assisted segmentation, quantitative analysis, and improved integration of vEM into broader biological workflows. The overall aim is to illustrate what vEM can reveal, what its successful application requires, and how to determine whether it is the most appropriate approach for a particular biological question.

PLENARY LECTURES

MATERIAL SCIENCE

SEM in Textile Science: Advances in Topological, Morphological and Chemical Characterization

Bischof Sandra, Kovačević Zorana

University of Zagreb Faculty of Textile Technology, Textile Science Research Centre, Prilaz baruna Filipovića 28a, 10000 Zagreb, Croatia

Corresponding author: sbischof@ttf.unizg.hr

Scanning Electron Microscopy (SEM) has become an indispensable analytical platform in contemporary textile science, enabling precise, multiscale investigation of fibers, fabrics, and complex material structures [1]. This presentation traces the historical development of SEM applications in textiles and highlights recent advances in topological, morphological, and chemical characterization that are transforming research, quality control, and sustainable innovation across the textile value chain. Emphasis is placed on high-resolution imaging for mapping fiber surface topology, quantifying morphological parameters such as fibrillation, porosity, and damage progression, and visualizing intricate yarn and fabric architectures (Figure 1). Beyond structural imaging, SEM has become a powerful tool for chemical characterization through Energy-Dispersive X-ray Spectroscopy (EDS) and correlative analytical workflows. SEM–EDS is increasingly applied to verify elemental composition in functional finishes, e.g. flame-retardant finishes, conductive coatings or bio-based composites, further reinforcing SEM's role as a decision-making tool in sustainable textile development. SEM–EDS elemental analysis, combined with other emerging techniques, e.g. 3D surface reconstruction, and *in situ* deformation studies, clearly demonstrate how SEM now provides integrated structural and chemical insights essential for understanding material performance, functionalization pathways, so as the degradation mechanisms, ultimately supporting improvements aimed at prolonging material lifespan. Case studies illustrate applications in natural and regenerated fibers, technical textiles, bio-based materials, and recycling streams, showing how SEM supports eco-design, circularity assessment, and verification of sustainable processing technologies. The presentation concludes by emphasizing the frontiers of SEM in textile science and its growing role as a powerful decision-making tool for innovation, standardization, and responsible material development.

References

1. M. Turalija et al., Tekstil 58 (2009) 640–649.
2. S. Bischof and Z. Kovačević, in: S. Bischof (Ed.), Sustainable Development of Biocomposites and Biofuels from Energy Efficient Sources, University of Zagreb Faculty of Textile Technology (2023).

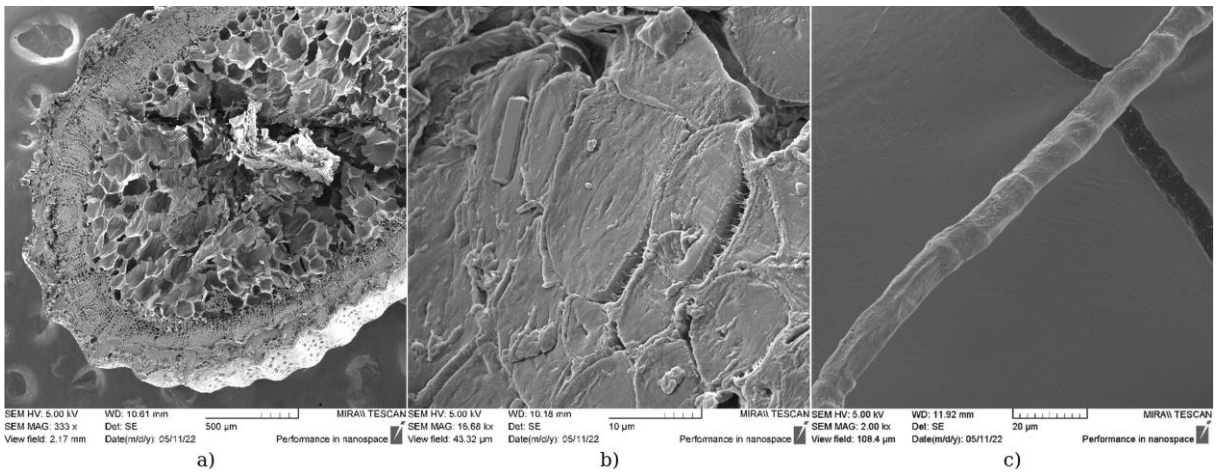

Figure 1. SEM micrographs of Spanish broom (*Spartium junceum* L): a) Cross-section of stem, b) Cross-section of elementary fiber and c) Longitudinal elementary fiber [2].

Transmission Electron Microscopy of Nanoparticle Nucleation, Growth and Dissolution: From Stardust to Nanoconfined Electrochemistry

Šturm Sašo[a,b,c]

[a]*Jožef Stefan Institute, Jamova cesta 39, 1000 Ljubljana, Slovenia*
[b]*University of Ljubljana, Faculty of Natural Sciences and Engineering, Aškerčeva cesta 12, 1000 Ljubljana, Slovenia*
[c]*Jožef Stefan International Postgraduate School, Jamova 39, 1000 Ljubljana, Slovenia*

Corresponding author: saso.sturm@ijs.si

Nanoparticle nucleation, early growth, and dissolution are key processes that determine how materials form, evolve, or degrade. However, these processes often proceed through transient intermediate states that persist only briefly and can change rapidly. As a result, they are difficult to preserve, isolate, or reconstruct using conventional *ex situ* characterisation methods. This lecture will focus on Transmission Electron Microscopy (TEM) as a tool for observing these processes directly, combining high-resolution imaging, electron diffraction, analytical TEM, and *in situ*/*in operando* approaches across two seemingly distant but mechanistically connected systems. The first part focuses on the formation of stardust analogues under microgravity conditions. In this environment, suppressed convection and local density fluctuations strongly affect nucleation pathways and the earliest stages of particle growth, providing insight into processes relevant to dust formation in stellar outflows. TEM-based structural and chemical analysis reveals how particle size, crystallinity, and composition develop during the earliest stages of alumina stardust analogue formation [1]. The second part turns to liquid-cell electrochemical TEM as a tool for studying the dissolution of metallic nanoparticles in nanoconfined liquid volumes under applied bias. We show that nanoparticle dissolution is strongly coupled to electron-beam radiolysis [2], radical chemistry, mass transport, and electrochemical driving forces, creating local reaction environments that differ substantially from those in macroscopic electrochemistry. Direct TEM observation reveals that dissolution can be governed by a delicate redox balance between solid metallic and ionic states, leading to phenomena such as core–shell formation and pit–induced dissolution [3]. By combining advanced TEM with controlled environmental stimuli, these examples demonstrate how TEM can move beyond conventional *post-mortem* characterisation tools and serve as an experimental platform for real-time studies of matter formation and transformation.

References

1. Y. Kimura et al., Int. J. Microgravity Sci. Appl. 35 (2018) 350305.
2. B. Ambrožič et al., Chem. Sci. 10 (2019) 8735–8743.
3. M. Bernal et al., Electrochim. Acta 492 (2024) 144302.

Acknowledgements

ARIS is acknowledged for financial support under P2-0084, PR-13066-5, J2-60043, GC-0004-3, N1-0401-2, PR-12334 and Z2-50057.

JEOL

Scientific / Metrology Instruments
Cryo Electron Microscope

CRYO ARM™ 300

Ultimate instrument
for Protein/Virus
structure study





Cold FEG
Omega energy filter
Phase plate
Single Particle Analysis

www.jeol.com

INVITED LECTURES

LIFE SCIENCE

Changing Significance of Electron Microscopy in the Investigation of Extracellular Vesicles

Kittel Ágnes
HUN-REN Institute of Experimental Medicine
Corresponding author: kittel.agnes@koki.hun-ren.hu

The history of extracellular vesicles is generally – and rightly so – traced back to the articles by Chargaff [1] and Chargaff and West [2]. According to the hypothesis proposed by the two authors, the fraction that Chargaff obtained during centrifugation at 31,000 g – using a protocol he developed for the separation of coagulation factors – and which possessed significant coagulation potential, "likely contains, in addition to the thromboplastic substance, numerous minute degradation products derived from blood cells" [2]. The electron microscope, which is essential for visualizing these "degradation products", is generally not mentioned in the history of extracellular vesicles, even though this remarkable instrument was developed as early as 1931–1933 by the German physicists Ernst Ruska and Max Knoll. Moreover, as a result of their collaboration with Siemens, the first commercially available model was ready as early as 1939. It took another twenty years before Wolf was able to identify these particles alongside platelets during his electron microscopic examinations in 1967, but he simply referred to them as "cell dust" [3]. Despite numerous high-quality electron microscopic studies that followed, it was not until 2009 that Meldolesi and colleagues published a review article in which they stated that these microscopic vesicles or microparticles have physiological significance [4]. Even if the extracellular vesicles released by cells do not provide a complete explanation, they can at least offer new answers and possible solutions to numerous questions and problems for which we have not yet found comprehensive answers or solutions. Furthermore, electron microscopy has played – and continues to play – a significant role in making research on extracellular vesicles one of the most dynamically developing fields in cell biology. The classical transmission technique was indispensable for visualizing these minute structures, classifying them based on their morphological and – to a certain extent – molecular composition, and elucidating their physiological and pathophysiological significance, thereby facilitating their application for diagnostic and therapeutic purposes (Figure 1). The use of cryogenic electron microscopes allows for the examination of cells – and even individual molecules – in their natural state [5]. This offers great potential for further discoveries regarding extracellular vesicles, but there are also numerous questions that remain to be answered, where the combined use of classical TEM, other microscopic techniques, and various methods is sufficient to provide the answers. Extracellular vesicles still hold many secrets, which we must uncover as soon as possible for our own benefit.

References

1. E. Chargaff, J. Biol. Chem. 160 (1945) 351–359.
2. E. Chargaff and R. West, J. Biol. Chem. 166 (1946) 189–197.
3. P. Wolf, Br. J. Haematol. 13 (1967) 269–288.
4. E. Cocucci et al., Trends Cell Biol. 19 (2009) 43–51.
3. A. Enciso-Martinez et al., J. Extracell. Vesicles 15 (2026) e70273.

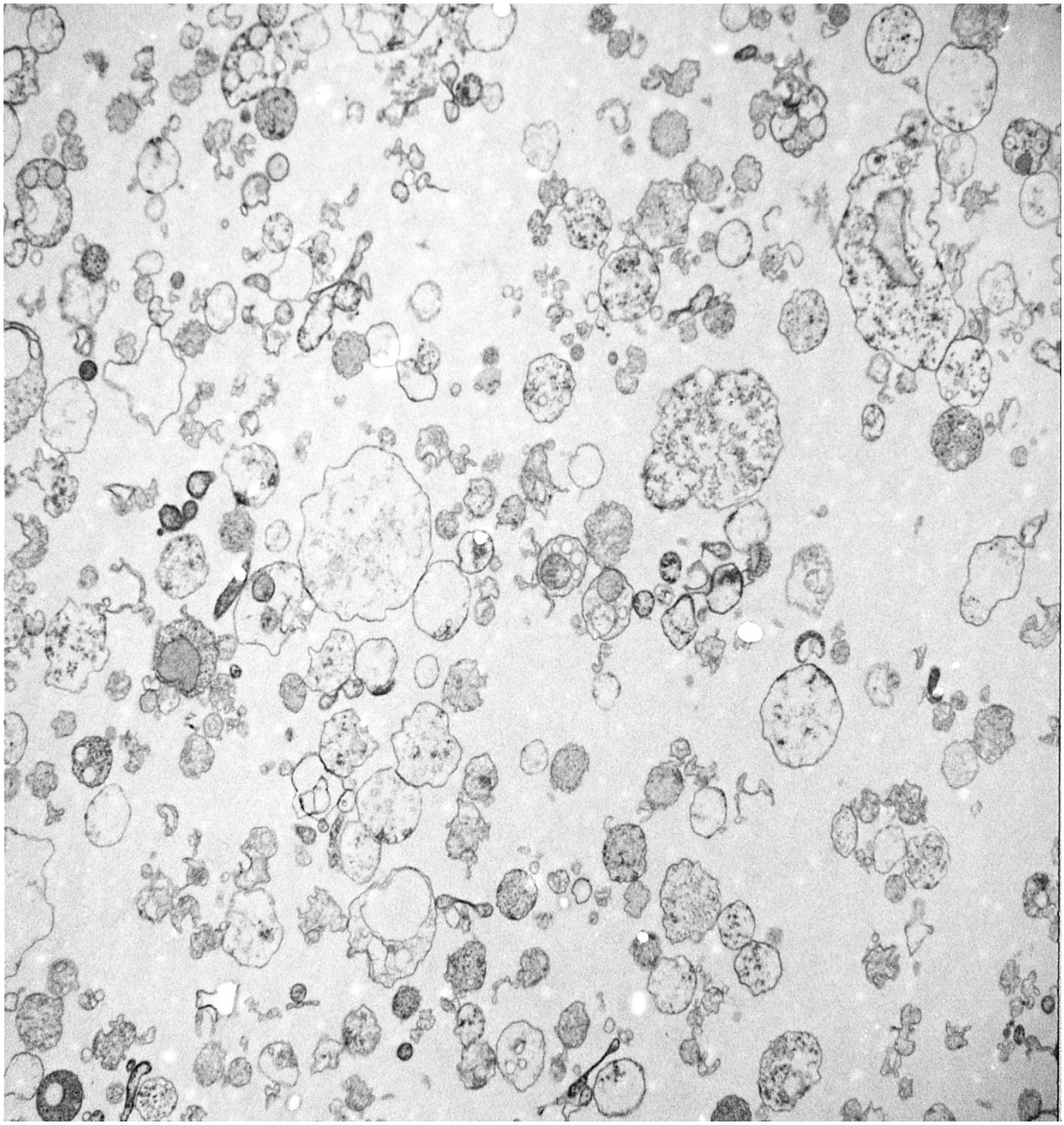

Figure 1. Microparticles isolated from the supernatant of A2058 cell culture (original magnification: 10 000×).

Ultrastructural and Biochemical Characterisation of the Renal Parenchyma in Rainbow Trout (*Oncorhynchus mykiss*) under Intensive Cage-Farming Conditions

Restović Ivana[a], Ugrin Marina[b], Fernandez Godoy María[c], Hrabar Jerko[d], Rudan Marina Dimlić[e], Kević Nives[f], Bočina Ivana[f]

[a]*Faculty of Humanities and Social Studies, University of Split, Poljička Cesta 35, 21000 Split, Croatia*
[b]*Doctoral Study Program in Biophysics, Faculty of Science, University of Split, Ruđera Boškovića 33, 21000 Split, Croatia*
[c]*Faculty of Sciences, University of Málaga, Blvr. Louis Pasteur 31, Puerto de la Torre, 29010 Málaga, Spain*
[d]*Institute of Oceanography and Fisheries, Šetalište Ivana Meštrovića 63, 21000 Split, Croatia*
[e]*Mediterranean Institute for Life Sciences, University of Split, Meštrovićevo Šetalište 45, 21 000 Split, Croatia*
[f]*Department of Biology, Faculty of Science, University of Split, Ruđera Boškovića 33, 21000 Split, Croatia*

Corresponding author: irestovic@ffst.hr

Intensive cage-farming aquaculture exposes salmonid fish to chronic environmental and confinement stressors, inducing systemic physiological disturbances. Because the teleost kidney functions as the primary osmoregulatory, excretory, and haematopoietic organ [1], this study conducted a longitudinal evaluation of the histopathological, ultrastructural, and molecular responses of renal tissue in rainbow trout (*Oncorhynchus mykiss*) across four successive growth stages (I–IV), compared with a wild-caught control group from a natural habitat. Light microscopy (haematoxylin and eosin staining) and transmission electron microscopy (TEM) identified progressive nephropathic alterations (Figure 1). Ultrastructural analysis revealed cellular and subcellular abnormalities, including extensive vacuolation of the tubular epithelium, basement membrane degradation, and loss of proximal tubular microvilli. These morphological lesions were significantly correlated with elevated Tubular Injury Scores (TIS) and Interstitial Fibrosis Scores (IFS), with the highest values observed at stage IV [2]. Histopathological damage was accompanied by specific molecular alterations. Immunohistochemical and immunofluorescence analyses demonstrated significant upregulation of caspase-3 expression, indicating activation of the apoptotic pathway, along with increased fibronectin deposition, confirming extracellular matrix (ECM) remodelling [2]. Methodological validation was strengthened by the initial characterisation of dendrin in the renal parenchyma of *O. mykiss*, with its baseline presence across all stages confirmed via Western blot. Multichannel immunofluorescence microscopy revealed a distinct spatial distribution of dendrin, diverging from the classical mammalian model, in which expression is restricted to glomerular podocytes. In *O. mykiss*, dominant and persistent dendrin expression was localised along the longitudinal axis of the proximal and distal renal tubules across all growth stages, whereas the glomerular signal remained limited and detectable only at stage IV. Digital image analysis and quantitative colocalisation confirmed a high degree of spatial overlap and stable functional association between dendrin and fibronectin signals within tubular structures. The positive correlation between the expression intensity of these molecular markers and histopathological scores (TIS/IFS) during development indicates direct involvement of dendrin and fibronectin in cellular stress responses, tissue remodelling, and progressive fibrosis. This research revises the established mammalian model of dendrin as a strictly glomerular marker by documenting its initial characterisation and pathological involvement within the teleost tubular compartment. Ultimately, these findings demonstrate cellular interactions between the tubular and glomerular compartments in teleosts and suggest the potential application of these proteins as molecular biomarkers for monitoring fish welfare and health status in aquaculture.

References

1. W.H. Dantzler, Comparative Physiology of the Vertebrate Kidney, Springer New York (2016).
2. M. Ugrin et al., Int. J. Mol. Sci. 26 (2025) 10876.

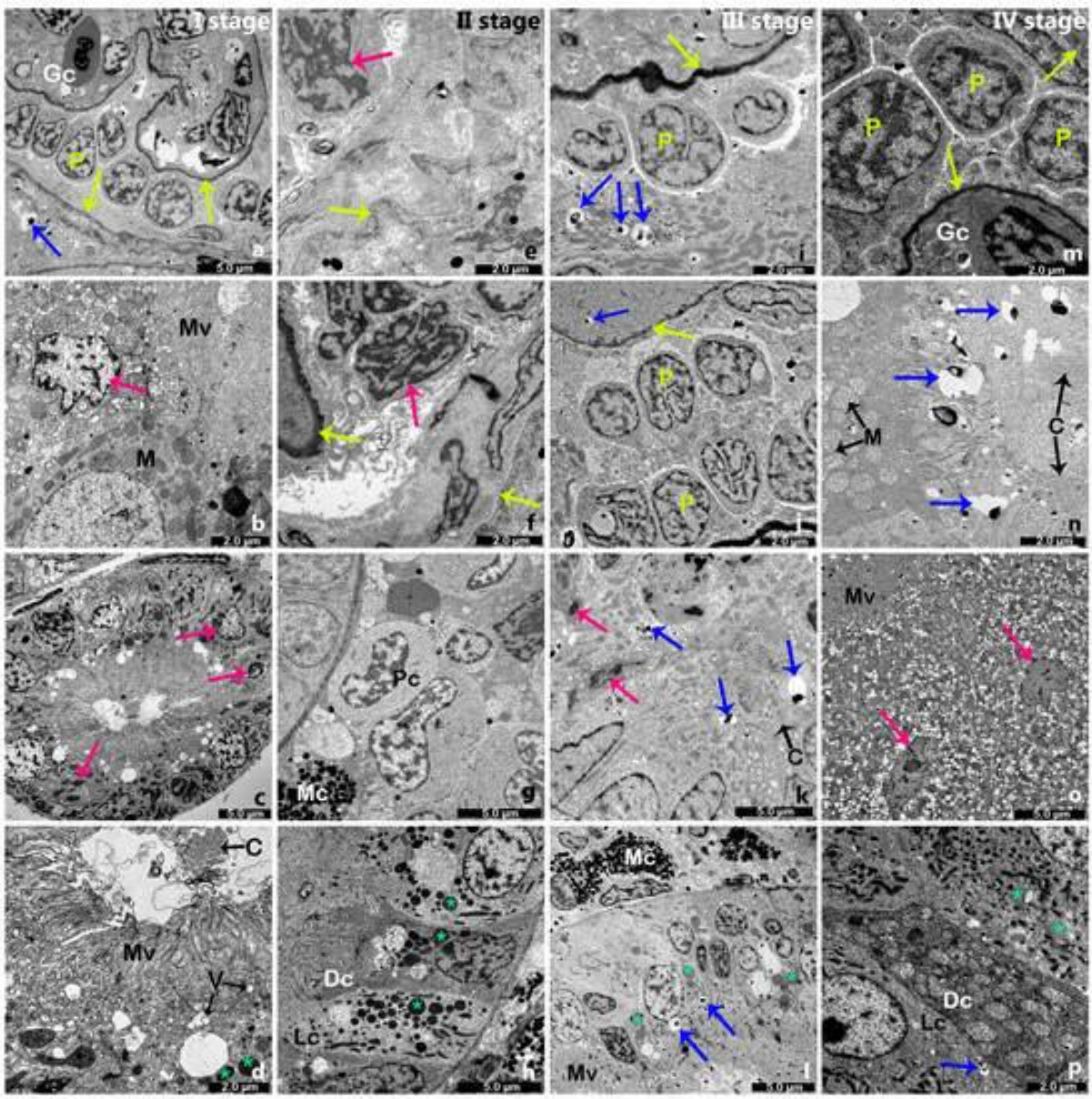

Figure 1. A cross-section throughout the kidney tissue in four growth stages of rainbow trout, *Oncorhynchus mykiss* (Walbaum, 1792). (a–d) – growth stage I; (e–h) – growth stage II; (i–l) – growth stage III; (m–p) – growth stage IV. Pink arrows – apoptotic cells and nuclei; blue arrows – apoptotic bodies; yellow arrows – capsular and glomerular basement membranes; Gc – glomerular capillary; P – podocytes; M – mitochondria; C – cilia; Mc – melanomacrophage centers; Pc – plasma-like cell; Mv – microvilli; V – vesicle; L – light cell; Dc – dark cell; asterisk – lipid droplets. Magnification: (a,l,o) 1200×; (b,e,j,p) 2500×; (c) 800×; (d,f,i,n) 3000×; (g,h,k) 1500×; (m) 4000×, TEM.

Inflammation Expands a Previously Unrecognized Osteoclast Progenitor Population

Rođak Edi[a,b], Jastrzebski Sandra[a], Kalajzic Ivo[c], Lorenzo Joseph[a], Novak Sanja[c,d]

[a]*Department of Medicine, UConn Health, 263 Farmington Avenue, Farmington, CT 06030, USA*

[b]*Department of Histology and Embryology, Faculty of Medicine Osijek, University of Osijek, Josipa Huttlera 4, 31000 Osijek, Croatia*

[c]*Center for Regenerative Medicine and Skeletal Development, UConn Health, 263 Farmington Avenue, Farmington, CT 06030, USA*

[d]*Department of Physiology and Cell Biology, University of Arkansas for Medical Sciences, 4301 W. Markham Street, Little Rock, AR 72205, USA*

Corresponding author: erodak@mefos.hr

Osteoclasts (OCs) are multinucleated bone-resorbing cells that arise through the fusion of osteoclast precursor cells (OCPs). During homeostasis, OCPs are predominantly derived from bone marrow-resident CX3CR1-expressing myeloid cells, while under inflammatory conditions circulating OCPs serve as a significant source of OCs. However, the role of CX3CR1 in circulating OCP engraftment during fracture repair and the identity of inflammation-induced OCPs remains unexplored. This study investigated the function of CX3CR1 in OCP migration and OC formation and identified a novel OCP population that expands in inflammatory conditions. CX3CR1 loss-of-function mice model, parabiosis, femoral fracture healing model, TNFα-induced systemic inflammation, flow cytometry, single-cell RNA sequencing, *in vitro* osteoclastogenesis assays, brightfield and fluorescence microscopy and *in vivo* transplantation experiments were used to characterize OCP dynamics and function in non-homeostatic conditions. During fracture repair (0-14 days), *Cx3cr1* expression transiently decreased whereas *Cx3cl1* expression increased. Despite these changes, fluorescence microscopy after parabiosis experiments showed that CX3CR1 deficiency did not impair circulating OCP migration, engraftment, or differentiation into OCs within fracture calluses, indicating that CX3CR1 is not crucial for these processes. However, CX3CR1 loss did alter circulating monocyte profile by increasing classical and reducing non-classical monocytes. Systemic TNFα treatment significantly enhanced osteoclastogenic potential of bone marrow and peripheral blood cells and also induced expansion of a previously uncharacterized inflammatory OCP population. Single-cell RNA sequencing identified that population as $CX3CR1^{+}CD115^{+}Adgre4^{+}$ non-classical monocyte population displaying the greatest transcriptional response to TNFα, including enrichment of OC differentiation pathways and reduced expression of genes associated with antigen presentation and phagocytosis. Flow cytometry confirmed expansion of $CD115^{+}Adgre4^{+}$ cells following TNFα treatment. These cells efficiently differentiated into functional, bone-resorbing OCs *in vitro*, fused with conventional OCPs to generate chimeric OCs, and successfully engrafted into fracture calluses following systemic transplantation, where they fused with resident precursors and contributed to OCs formation *in vivo*. Together, these findings demonstrate that CX3CR1 is not required for circulating OCP recruitment during fracture healing but can be used as a marker for OCPs. A distinct inflammatory $CX3CR1^{+}CD115^{+}Adgre4^{+}$ osteoclast precursor population that expands during TNFα-driven inflammation and directly contributes to osteoclastogenesis has been identified and explored. Selective targeting of this inflammatory OCP subset may represent a therapeutic strategy for inflammatory bone loss while preserving physiological bone remodelling mediated by homeostatic osteoclasts.

Computational Imaging for Routine Pathology and Cytology: Aberration Calibration, Real-Time Sparse Deconvolution and Deep Learning-Assisted Acquisition

Vinicki Krunoslav

Digicyte, Vukomerec 49A, 10000 Zagreb, Croatia

Corresponding author: kvinicki@gmail.com

Modern image restoration algorithms have largely remained confined to high-end research platforms, where computational cost and specialist operation are acceptable. Routine diagnostic microscopy in pathology and cytology, which relies overwhelmingly on brightfield imaging on manual or semi-automated stands, has been left largely untouched by them. We present a computational imaging pipeline that brings calibrated aberration correction, real-time sparse deconvolution and deep learning-assisted acquisition to routine clinical microscopes. Lateral chromatic aberration and geometric distortion are treated as a single polynomial deformation, calibrated per colour channel and per magnification from one dot-target exposure, with vignetting taken from a flat field. Characterising three apochromatic objectives across a 21.4 mm image circle, distortion at the extreme corner was a purely radial pincushion of +0.36 to +0.67 %, whereas uncorrected lateral chromatic aberration reached 5.8 to 7.5 px of red-to-blue separation, 2.5 to 3.6 times the Rayleigh limit in object space and therefore plainly visible: chromatic error, not distortion, is the dominant geometric defect. After correction, verified by re-detecting the target in the corrected output rather than by scoring the model against its own fit, red-to-blue separation fell to 0.2 to 0.5 times the diffraction limit, a reduction of up to 11.7-fold, and the residual magnification difference between channels fell from 800-2250 ppm to below 11 ppm. Relative illumination at the corner measured 72.6, 81.8 and 92.6 % at 10×, 20× and 40× and proved near-achromatic. For restoration, sparse deconvolution was implemented from the published method and applied to brightfield, separately for each colour channel. Although the sparsity assumption underlying the original fluorescence application does not hold for densely stained transmitted-light images, the sparsity and continuity constraints act as effective regularisers, suppressing noise amplification and ringing while recovering high-frequency detail. Rewritten for GPU execution, it reaches approximately 200-fold higher throughput than the reference implementation, allowing restoration to run on the live image rather than as offline post-processing. Two neural networks remove the remaining manual steps: one identifies the objective in use on manual stands, so the correct calibration is applied automatically, and one performs automatic white balance. Together these make image quality a property of the system rather than of the operator: the user selects the regions worth imaging, while the software takes care of the image.

INVITED LECTURES

MATERIAL SCIENCE

Atomic Scale Insights into the Formation Mechanism and Photocatalytic Properties of $SrTiO_3/Bi_4Ti_3O_{12}$ Nanoplatelets

Daneu Nina, Rooj Subhashis, Spreitzer Matjaž, Maček Kržmanc Marjeta
Advanced Materials Department, Jožef Stefan Institute, Jamova cesta 39, 1000 Ljubljana, Slovenia
Corresponding author: nina.daneu@ijs.si

Solar-driven photocatalytic water splitting is a simple, low-cost, and scalable approach for the production of green hydrogen. State-of-the-art catalysts are designed as nanosized 2D/2D epitaxial heterostructures with suitable band-gap alignment of the phases, and combined with single-atom co-catalysts. Among the most suitable precursors for the synthesis of heterostructural nanosized platelets are phases with layered crystal structure such as Aurivillius-type $Bi_4Ti_3O_{12}$ (BIT). In our work, we use BIT for gradual topochemical conversion into $SrTiO_3$ (STO) under hydrothermal conditions [1–3]. The dissolving BIT platelets represent the source of $Ti(OH)_6^{2-}$ ions, whereas excess $SrCl_2$ is added into the solution as a source of Sr^{2+} ions. The products after different stages of transformation and different synthesised under different conditions were inspected by scanning transmission electron microscopy (STEM; ARM 200CF, Jeol, Japan and Spectra 300, Thermo Fisher, Netherlands). In the presentation, we will show that nanoscale characterisation of the platelets at all stages of topochemical transformation and in top-down and edge-on orientations is vital for understanding the transformation mechanism, the correlation between microstructural and functional properties and enables rational design of the nanoparticles with improved photocatalytic performance. Molten-salt synthesised template BIT platelets have tabular morphology with side length of about 1–2 microns and thickness up to 100 nanometres. Both basal-plane surfaces are terminated by $(Bi_2O_2)^{2+}$ layers, which dissolve during pre-treatment in NaOH, exposing the $(Bi_2Ti_3O_{10})^{2-}$ perovskite-blocks. Such surface represents an ideal substrate for epitaxial growth of STO. The growth of STO starts at the edges on both basal plane surfaces of the BIT platelets and proceeds towards the interior. Simultaneously, dissolution of BIT from lateral sides of the platelets occurs. The specific transformation mechanism results in the formation of heterostructural BIT/STO platelets with a groove running along the edges that apparently splits the starting BIT platelets into two thinner parallel STO platelets. Each STO platelet contains Bi-rich monolayer running through the middle and multiple nanosized Bi-rich inclusions [1]. The morphology of the recrystallized STO platelets depends mainly on the Sr excess [2], and the size and crystalline quality of the starting BIT platelets. A higher excess of Sr (Sr/Ti = 15), smaller BIT template nanoplatelets, and pre-reaction etching of the template with hot NaOH promote the formation of high-surface-area nanoplatelets with BET > 60 m^2/g, which show more than 50 times higher H_2 evolution rates compared to smooth, low surface area platelets with BET ≈ 10 m^2/g (Figure 1) [3]. The results show that higher surface roughness facilitates effective surface trapping of bismuth species, which, through *in situ* reduction to metallic Bi◦ single atoms act as co-catalyst and enhance photocatalytic H_2 evolution.

References
1. M. Maček Kržmanc et al., ACS Appl. Mater. Interfaces 13 (2021) 370–381.
2. A. Čontala et al., Nanoscale Adv. 5 (2023) 3005–3017.
3. M. Maček Kržmanc et al., Chem. Eng. J. 527 (2026) 171758.

Acknowledgements
Funding within the M-ERA.NET project GRIPHUS (Contact No. C3360-25-452025) and by the Slovenian Research Agency (P2-0091) is gratefully acknowledged.

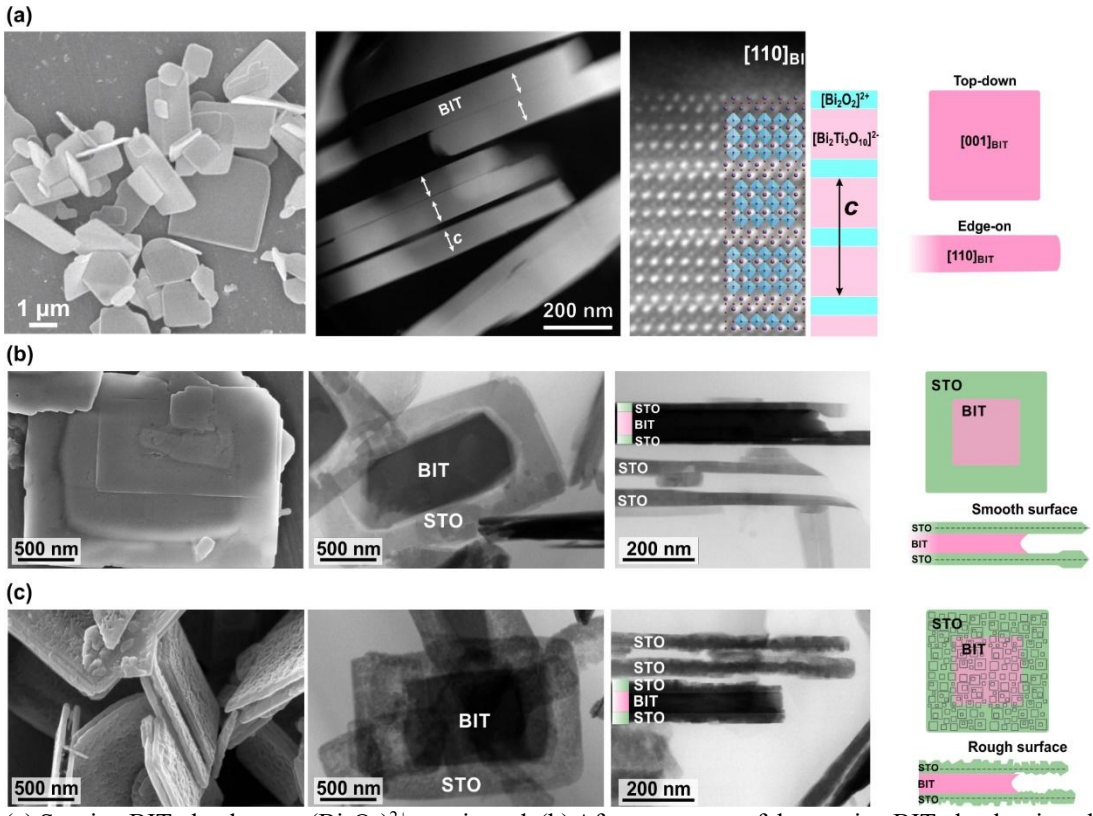

Figure 1. (a) Starting BIT platelets are $(Bi_2O_2)^{2+}$ terminated. (b) After treatment of the starting BIT platelets in cold NaOH, the STO/BIT heterostructural nanoparticles have smooth surface and low surface area. (c) After treatment of BIT in hot NaOH, the STO/BIT heterostructures have rough surface, large surface area and show about 50 times higher photocatalytic activity.

Spectromicroscopy of Epitaxial Borophene: Synthesis, Functionalization and Heterostructures

Petrović Marin
Institute of Physics, Bijenička 46, 10 000 Zagreb, Croatia
Corresponding author: mpetrovic@ifs.hr

Borophene, an atomically-thin 2D form of boron, has emerged as a promising material for nanotechnological applications due to its unique electronic and structural properties. Despite intensive research of borophene in recent years, many challenges from fundamental and applicative aspect still persist. In this talk, an overview of our recent advancements in addressing these challenges will be presented, with a focus on epitaxial borophene monolayer on iridium (111) surface. The main technique used in our investigation is spectroscopic photoemission and low-energy electron microscopy (SPE-LEEM), which allows *in situ* real-time monitoring of morphology and electronic properties of the examined systems. As will be elaborated, our borophene synthesis method is based on boron dissolution in iridium and its subsequent segregation to the surface, resulting in high-coverage, single-layer borophene of excellent crystallographic quality (Figure 1) [1]. Intrinsic properties of such high-quality borophene can be altered by adsorption of alkali atoms which readily induce modifications of borophene's crystal lattice and electronic structure [2]. One of the main factors governing these modifications are charge donation from the alkali atoms and high chemical reactivity of borophene. The reactivity of borophene also inhibits its use in applications, since exposure to air leads to severe contamination and deterioration of borophene's pristine properties. With this respect, vertical borophene-graphene heterostructures with promising ambient stability have been fabricated, where borophene was efficiently encapsulated by an inert graphene layer [3]. Overall, these results highlight the versatility of boron-based 2D systems and open new pathways for their integration into more complex nanoscopic devices.

References

1. K.M. Omambac et al., ACS Nano 15 (2021) 7421–7429.
2. S. Kamal et al., ACS Nano 20 (2026) 20198–20207.
3. M. Jugovac et al., Adv. Electron. Mater. 9 (2023) 2300136.

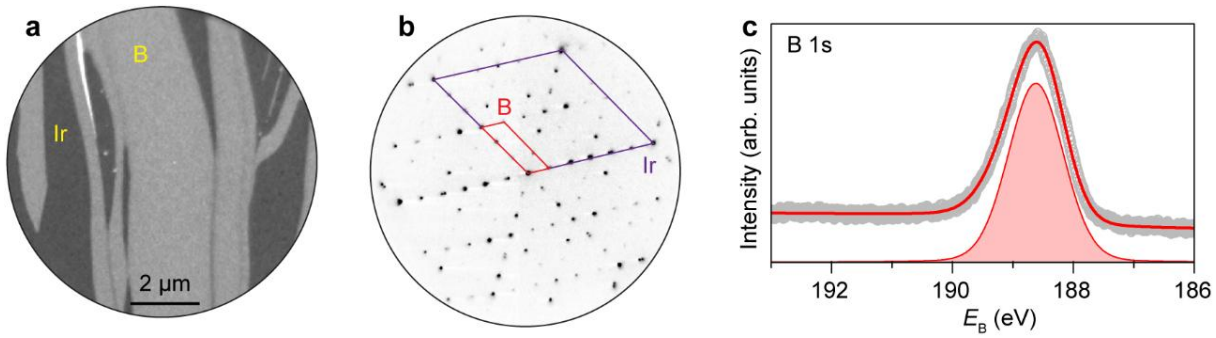

Figure 1. (a) Low-energy electron microscopy (LEEM) image, (b) low-energy electron diffraction (LEED) pattern and (c) X-ray photoelectron spectroscopy (XPS) spectrum (B 1s region) of a borophene monolayer on Ir(111). All data were recorded *in situ* on the same sample with the SPE-LEEM instrument.

Atomic Force Microscopy: A Powerful Tool for Studying Polyelectrolyte Multilayers

Klačić Tin

University of Zagreb Faculty of Science, Department of Chemistry, Horvatovac 102A, 10000 Zagreb, Croatia

Corresponding author: tin.klacic@chem.pmf.unizg.hr

Polyelectrolytes are macromolecules (*e.g.*, polymers) whose constitutional units bear ionic or ionizable groups that dissociate in polar solvents such as water. According to the sign of charge produced on the constitutional units after dissociation, polyelectrolytes are traditionally classified as polycations or polyanions. Nowadays, polyelectrolytes are building blocks of many interesting nanosystems, such as polyelectrolyte multilayers (PEMs). This type of organic thin film is commonly prepared through the layer-by-layer (LbL) method which consists of the alternative dipping of a solid substrate in polycation and polyanion solution, often with rinsing and drying steps between them. The substrate for PEM preparation can be a flat macroscopic object, but PEM can also be built up on colloidal particles of various geometries. The potential application of PEMs nowadays ranges from corrosion inhibitors, membranes, flame retardants, and sensors to antimicrobial coatings and drug delivery capsules [1]. The main reason for the widespread application potential of PEMs lies in the fact that their properties can be precisely controlled by varying the conditions of their preparation. Some of the experimental conditions that are typically varied to obtain PEMs of the desired properties are pH, ionic strength, molecular weight of polyelectrolytes, and the type of background salt present in polyelectrolyte solutions [2,3]. PEMs are usually characterized with methods such as ellipsometry, tensiometry, atomic force microscopy (AFM), UV-Vis spectrophotometry, and small-angle X-ray scattering. Among these methods, AFM is the most versatile for the characterization of PEMs. AFM primarily allows the determination of the morphology and roughness parameters of the PEM surface. However, if a part of the PEM is removed from the substrate surface, the thickness and structure of the PEM can be determined by AFM. Generally, a PEM structure can be compact, porous, or island-like. If PEM is porous or if it forms islands on the substrate surface, AFM can be used to estimate the surface coverage of the substrate with PEM. AFM can also be used to investigate the mechanical properties of the PEMs, *i.e.*, determine the elastic (Young) modulus of the PEMs. Since PEMs are relatively soft materials, they are suitable for nanolithography, which can be performed using an AFM instrument. From all of the above, it can be seen that AFM is a powerful tool for studying PEMs. Therefore, in my presentation, I will use real examples to show the possibilities of studying PEMs with AFM.

References

1. S. Zhao et al., ACS Nano 13 (2019) 6151–6169.
2. S.T. Dubas and J.B. Schlenoff, Macromolecules 32 (1999) 8153–8160.
3. T. Klačić et al., Macromolecules 55 (2022) 9571–9582.

Acknowledgements

This activity was supported by the European Union – NextGenerationEU through the National Recovery and Resilience Plan 2021–2026 via Institutional grant of the University of Zagreb Faculty of Science (PMF-PRESTIGE-2026-03).

Corrosion of Archaeological and Art Objects – Combined Electrochemical, Microscopic and Spectroscopic Studies

Otmačić Ćurković Helena[a], Mikić Dajana[a], Blažanović Angela[a], Hmelina Karla[a], Močnik Petra[b], Kosec Tadeja[b]

[a]*University of Zagreb Faculty of Chemical Engineering and Technology, Marulićev trg 19, 10000 Zagreb, Croatia*
[b]*Slovenian National Building and Civil Engineering Institute, Dimčeva ulica 12, 1000 Ljubljana, Slovenia*

Corresponding author: hotmac@fkit.unizg.hr

Corrosion of metallic materials generally proceeds as an electrochemical process, for that reason electrochemical methods are dominant in corrosion studies. On the other hand, spectroscopic and microscopic methods reveal the degree and form of surface damage and the composition of corrosion products. In this work, corrosion studies of bronze archaeological samples as well as of the weathering steel used for modern sculptures, were conducted by electrochemical, microscopic and spectroscopic methods. Archaeological samples usually contain layers of corrosion products, which have formed under changing conditions during the years. Knowledge on their composition can reveal how corrosion proceeded in time as well as which is the level of current reactivity of the sample. In this work the morphology and composition of two small archaeological samples were examined by SEM/EDS (Figure 1). FTIR spectroscopy and cyclic voltammetry were employed for surface characterization, enabling the identification of various compounds on the surfaces of the artefacts. Weathering steel has become a popular material for sculptures exposed outdoors and architecture as the gradual formation of corrosion products results in slow transformation of its visual appearance. In time corrosion resistance of weathering steel surface should be increasing as less protective corrosion products transform to more protective ones. However, this process depends on the presence of pollutants in the atmosphere, humidity and number and duration of drying cycles. In our study weathering steel samples were pre-patinated in several ways in order to simulate varying environmental conditions. Afterwards samples were exposed to outdoor urban atmosphere and their evolution in time was followed by electrochemical measurements, SEM/EDS, XRD and Raman spectroscopy. Based on the obtained results the correlation between the composition of corrosion products layer and corrosion resistance was established.

Acknowledgements
This research is partially financed by the bilateral Croatian-Slovenian project (Ministry of Science Education and Youth) “Environmental impact on metal cultural heritage”.

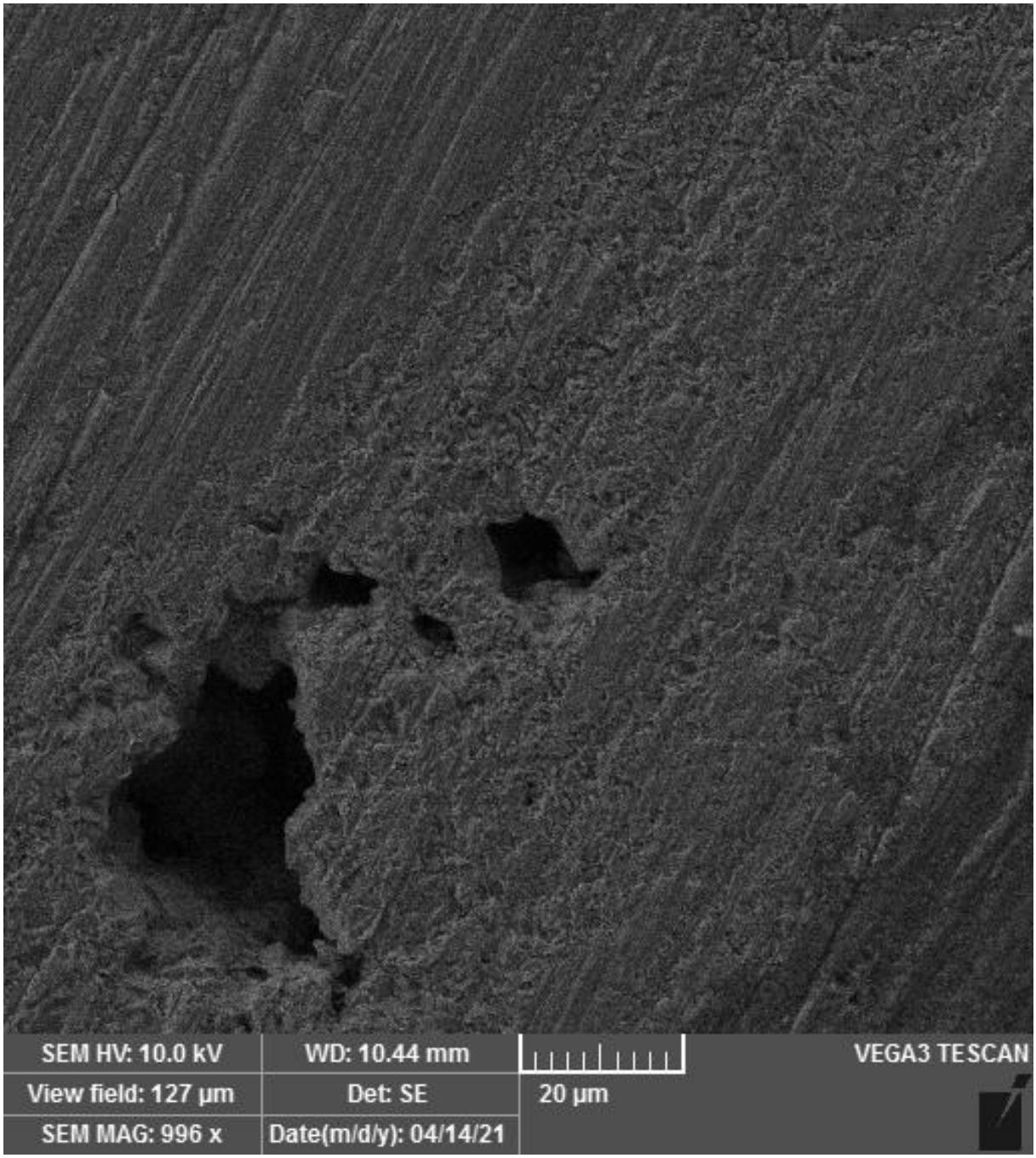

Figure 1. SEM image of archaeological bronze sample.

SpeciOn

SEE THE COMPLETE PICTURE

Explore your samples across scales.

TISSUE DETAIL

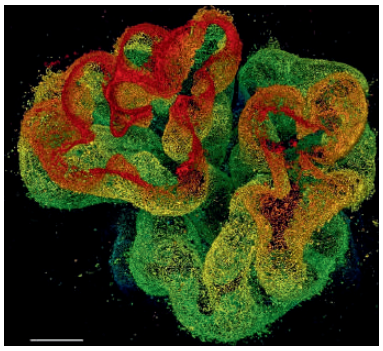

CELLULAR DETAIL

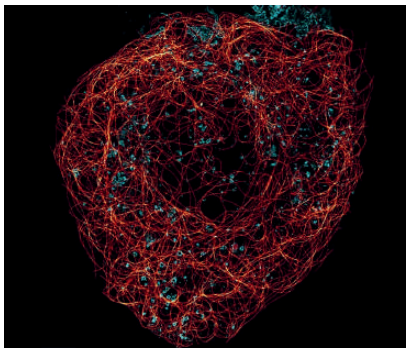

MATERIAL / SURFACE DETAIL

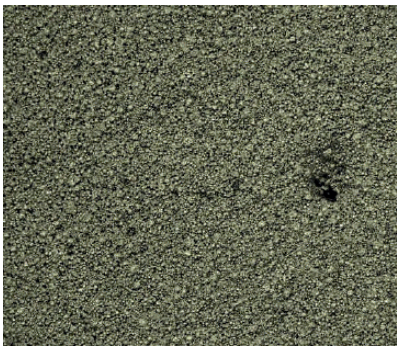

STED / ADVANCED FLUORESCENCE → CONFOCAL MICROSCOPY → EM SAMPLE PREPARATION

One partner. Multiple scales. Complete insight.

Specion provides a complete portfolio of advanced microscopy instruments and workflow solutions, application expertise, technical support and service for life sciences, pharmaceutical research, drug development, cancer research, materials science, industrial applications and quality control.

LIFE SCIENCES | MATERIALS SCIENCE | INDUSTRY & QUALITY

YOUR MICROSCOPY PARTNER IN SLOVENIA AND CROATIA

FIND THE RIGHT SOLUTION FOR YOUR LAB.
SCAN TO SPEAK WITH OUR MICROSCOPY SPECIALISTS.

WWW.SPECION.SI

WWW.SPECION.HR

SpeciOn | Leica MICROSYSTEMS AUTHORIZED PARTNER | HITACHI

SELECTED ORAL PRESENTATIONS

LIFE SCIENCE

Defining the Sequence Signals Governing NME6 Mitochondrial Targeting

Vrbančić Lea, Proust Bastien, Šutić Maja, Škrobot Vidaček Nikolina, Jazvinšćak Jembrek Maja, Štimac Valentina, Gudlin Lovro, Tolić Iva Marija, Herak Bosnar Maja

Ruđer Bošković Institute, Bijenička cesta 54, 10000 Zagreb, Croatia

Corresponding author: mherak@irb.hr

Nucleoside diphosphate kinases (NDPKs/NME) form an evolutionarily conserved enzyme family involved in diverse cellular processes, including metastasis suppression. The ten human NME genes cluster into two phylogenetic groups distinguished by exon–intron organization and protein homology. Group I members (NME1–4) are highly similar, assemble into hexamers, and display classical NDPK activity via a phospho-histidine intermediate. In contrast, Group II proteins (NME5–9) are more heterogeneous, and their catalytic properties and cellular roles remain poorly defined. Recent studies have identified NME6 as an exception within this group. We previously demonstrated that NME6 exists in two isoforms and localizes specifically to the mitochondrial matrix, likely adjacent to the inner membrane [1]. There, it colocalizes with the GTPase RCC1L and participates in mitochondrial RNA maturation, ribosome assembly, and translation. Notably, its NDPK activity requires direct interaction with RCC1L, distinguishing NME6 from Group I enzymes [2]. Despite its mitochondrial localization, NME6 lacks a canonical N-terminal targeting sequence, prompting our investigation into alternative import signals within its sequence [3]. Guided by TargetP and iMTS-L predictions, we generated a panel of GFP-tagged NME6 deletion and point mutants to identify regions essential for mitochondrial targeting. Their localization was examined in live HeLa and MDA-MB-231T cells using confocal microscopy, and validated by cellular fractionation. To refine spatial resolution, we are applying dual-color STED microscopy to visualize NME6 relative to markers of specific submitochondrial compartments. Our results indicate that the primary import determinant resides within the first seven N-terminal amino acids of NME6. Additionally, positively charged residues – particularly arginines within predicted internal mitochondrial targeting segments – substantially contribute to efficient mitochondrial entry. Preliminary STED imaging excludes NME6 presence at the outer mitochondrial membrane and reveals partial overlap with the inner membrane, a finding that will be further examined through ongoing high-resolution analyses.

References

1. B. Proust et al., Cell Biosci. 11 (2021) 195.
2. N. Grotehans et al., EMBO J. 42 (2023) e113256.
3. B. Proust et al., Int. J. Mol. Sci. 27 (2026) 4871.

Acknowledgements

This work was supported by the Croatian Science Foundation under the project numbers IP-2022-10-7420 and HRZZ-DOK-NPOO-2023-10-8602 to MHB.

Establishment and Microscopic Characterisation of an *In Vitro* Adipogenesis Model in 3T3-L1 Cells

Igrec Dunja[a], Matić Anita[a], Vuković Popović Ana[b]

[a]*Faculty of Dental Medicine and Health Osijek, Josip Juraj Strossmayer University of Osijek, Crkvena 21, 31000 Osijek, Croatia*

[b]*Department of Biology, Josip Juraj Strossmayer University of Osijek, Trg Ljudevita Gaja 6, 31000 Osijek, Croatia*

Corresponding author: anitamatic@fdmz.hr

Adipogenesis is a highly regulated biological process in which preadipocytes differentiate into mature adipocytes. Understanding this process is critical for elucidating the mechanisms of obesity, lipid metabolism, and adipose tissue development. *In vitro* adipogenesis models enable controlled analysis of cellular and metabolic changes and serve as essential tools in experimental research [1,2]. This study established an *in vitro* adipogenesis model using the 3T3-L1 murine cell line. It evaluated the effectiveness of microscopy and Oil Red O staining for monitoring morphological changes and intracellular lipid accumulation during differentiation. Frozen 3T3-L1 cells were thawed and cultured under sterile conditions until reaching 80% confluence, designated as day 0. Adipogenic differentiation was induced over a 10-day protocol using three culture media: growth medium, differentiation-induction medium supplemented with IBMX, dexamethasone, and insulin, and insulin medium, followed by recultivation in standard growth medium. Differentiation was assessed on days 0, 4, 7, and 10. At each time point, cells were stained with Oil Red O to visualise intracellular lipid droplet formation and accumulation. During early differentiation, cells exhibited initial lipid droplet formation and morphological changes. By day 4, cells became more rounded and displayed prominent intracellular lipid vacuoles, indicating ongoing adipogenic conversion. By day 10, cells exhibited morphological features characteristic of mature adipocytes, including enlarged lipid droplets and cytoplasm extensively filled with lipids, confirming successful adipogenic differentiation. The sequential morphological changes observed aligned with the expected progression from fibroblast-like preadipocytes to mature adipocyte-like cells. These results demonstrate that Oil Red O staining combined with light microscopy provides a straightforward and informative method for assessing adipogenesis *in vitro*. The established 3T3-L1 model offers an experimental platform for future investigations of adipocyte biology, metabolic regulation, obesity-related mechanisms, and the evaluation of potential therapeutic interventions.

References

1. K. Zebisch et al., Anal. Biochem. 425 (2012) 88–90.
2. I. Kaczmarek et al., STAR Protoc. 5 (2024) 102977.

Acknowledgements

The European Union funded research presented in this abstract through NextGenerationEU under the National Recovery and Resilience Plan 2021–2026 (Project No. 581-UNIOS-44).

Confocal Microscopy Reveals F-Actin Remodelling Associated with Hepatic Lipid Accumulation Following Gonadectomy and Aging

Mihajlović Lovro[a], Čurila Viktoria[b], Eržić Ema[b], Balog Marta[b], Viljetić Barbara[b], Pavić Valentina[a], Heffer Marija[b]

[a]*Department of Biology, J.J. Strossmayer University of Osijek, Ulica cara Hadrijana 8/A, 31000 Osijek, Croatia*
[b]*Faculty of Medicine Osijek, J.J. Strossmayer University of Osijek, Ulica Josipa Huttlera 4, 31000 Osijek, Croatia*

Corresponding author: lmihajlovic@biologija.unios.hr

Sex hormone loss, through either gonadectomy or aging, has been linked to increased hepatic lipid droplet accumulation, likely due to impaired fatty acid oxidation and triglyceride export [1]. Recent evidence suggests that lipid droplet accumulation is associated with alterations in cortical F-actin organization in hepatocytes [2]. To date, however, no study has directly examined whether sex hormone loss and aging affect cortical F-actin organization in the liver, or whether this occurs through lipid droplet-mediated mechanisms. Here, we investigated lipid droplet accumulation and cortical F-actin reorganization in the liver of young, middle-aged, and middle-aged gonadectomized male and female Sprague-Dawley rats. Young (3 months, n=6 males/6 females), middle-aged (10 months, n=7/7), and middle-aged gonadectomized (n=8/8) Sprague-Dawley rats were used. Gonadectomy (orchiectomy in males, ovariectomy in females) was performed at 10 months of age, with animals sacrificed 4 weeks later. Liver cryosections (10 µm) were stained with Oil Red O to visualize lipid droplets, imaged by bright-field microscopy, and quantified as the stained area (µm²) per field using Fiji/ImageJ. Separate cryosections were stained with rhodamine-phalloidin to label F-actin and DAPI for nuclei, and acquired using confocal laser scanning microscope (FLUOVIEW™ FV5000) where F-actin organization was assessed only qualitatively. Group differences were analysed by two-way ANOVA, with Games-Howell post hoc test. Oil Red O analysis revealed a significant main effect of group on lipid droplet staining area ($F(2,24)=20.71$, $p<0.001$, $\omega^2=0.59$). Gonadectomized rats showed significantly greater lipid droplet staining area (µm²) than both young and middle-aged intact rats, while no difference was found between young and middle-aged intact animals. Neither the effect of sex nor the group × sex interaction reached significance, and Games-Howell post hoc tests confirmed this pattern despite a violation of homogeneity of variance. Qualitative confocal imaging revealed marked cortical redistribution of F-actin, with prominent membrane-associated staining outlining hepatocyte borders exclusively in gonadectomized animals (Figure 1). These findings indicate that loss of gonadal hormones, rather than aging itself, drives hepatic lipid droplet accumulation in Sprague-Dawley rats. The parallel emergence of cortical F-actin reorganization specifically in gonadectomized animals suggests that this cytoskeletal reorganization is linked to lipid droplet accumulation rather than to aging-related processes independent of hormone status.

References

1. H. Malínská et al., Int. J. Mol. Sci. 22 (2021) 4527.
2. A.E. Loneker et al., Proc. Natl. Acad. Sci. U.S.A. 120 (2023) e2216811120.

Acknowledgements

This research was funded by the Croatian Science Foundation under project HRZZ-IP-2025-02-7869: Metabolomics of Targeted Tissues in Sex-Specific Prediction of Type 2 Diabetes and Neurodegeneration Risk in Response to Western and Keto Diets (MeDiet), led by Prof. Marija Heffer, PhD.

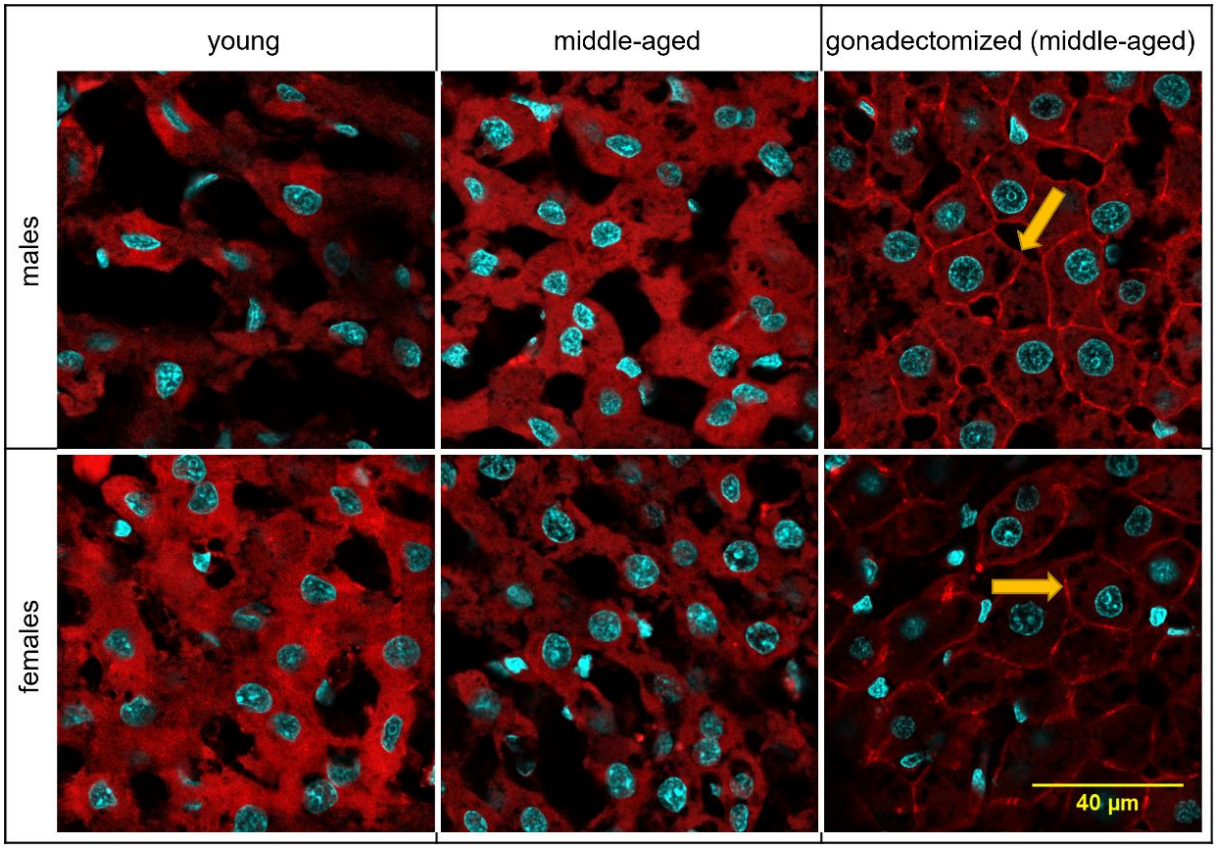

Figure 1. Representative confocal images of rhodamine-phalloidin (F-actin, red) and DAPI (nuclei, cyan) staining in rat liver cryosections from young, middle-aged, and gonadectomized (middle-aged) animals, shown separately for males and females (40× objective; scale bar indicated). Qualitative analysis revealed marked cortical redistribution of F-actin, with prominent membrane-associated staining outlining hepatocyte borders in a honeycomb-like pattern (yellow arrows), observed exclusively in gonadectomized animals of both sexes.

Dermoscopy as an Important Tool in Everyday Clinical Practice and in the Diagnosis of Various Dermatological Entities

Ilić Ivana[a,b], Delaš Aždajić Marija[c], Mujkić Robert[a]

[a]*Department of Anatomy, Histology, Embryology, Pathological Anatomy and Pathological Histology, Faculty of Dental Medicine and Health, Josip Juraj Strossmayer University of Osijek, Crkvena Street 21, 31 000 Osijek, Croatia*
[b]*Department of Histology and Embryology, Faculty of Medicine Osijek, Josip Juraj Strossmayer University of Osijek, Josipa Huttlera 4, 31 000 Osijek, Croatia*
[c]*Department of Dermatovenereology, Sestre milosrdnice University Hospital Centre, Vinogradska 29, 10 000 Zagreb, Croatia*

Corresponding author: ilic.ivana@gmail.com or ilovric@fdmz.hr

Dermoscopy is a non-invasive diagnostic method in dermatology that enables direct microscopic examination of skin lesions using a specialized device known as a dermatoscope. A dermatoscope is a non-invasive optical instrument used to magnify skin lesions. Handheld dermatoscopes are most commonly used, while digital dermatoscopes, as well as devices integrated with photographic systems, have become increasingly widespread in recent years. The essential components of every dermatoscope are a light source and a lens. The lens represents the central component of the instrument, providing 10–20× magnification in handheld dermatoscopes and up to 70× magnification in digital devices. The instrument is placed directly on the skin surface over the lesion of interest, allowing *in vivo* visualization of structures within the epidermis, the dermoepidermal junction, and the papillary dermis. The diagnostic value of dermoscopy is primarily associated with the evaluation of skin tumors, including both melanocytic and non-melanocytic lesions. Based on their dermoscopic features, lesions may be classified as benign or malignant. In addition to its role in the diagnosis of neoplastic skin lesions, dermoscopy is also applied in the assessment of parasitic and inflammatory skin diseases, as well as disorders of the scalp [1]. These applications include inflammoscopy, entodermoscopy, and trichoscopy. It is essential to interpret dermoscopic findings in correlation with the clinical presentation and, when indicated, with histopathological findings. This approach emphasizes the importance of collaboration among medical specialties and contributes to improving the sensitivity and specificity of dermoscopy as a diagnostic method. We invite you to embark on a “dermatological journey” through common entities encountered in everyday dermatology practice, demonstrating the heterogeneity of dermoscopic patterns across different dermatological conditions. More importantly, we aim to emphasize that microscopy as a diagnostic approach is not limited to research laboratories or large university centers, but is also an integral part of daily clinical practice across numerous medical specialties, including dermatology [2].

References

1. A. Lallas et al., Dermatol. Clin. 31 (2013) 679–694.
2. D. Sgouros et al., J. Clin. Med. 13 (2024) 972.

Insight into the Intracellular Dynamics of Rac1 GTPases by Confocal Microscopy and Mathematical Modelling

Šoštar Marko[a], Filić Vedrana[a], Pavin Nenad[b] and Weber Igor[a]

[a]*Ruđer Bošković Institute, Division of Molecular Biology, Bijenička 54, 10000 Zagreb, Croatia*
[b]*Faculty of Science, University of Zagreb, Department of Physics, Bijenička 32, 10000 Zagreb, Croatia*
Corresponding author: iweber@irb.hr

Biological oscillations are ubiquitous across all levels of organisation of living matter, from ecosystems down to individual cells. Within cells, proteins regulating polarisation and motility are particularly prone to cyclic spatial and temporal fluctuations. A prominent example is the Rho family of small GTPases, which act as master regulators of the actin cytoskeleton to control cell motility and polarity across diverse species, including yeast, plants, and mammals [1]. This study investigates the spatio-temporal dynamics of the Rho GTPase Rac1 and its effector, the IQGAP-related protein DGAP1, in free-living amoeboid cells of the protist *Dictyostelium discoideum*. Using specific live-cell fluorescent probes, we show that the active form of Rac1 (Rac1-GTP) displays highly dynamic, polarised, and oscillating intracellular patterns in the plasma membrane. Specifically, active Rac1 exhibits both oscillations, moving repeatedly from one side of the cell to the other as standing waves, and rotations, moving along the cell membrane as travelling waves, with a characteristic period of 2 to 5 minutes. Concurrently, cortical domains enriched in active Rac1 show a counterintuitive anti-correlation with DGAP1, which is predominantly depleted from these regions [2]. To capture and quantitatively understand these complex dynamics, we developed a mass-conserving reaction-diffusion model. This theoretical framework simulates the biochemical system based on the circulation of Rac1 between the cell membrane and the cytoplasm, its activation by guanine nucleotide exchange factors (GEFs), its deactivation by GTPase-activating proteins (GAPs), and its competitive interaction with DGAP1. Our mathematical model accurately reproduces the experimentally observed periods, amplitudes, and precise wave shapes of both active Rac1 and DGAP1 [3]. Furthermore, the modelling reveals distinct regulatory contributions from the negative regulators: while GAPs primarily dictate the temporal aspects of pattern formation, DGAP1 significantly influences the spatial dynamics. Crucially, the reaction-diffusion model predicted a novel colocalisation regime for active Rac1 and DGAP1 within stably polarised cells, which we subsequently confirmed through targeted *in cellulo* imaging experiments. Our findings demonstrate that transitions between homogeneous distribution, stable polarisation, and oscillatory regimes depend tightly on physical cell size, absolute protein amounts, and specific biochemical reaction kinetics. In summary, this study expands our knowledge of Rho GTPase behaviour in *Dictyostelium discoideum* and offers a quantitative blueprint for how feedback loops involving small signalling proteins generate complex self-organising patterns to regulate cell motility.

References

1. V. Filić et al., Cells 10 (2021) 1592.
2. V. Filić et al., Cell. Mol. Life Sci. 71 (2014) 2775–2785.
3. M. Šoštar et al., PLoS Comput. Biol. 20 (2024) e1012025.

Acknowledgements

This work was supported by the Croatian Science Foundation under the project number HRZZ-IP-2024-05-6331.

Cytotoxic and Genotoxic Activity of Invasive Alien Plant Extracts Reveals Their Selective Antitumor Potential in Human Cell Lines

Poljuha Danijela[a], Cvjetko Petra[b], Caput Mihalić Katarina[b], Sladonja Barbara[a], Uzelac Božac Mirela[a] and Modrušan Vanja[a]

[a]*Institute of Agriculture and Tourism, Karla Huguesa 8, 52440 Poreč, Croatia*
[b]*Faculty of Science, University of Zagreb, Horvatovac 102a, 10000 Zagreb, Croatia*

Corresponding author: danijela@iptpo.hr

Invasive alien plant species are a promising source of bioactive metabolites with potential antitumor activity. Evaluating their cytotoxicity, genotoxicity and selectivity towards tumor cells is essential for identifying promising antitumor candidates. The aim of this study was to assess the cytotoxic and genotoxic effects of leaf and flower extracts of four invasive alien plant species (*Ailanthus altissima* (Mill.) Swingle, *Helianthus tuberosus* L., *Robinia pseudoacacia* L., and *Solidago canadensis* L.) and to identify extracts possibly showing the greatest potential for further investigation as selective antitumor agents. Plant extracts were prepared using finely minced air-dried leaves and inflorescences collected and pooled from 15 locations in Istria (Croatia) and dissolved in 2% dimethyl sulfoxide (DMSO). Leaf and flower extracts were tested on three human cell lines: U2OS osteosarcoma cells, HeLa cervical adenocarcinoma cells and non-tumor HEK293 embryonic kidney cells. Cell viability was determined using the MTT assay [1] following exposure to three extract concentrations (0.5, 1.0 and 2.0 mg mL^{-1}), while DNA damage was assessed by the comet assay [2] using the percentage of tail DNA (% tDNA) as the primary indicator of genotoxicity. Statistical analyses were performed using ANOVA followed by appropriate post hoc tests ($p < 0.05$). The extracts exhibited distinct biological activities. *S. canadensis* extracts showed strong cytotoxic and genotoxic effects in all tested cell lines, indicating pronounced but non-selective toxicity. *H. tuberosus* leaf extracts also induced substantial cytotoxic and genotoxic responses, while flower extracts showed a concentration-dependent shift from proliferation stimulation to cytotoxicity. *R. pseudoacacia* displayed the weakest activity, including hormetic responses at lower concentrations. Among the tested species, *A. altissima* showed the most promising profile, with moderate cytotoxicity of leaf extracts and concentration-dependent genotoxic effects of flower extracts. Importantly, leaf extracts demonstrated differential responses between tumor and non-tumor cells (Figure 1), suggesting the presence of a potential concentration range for selective activity. Overall, most extracts exhibited limited therapeutic potential due to insufficient selectivity, whereas *A. altissima* represents the most promising candidate for further antitumor investigations. Future studies will focus on lower, micromolar concentrations and molecular mechanisms underlying its cytotoxic and genotoxic effects to define a potential therapeutic window.

References

1. M. Ledinski et al., Polymers 14 (2022) 1751.
2. P. Cvjetko et al., Environ. Sci. Pollut. Res. 25 (2018) 5590–5602.

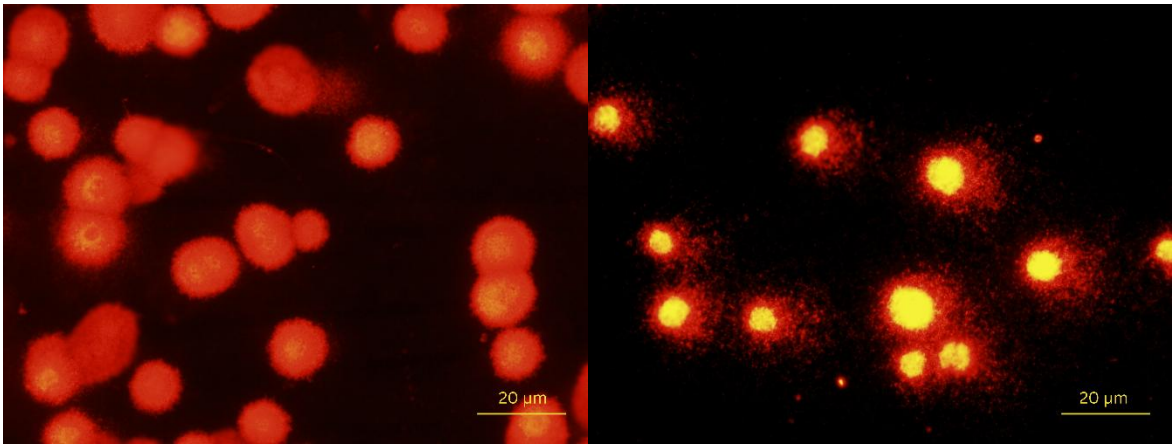

(a) **(b)**

Figure 1. *Ailanthus altissima* leaf extract induced differential DNA damage responses in non-tumor-derived HEK293 human embryonic kidney cells (a) and tumor-derived U2OS human osteosarcoma cells (b) after 24 h of treatment at a concentration of 0.5 mg mL^{-1}. Images were acquired using a ZEISS Axioscope 5 fluorescence microscope.

SELECTED ORAL PRESENTATIONS

MATERIAL SCIENCE

Morphology of Lead Halide Perovskite Thin Films via Spin Coating and Slot Die Coating

Kojić Vedran, Klobučar Lucija, Dolić Stjepan, Juraić Krunoslav, Čižmar Tihana, Gajović Andreja
Ruđer Bošković Institute, Division of Materials Physics, Laboratory for Energy Conversion Materials and Sensors, Bijenička cesta 54, 10000 Zagreb, Croatia
Corresponding author: vkojic@irb.hr

The solution processing of organometal halide perovskite absorber films is governed by a complex hierarchy of solvent–precursor interactions. These range from molecular-level coordination chemistry in the precursor solution to mesoscale crystallization dynamics during film formation, particularly under antisolvent treatment. A key parameter controlling these interactions is Gutmann's donor number (DN), which quantifies solvent Lewis basicity and its ability to coordinate with Pb^{2+} ions in lead halide precursors [1]. High-DN solvents, such as dimethyl sulfoxide (DMSO), strongly coordinate with Pb^{2+}, suppressing iodoplumbate complex formation. This stabilizes precursor solutions and enables controlled thin-film deposition. In contrast, low-DN solvents, such as dimethylformamide (DMF), facilitate iodide coordination and promote perovskite crystallization, which can support the growth of large single crystals. However, relying solely on solvent-driven crystallization often results in thin films that lack uniformity and reproducibility. To address this limitation, antisolvents are introduced to accelerate solvent removal and induce rapid perovskite precipitation [2]. Antisolvents can be categorized into three types based on their solubility for organic precursors and their miscibility with host solvents: Type I antisolvents (e.g., alcohols), which have high solubility for organic precursors. Type II antisolvents (e.g., chlorinated and ester-based solvents) exhibit low solubility for organic components and high miscibility with host solvents. Type III antisolvents (e.g., nonpolar aromatic solvents), which are immiscible with host solvents. In slot-die coating, the absence of a centrifugal force – as present in spin coating – necessitates alternative quenching strategies, such as air-knife gas flow or antisolvent bathing, to drive crystallization [3]. High-DN, high-boiling-point co-solvents like DMSO are used to extend the processing window and stabilize intermediate phases, while low-boiling-point primary solvents, such as acetonitrile and 2-methoxyethanol, enable rapid coating speeds suitable for scalable manufacturing. In this work, we compare thin films prepared via spin coating and slot-die coating using identical primary solvents and antisolvents, with the aim of elucidating differences in film morphology and optical properties.

References

1. J.C. Hamill et al., ACS Energy Lett. 3 (2018) 92–97.
2. A.D. Taylor et al., Nat. Commun. 12 (2021) 1878.
3. K.K. Shin Thant et al., Adv. Energy Mater. 15 (2025) 2403088.

Acknowledgements

We acknowledge the cooperation between the Government of the Republic of Croatia and the Government of the State of Israel with co-financing from the Ministry of Science, Education and Youth Croatia, project „Novel perovskite solar cells with enhanced performance based on hybrid halide perovskite/transition-metal disulfides nanocomposites (Sol-HP-TMD-NanoComp)".

The Atomic Resolution Electron Microscopy Study of the WTaVCr Intended for Fusion Application

Gajović Andreja[a], Drev Sandra[b], Tomić Luketić Kristina[a], Dunatov Toni[a], Matić Mario[a], Ovčar Juraj[a], Gunde Miha[a], Popović Jasminka[a], Skoko Željko[c], Tadić Tonči[a], Čeh Miran[b]

[a]*Ruđer Bošković Institute, Bijenička cesta 54, 10000 Zagreb, Croatia*
[b]*Jožef Stefan Institute, Jamova cesta 39, 1000 Ljubljana, Slovenia*
[c]*University of Zagreb, Faculty of Science, Department of Physics, Bijenička cesta 32, 10000 Zagreb, Croatia*
Corresponding author: gajovic@irb.hr

Fusion-based power plants are central to efforts to reduce carbon emissions, but their development depends on materials that can withstand high-energy fusion neutrons and heat fluxes of approximately 10 MW m^{-2}. Tungsten and W-based alloys are leading candidates for plasma-facing components [1]. To screen different compositions, we prepared WTaVCr thin films by magnetron sputtering and investigated irradiation-induced changes using X-ray diffraction (XRD), scanning electron microscopy, energy-dispersive X-ray spectroscopy and atomic-resolution scanning transmission electron microscopy (STEM), complemented by atomistic simulations based on a machine-learned interatomic potential [2,3]. Films deposited on Si were characterized before and after irradiation with 8 MeV Cu^{3+} ions to a dose of 1 dpa. XRD revealed two body-centred cubic high-entropy-alloy phases in the as-deposited films, with unit-cell parameters of a = 3.191(2) Å and a = 3.126(3) Å. After irradiation, the material transformed completely into the phase with the smaller unit cell. This finding indicates irradiation-induced lattice relaxation and ordering rather than the expected increase in structural defects. Simulations confirmed that a unit-cell length of approximately 3.12 Å represents the global minimum of the WTaVCr BCC lattice. Atomic-resolution STEM and EDS mapping further showed a homogeneous distribution of W, Ta, V and Cr within irradiated grains (Figure 1). Rietveld line-broadening analysis demonstrated that the as-deposited phase with the larger unit cell had a higher microstrain than the irradiated phase. The reduced microstrain after irradiation therefore reflects a decrease in lattice distortions and relaxation of deformations initially introduced during deposition. These results suggest that the as-deposited alloy is retained in a substrate-induced local energy minimum, whereas heavy-ion irradiation promotes relaxation towards a more thermodynamically stable BCC phase.

References

1. G. Pintsuk et al., Fusion Eng. Des. 174 (2022) 112994.
2. J. Byggmästar et al., Acta Mater. 296 (2025) 121276.
3. J. Byggmästar et al., Phys. Rev. Mater. 6 (2022) 083801.

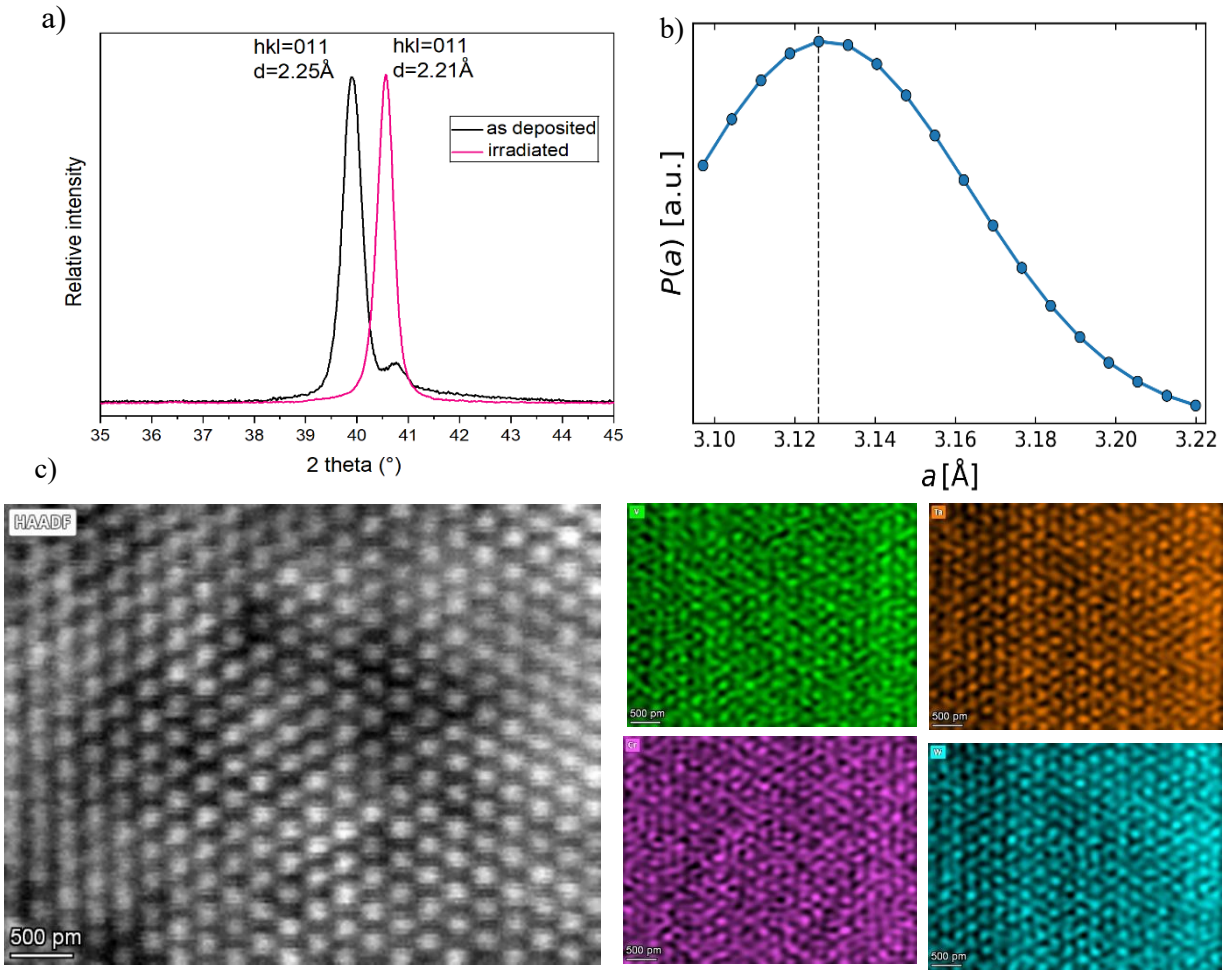

Figure 1. X-ray diffraction pattern of WTaVCr film as deposited and after irradiation by 8 MeV Cu (a), probability of WTaVCr to form a BCC bulk crystal of unit cell length "a" (b), and HAADF and EDS maps of WTaVCr film after irradiation by 8 MeV Cu. Scale bars are 500 pm (c).

Designing Infection-Resistant Surfaces: Physico-Chemical and Antibacterial Characterization of Calcium Phosphates/Silver Nanoparticles Composite Coatings for Titanium Implants

Inkret Suzana[a], Bojanić Krunoslav[a], Erceg Ina[a], Christiansen Silke[b,c], Dutour Sikirić Maja[a]

[a]*Ruđer Bošković Institute, Bijenička cesta 54, 10000 Zagreb, Croatia*

[b]*Fraunhofer Institute for Ceramic Technologies and Systems IKTS, Äussere Nürnberger Strasse 62, 91301 Forchheim, Germany*

[c]*Innovation Institute for Nanotechnology and Correlative Microscopy – INAM, Äussere Nürnberger Strasse 62, 91301 Forchheim, Germany*

Corresponding author: sinkret@irb.hr

Titanium implants are widely used for their mechanical stability, chemical inertness, and biocompatibility [1]. However, the inertness impairs osseointegration, i.e., the incorporation of an implant into bone, prompting the use of bioactive calcium phosphates (CaPs) coatings. CaPs mimic the main inorganic component of bone [2] and have therefore been studied and applied for decades in bone implantation. Currently, implant-associated infections are a key problem in treating bone defects with implants. A possible solution to this problem is antibacterial CaP-based coatings containing antimicrobial agents. Silver nanoparticles (AgNPs) are a promising candidate, as silver exhibits a broad spectrum of antibacterial activity and is unlikely to cause bacterial resistance. CaPs/AgNPs coatings were prepared by wet chemistry method on etched titanium substrates. Etching with a mixture of sulphuric and hydrochloric acids followed the method described by Lu et al. [3] AFM, SEM, and contact angle measurements showed increased surface roughness, altered surface topography, and wettability due to etching, all of which favour osteoblast cell adhesion, as reported in previous studies. Furthermore, SEM and optical profilometry showed more uniform coating distribution on the etched titanium surface compared to the unetched surface. Antibacterial efficacy was assessed using indirect (crystal violet staining) and direct (CFU counting) methods and visualised by SEM. Both demonstrated reduced biofilm formation by *Staphylococcus aureus* and *Escherichia coli* on CaPs/AgNPs-coated titanium compared to uncoated titanium. The obtained results indicate that functional, antimicrobial coatings can be prepared through the simple wet method, which could contribute to further development of affordable antibacterial implant materials.

References

1. X. Lu et al., Front. Bioeng. Biotechnol. 9 (2021) 783816.
2. S. Weiner et al., Annu. Rev. Mater. Res. 28 (1998) 271–298.
3. X. Lu et al., Mater. Sci. Eng. C 27 (2007) 700–708.

Acknowledgements

Financial support from Croatian Science Foundation, grants DOK2021-02-5447 and MOBDOK-2023-4472.

Synthesis of Multicomponent Transition-Metal Alloys and Oxides for Dual Photocatalytic and Antibacterial Applications

Čižmar Tihana[a], Kojić Vedran[a], Skelin Ilić Josipa[a], Radetić Lucija[b]
[a]*Ruđer Bošković Institute, Bijenička cesta 54, Zagreb*
[b]*University of Zagreb Faculty of Geotechnical Engineering, Hallerova aleja 7, Varaždin*
Corresponding author: tcizmar@irb.hr

Multicomponent transition-metal systems [1,2], including alloys and their corresponding oxide thin films obtained either by magnetron sputtering in an oxygen atmosphere or by electrochemical anodization, have emerged as promising candidates for the preparation of functional surfaces with combined photocatalytic [3] and antibacterial [1] properties. Their compositional complexity enables fine-tuning of physicochemical properties, which is highly relevant in addressing environmental pollution and microbial contamination. In particular, the rapid global rise of multidrug-resistant bacteria represents a critical public health challenge, significantly reducing the effectiveness of conventional antibiotics and requiring the development of alternative antimicrobial strategies. In this study, multicomponent alloy thin films were deposited by magnetron sputtering onto fluorine-doped tin oxide (FTO) substrates and afterwards transformed into nanostructured oxide layers through electrochemical anodization. Emphasis was put on detailed morphological and compositional analysis using scanning electron microscopy (SEM) coupled with energy-dispersive X-ray spectroscopy (EDS). SEM imaging revealed the formation of highly ordered surface structures (Figure 1), while EDS mapping provided spatially resolved insight into elemental distribution and homogeneity across the films, highlighting the role of multicomponent composition in governing nanoscale organization. X-ray diffraction (XRD) was used as a complementary technique to assess the crystalline phases developed during magnetron sputtering and electrochemical anodization. The photocatalytic activity of the obtained thin films was tested using Ciprofloxacin under UV–visible irradiation. The results indicate a strong dependence of photocatalytic activity on surface morphology and compositional uniformity, as determined by SEM/EDS analysis. Furthermore, the antibacterial properties of the oxide thin films were evaluated against Gram-positive *Bacillus subtilis* and Gram-negative *Escherichia coli*. Variations in bacterial inhibition efficiency were correlated with differences in surface features and elemental distribution, suggesting that nanoscale heterogeneity and surface chemistry play a crucial role in antibacterial activity. Overall, these findings support the development of advanced multifunctional materials for water treatment and antibacterial applications, highlighting the potential of thin film systems for the removal of antibiotic pollutants such as Ciprofloxacin and for addressing the growing threat of multi-drug resistant bacteria.

References

1. Z. Shi et al., Adv. Eng. Mater. 25 (2023) 2300968.
2. M. Anandkumar et al., J. Alloys Compd. 960 (2023) 170690.
3. R. Huang et al., Nano Mater. Sci. 8 (2026) 264–283.

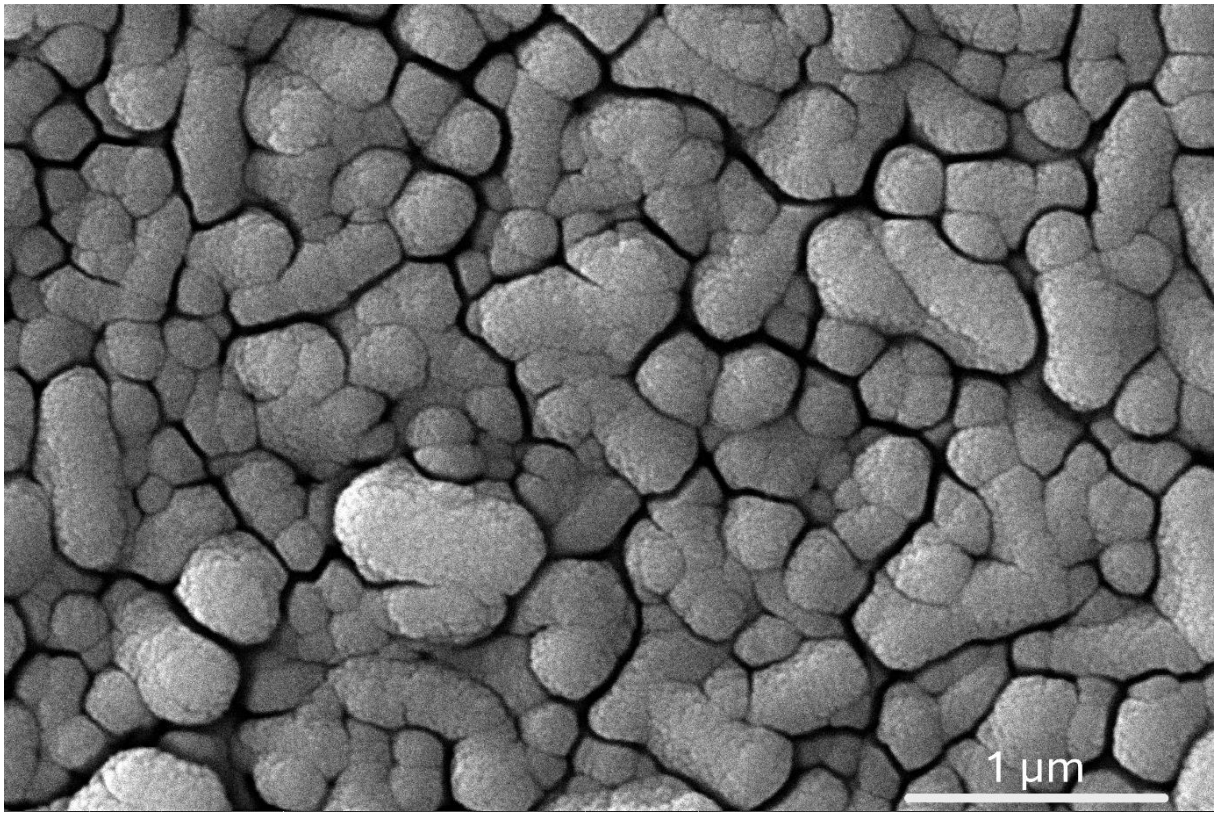

Figure 1. SEM micrograph of FeCuCoMnNi prepared by magnetron sputtering.

Light and Electron Microscopy in Research of Historical Papers

Macan Jelena[a], Dragojević Andreja[b]

[a]*University of Zagreb Faculty of Chemical Engineering and Technology, Trg Marka Marulića 19, 10000 Zagreb, Croatia*

[b]*Croatian State Archives, Trg Marka Marulića 21, 10000 Zagreb, Croatia*

Corresponding author: jmacan@fkit.unizg.hr

Microscopical investigation of historical papers from the collection of Croatian State Archives can help determine their composition, from the source of fibres and the choice of sizes and fillers to pigments used to colour them. Analysis of paper surface and fibre morphology was performed by Dino-Lite Pro-AM-413T5 digital light microscope, Micros Austria MCx500 light microscope and by Tescan Vega III Easyprobe scanning electron microscope (SEM) with an energy dispersive X-ray spectroscopy (EDS) detector. EDS analysis allowed for elemental analysis of filler and pigment particles. Before 18th ct., papers were mostly made from cast-off textile (comprising cellulosic fibres from flax and hemp, with some cotton) sized with gelatine, sometimes with addition of calcium carbonate as filler. Fibers can be differentiated based on their morphological characteristics. Flax fibres appear as long, transparent, cylindrical tubes that may be smooth or longitudinally striated, while hemp fibres are cylindrical in shape, with joints, cracks, nodes, and other surface irregularities and cotton fibres are characterised by their twisted shape. Investigated papers were composed mostly from flax and hemp fibres, with the exception of paper from 1808 which was made from flax and cotton (Figure 1). SEM image also showed larger quantity of sizing material in the papers from 18th and 19th ct. compared to older samples. EDS analysis showed the presence of calcium, most likely as part of calcium carbonate or gypsum filler, as well as aluminium and silicon which are likely present in clay minerals used as filler or present in water used for preparation of paper. Blue papers were investigated to determine how they were dyed. Three distinct ways were found: incorporating coloured fibres into the paper pulp to tint the paper, adding blue pigments to the filler, or applying a blue dye to the paper's surface. It was impossible to obtain unambiguous identification of elemental composition of blue fibres and pigment particles without first isolating them from the paper. The blue dye contained iron, which together with infra-red spectroscopy allowed us to identify Prussian blue as the dye used. Green colour on maps and plans from the cartographic collection of Croatian State Archives was also investigated. It was mostly due to presence of particles of green pigment, largely copper based. Most likely green pigments are thus 7erdigris and malachite, both of which contain only carbon, oxygen and hydrogen alongside copper, which makes their identification solely using EDS difficult.

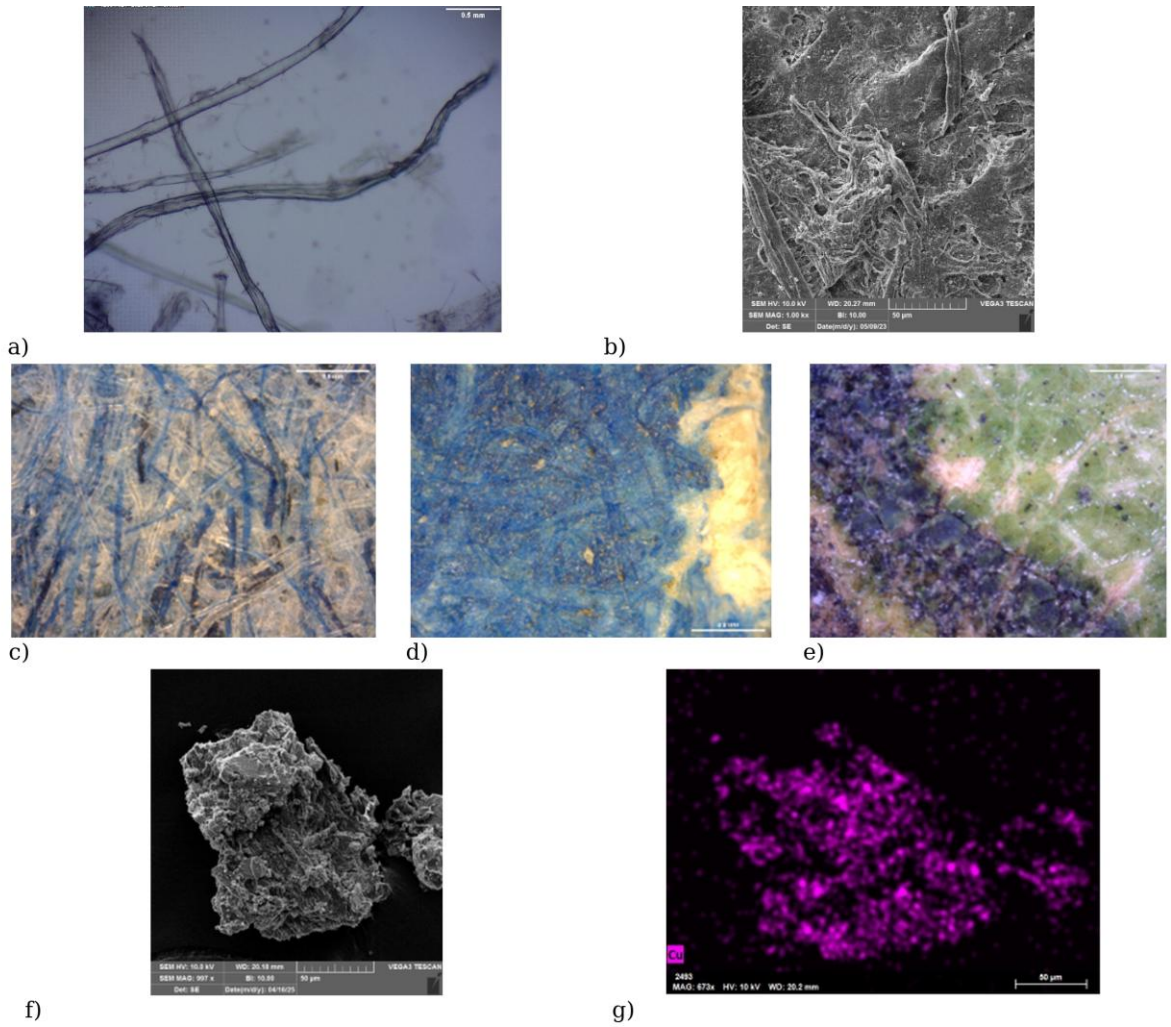

Figure 1. Morphology of paper from 1808 investigated by (a) light microscopy in transmission and (b) electron scanning microscopy, showing presence of cotton fibre; light microscopy images of coloured papers: (c) blue fibres in paper from 1830, (d) blue dye on a paper from 1901 and € green pigment on a map from 1711; (f) SEM micrograph and (g) EDS elemental mapping of copper of the detached pigment particle from a map from 1572.

Advanced Light Microscopy and Digital Image Analysis in Textile Structure Characterization

Vyšanská Monika

Department of Technologies and Structures, Faculty of Textile Engineering, Technical University of Liberec, Studentská 2, Liberec, 461 17, Czech Republic

Corresponding author: monika.vysanska@tul.cz

The historically first recorded use of the light microscope for investigating textile structures dates back to the 17th century, while its scientific application in textile research has been documented since approximately the mid-19th century [1]. Generally achievable magnification with an optical microscope is around 1000×, which is sufficient for the observation, identification, and analysis of textile structures. When evaluating a larger sample area is required, a light macroscope can be utilized; however, at the expense of recording a larger area, it does not allow for such high object magnifications as a microscope. Our workplace – the Department of Technologies and Structures, Faculty of Textile Engineering, Technical University of Liberec – operates both types of magnification tools. The initial step in analyzing textile structures is obtaining a sufficiently magnified digital image, which can represent the end of the entire analysis. However, if it is necessary to quantify the structure through structural parameters, digital image analysis follows. In our case, we utilize NIS Elements, a software product developed by the Czech company Laboratory Imaging. On this platform, we have established a set of non-standard procedures for analyzing the structural parameters of linear textiles (fibers, yarns) and planar textiles (woven, knitted, and nonwoven fabrics). Furthermore, thanks to our specialized methodology of modified paraffin sections, we can evaluate the internal structure of textiles in addition to their external morphology. Through image sequences, it is also possible to analyze the dynamic processes of structural changes in textiles, such as mechanical stress, liquid transport through the textile medium, or the propagation of defects in a stressed textile material. This presentation aims to demonstrate the wide scope of our capabilities and expertise in evaluating the qualitative structural properties of textiles through these advanced techniques. Figure 1 illustrates the use of micro- and macro-images obtained under reflected and transmitted light for textile analysis.

References

1. V.W. Tripp, in: Symposium on Light Microscopy, ASTM International (1953) 25–34.

Micro images	Macro images
transmitted light *cross-sections*	**reflected light** *planar view*
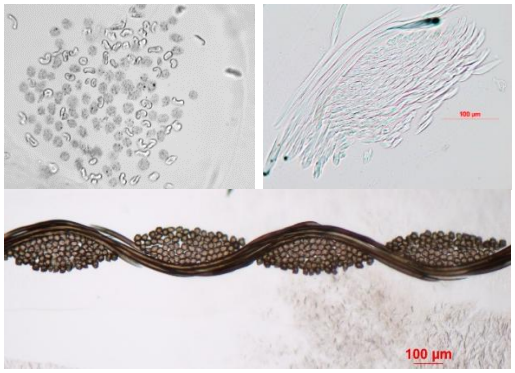 **evaluated parameters:** material type, # fibers, yarn packing density, yarn diameter, fibers' orientation; fabric thickness, binding wave length, yarn deformation in binding point, … *+planar view*	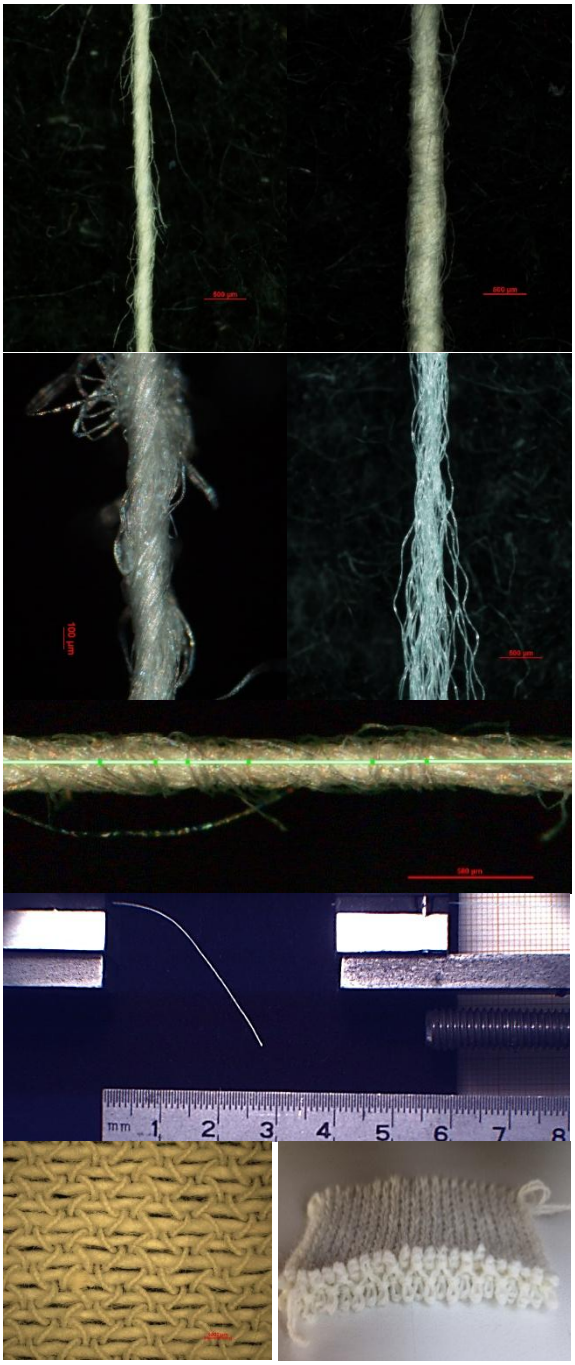
 **evaluated parameters:** cover x porosity of fabric; yarn diameter, hairiness, imperfections (joints, pills, …)	 **evaluated parameters:** yarn identification, belt fibers' parameters, yarn bending rigidity; fabric identification, warp, weft sett, wale, course density; textile filters – fibers' artifacts parameters; liquid transport in textile; defect propagation in knitted fabric, …
reflected light *planar view*	
 **evaluated parameters:** fibers' orientation in yarn	

Figure 1. Micro- and macro-images obtained under reflected and transmitted light for textile analysis.

ANSAR-ANALITIKA
ANALYTICAL EQUIPMENT

Imamo rješenja i tehnologije za istaživačke, analitičke,
i kontrolne laboratorije

Tel.+385 1 7980 857
E-mail: ansar@ansar-analitika.hr
Web: www.ansar-analitika.hr

OXFORD INSTRUMENTS

Oxford Instruments plc vodeći je proizvođač visokotehnoloških instrumenata i tehnologija:
Mikroskopi atomske sile (AFM)
Kriostati za mikroskopiju i spektroskopiju (Microstat i Optistat)
Dilucijski kriostati s magnetima (wet i dry)

biosistemi
YOUR TRUSTED PARTNER IN CREATING THE FUTURE

Od rutinske analize
staničnih kultura do
prostorne analize tkiva

Biosistemi d.o.o. predstavlja Thermo Fisher Scientific rješenja za modernu mikroskopiju - intuitivne, pouzdane i učinkovite sustave koji znanstvenicima omogućuju brži put od uzorka do kvalitetne slike

EVOS™ sustavi za svaku fazu istraživanja



EVOS™ M3000
pouzdano rješenje za svakodnevni rad u staničnoj kulturi i rutinsko snimanje



EVOS™ M5000
fleksibilan sustav za fluorescentnu mikroskopiju, analizu stanica i tkiva te napredne istraživačke primjene



EVOS™ M7000
potpuno automatizirano snimanje za veći broj uzoraka, zahtjevne eksperimente i višedimenzionalna snimanja



EVOS™ S1000
nova generacija prostorne analize tkiva s mogućnošću višekanalnog fluorescentnog snimanja



Više od mikroskopa
Uz EVOS™ sustave nudimo i kompletan portfelj Thermo Fisher Scientific potrošnog materijala za staničnu biologiju i mikroskopiju: laboratorijsku plastiku i posuđe za staničnu kulturu, pločice i posude za mikroskopiju, fluorescentne boje i reagense za označavanje stanica i tkiva te reagense za pripremu uzoraka i svakodnevni laboratorijski rad

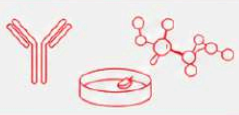

Sve što Vam je potrebno -
od uzorka do vrhunske
slike

ThermoFisher
SCIENTIFIC

Posjetite nas tijekom 5. Hrvatskog mikroskopijskog kongresa 16.-18. rujna

POSTER PRESENTATIONS

LIFE SCIENCE

Leaf Anatomy and Ultrastructural Characteristics of the Endemic *Seseli tomentosum* Vis.: Insights into Species-Specific Adaptations

Vuko Elma[a], Bočina Ivana[a], Kamenjarin Juraj[a], Radman Sanja[b], Fredotović Željana[a]

[a]*Faculty of Science, University of Split, R. Boškovića 33, Split, Croatia*

[b]*Faculty of Chemistry and Technology, University of Split, R. Boškovića 35, Split, Croatia*

Corresponding author: elmal@pmfst.hr

Seseli tomentosum Vis. is an endemic species of the coastal Dinarides whose leaf anatomy has not previously been described. Among the scarce anatomical studies within the genus, Georgescu et al. [1] reported the leaf anatomy of *S. gigantissimum*, describing sparse, needle-shaped epidermal trichomes and secretory ducts located in the fundamental parenchyma. The present study provides the first detailed anatomical description of the leaf of *S. tomentosum*, contributing to the biological knowledge of Apiaceae, offering insights into species-specific structural adaptations to local ecological conditions, and facilitating accurate taxonomic identification. Plant material was harvested before flowering (May) from degraded, stony pasture habitats in the Municipality of Klis, Croatia. Leaf tissue samples were initially fixed in 2.5% glutaraldehyde for 2 h and further prepared for semithin and ultrathin sections as described by Vuko et al. [2]. Semithin sections were stained with Toluidine Blue and observed using a Leica DM 3000 LED light microscope. Ultrathin sections were examined using a JEM JEOL 1400 Flash transmission electron microscope. Microscopic analysis revealed that the leaves of *S. tomentosum* are glabrous. Their internal structure is characterized by the following sequence of tissues: the epidermis consists of a single layer of cells protected by a thick cuticle on the outer walls and containing retracted stomata; the spatial arrangement of collenchyma cells below the epidermis corresponds to that of the vascular bundles in the central part of the leaf; the photosynthetic mesophyll extends to the Kranz cells, which separate the mesophyll from the central region containing vascular bundles arranged in a semicircle. These anatomical features can be compared with those of *S. gigantissimum*, which exhibits a generally similar leaf anatomy but lacks Kranz cells in the central part of the leaf [1]. In addition, secretory ducts are located above the phloem, within the phloem, and beneath the xylem part of the vascular bundle. Secretory ducts in the phloem area have a smaller diameter than those outside the vascular bundles. The ducts are surrounded by secretory epidermal cells containing chloroplasts, gray oil droplets, and electron-dense droplets corresponding to the oil content. These droplets are also present in the phloem parenchyma as well as in the lumen of the duct. This study provides the first anatomical description of the leaf of the endemic *S. tomentosum*. The results contribute to a better understanding of this species and highlight the importance of anatomical studies of endemic plants for advancing biodiversity research.

References

1. M. Georgescu et al., Sci. Pap. Ser. B Hortic. 59 (2015) 347–349.
2. E. Vuko et al., Plant Direct 9 (2025) e70119.

Dark-Field Microscopy-Based Tracking of *Dictyostelium discoideum* Cells Lacking the Small GTPase Rac1 Isoforms

Cerovski Sara, Šimić Marija, Filić Vedrana, Weber Igor

Laboratory of Cell Dynamics, Division of Molecular Biology, Ruđer Bošković Institute, Bijenička cesta 54, 10000 Zagreb, Croatia

Corresponding author: igor.weber@irb.hr

Small monomeric guanosine triphosphatases (GTPases) of the Rho family are signaling proteins that play a central role in regulating cell motility by controlling the remodeling of the actin cytoskeleton. As molecular switches, Rho GTPases cycle between an active GTP-bound state and an inactive GDP-bound state. Activation is facilitated by guanine nucleotide exchange factors (GEFs), and inactivation by GTPase-activating proteins (GAPs). In their active state, Rho GTPases bind and activate effector proteins, including actin-binding proteins, actin polymerases, and their direct regulators. The best studied Rho family GTPases in animals belong to the Rac, Rho, and Cdc42 groups. While the model protist *Dictyostelium discoideum* lacks clear orthologs of Rho and Cdc42, it has three Rac1 isoforms - Rac1A, Rac1B, and Rac1C - which are more than 90% identical in amino acid sequence and share about 80% amino acid sequence identity with human Rac1. Similar to mammalian Rac1, they are involved in regulating actin-based processes such as cell motility, adhesion, phagocytosis, and chemotaxis [1]. Given their high sequence conservation, it is unclear which functions can be assigned to individual *Dictyostelium discoideum* Rac1 isoforms and in which they are redundant. No systematic and comprehensive analysis of mutants lacking different combinations of Rac1 isoforms has been published to date. We therefore generated a panel of mutants in which *rac1* genes were deleted individually, or in double and triple combinations. Using this panel of knockout mutants, our aim is to systematically distinguish redundant from isoform-specific functions by comprehensive phenotypic characterization of mutants. Since *Dictyostelium discoideum* cells are highly motile, quantitative characterization of their migration is one of the main methods used to screen mutant phenotypes. We therefore used a cell tracking assay based on dark-field microscopy to measure the random migration of vegetative cells [2]. Cells were placed in a 35 mm diameter glass-bottom dish filled with nutrient medium, and the cell density was adjusted so that 20–30 cells were present in the field of view. Cells were imaged using a custom dark-field setup assembled on a Zeiss Axiovert 10 inverted microscope equipped with a 5×/0.15 NA Plan-Neofluar objective and a long working distance condenser (LD 0.55 H, WD 22 mm) with an annular aperture (INAI = 0.34) [2]. In a single experiment, high-contrast images of cells were captured using a pco.panda 4.2 sCMOS camera every 10 seconds for 60 minutes (Figure 1). Cell trajectories were reconstructed using the ImageJ plugin TrackMate [3], and statistical analysis was performed using Microsoft Excel. Trajectories of individual cells were characterized by their average instantaneous velocity and persistence. Our results indicate that, among the three Rac1 isoforms, Rac1A has the greatest influence on the velocity of random migration of vegetative *Dictyostelium discoideum* cells.

References

1. V. Filić et al., Cells 10 (2021) 1592.
2. V. Antolović et al., J. Microbiol. Methods 104 (2014) 9–11.
3. R. Gorelik et al., Nat. Protoc. 9 (2014) 1931–1943.

Acknowledgements

This work was supported by the Croatian Science Foundation under project numbers HRZZ-IP-2024-05-6331 and DOK-2025-02-6267.

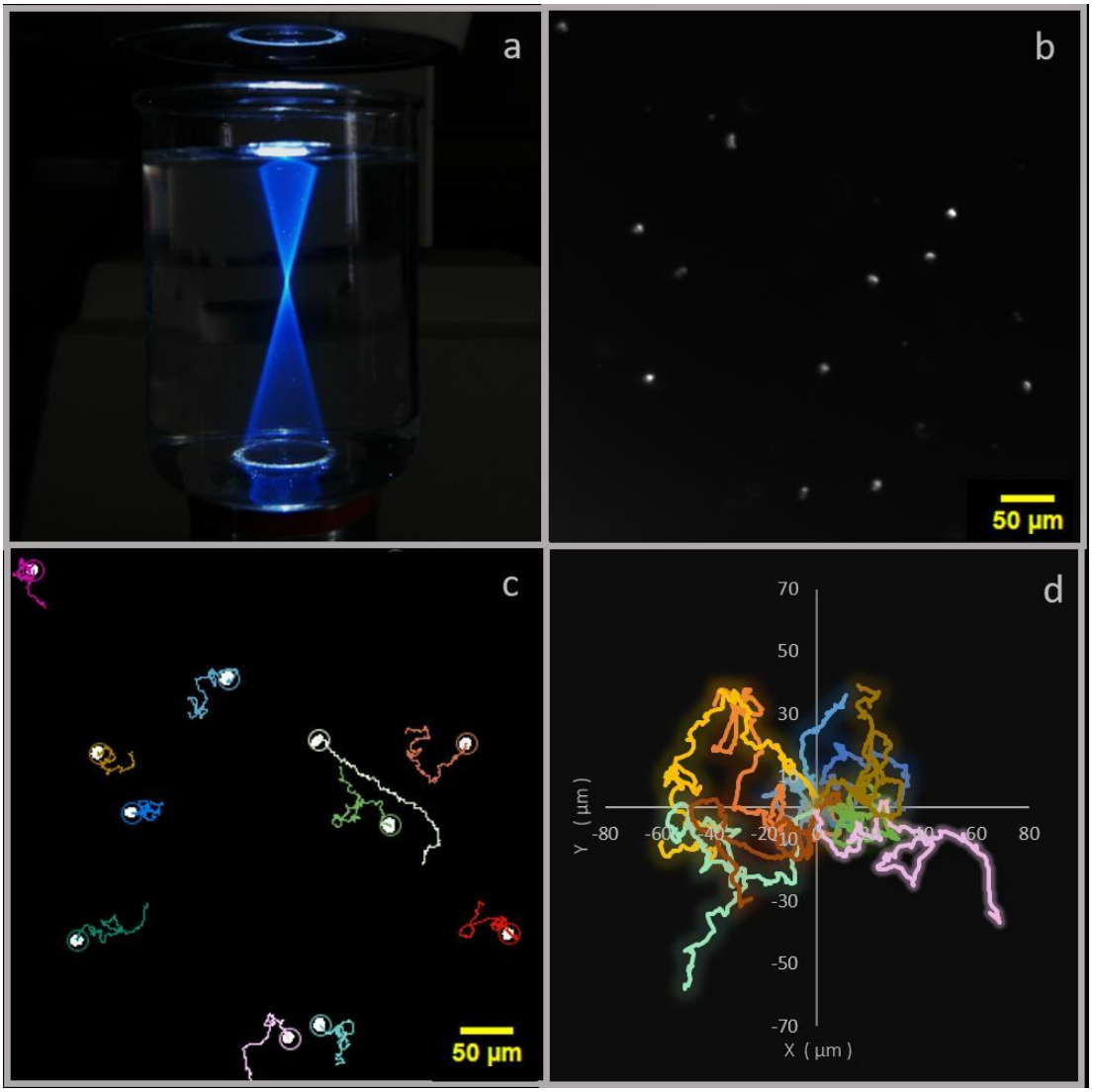

Figure 1. Experimental methodology. (a) Lateral view of the hollow cone of light emanating from the annular aperture of a phase-contrast condenser used for sample illumination in dark-field microscopy. The light beam between the condenser and the objective is visualized by the fluorescence of quinine from tonic water. In dark-field microscopy, direct light does not enter the front objective lens, and the image is formed by light scattered from the sample. (b) Image of vegetative *Dictyostelium discoideum* cells obtained by dark-field microscopy. (c) Trajectories of cells shown in panel (b) traced over an interval of 60 minutes using the ImageJ plugin TrackMate. The image was binarized to separate the cells, as bright light-scattering objects, from the background. (d) Individual cell trajectories plotted from a common origin using Microsoft Excel.

Possible Alternative BPM2 Isoforms Influence the Subcellular Localization of Target Proteins

Jagić Mateja[a], Keresteš Gaj[a], Vitko Sandra[a], Štancl Paula[a], Stepinac Emma[a], Miškec Karlo[a], Frlin Marta[a], Karlić Rosa[a], Lorković Zdravko[b], Berger Frédéric[b], Vidaković-Cifrek Željka[a], Leljak-Levanić Dunja[a], Bauer Nataša[a]

[a]*Department of Biology, University of Zagreb Faculty of Science, Horvatovac 102a, 10000 Zagreb, Croatia*
[b]*Gregor Mendel Institute, Austrian Academy of Sciences, Vienna BioCenter, Dr. Bohr-Gasse 3, 1030 Vienna, Austria*

Corresponding author: mateja.jagic@biol.pmf.hr

MATH-BTB proteins play diverse developmental and stress-related roles in eukaryotes by acting as substrate-specific adaptors for CUL3-based E3 ubiquitin ligases, directing specific proteins for ubiquitin-dependent proteasomal degradation [1]. In this process, the N-terminal MATH domain binds the target protein, while the C-terminal BTB domain binds CUL3, leading to ubiquitination and subsequent degradation of the target protein. The MATH-BTB gene family is greatly expanded in some organisms, such as grasses (Poaceae), with genomes containing dozens of mainly intronless MATH-BTB genes [2]. Others, like *Arabidopsis thaliana*, contain only a few MATH-BTB genes. *A. thaliana* has six such genes (BPM1–6), all of which have introns that enable posttranscriptional mRNA processing. All BPM genes undergo alternative splicing and encode a total of 56 transcript variants, which may produce 38 different putative protein isoforms. BPM2 has the greatest alternative splicing diversity, with 16 transcript variants predicted to encode nine proteins. By whole CDS Sanger sequencing we confirmed the presence of three variants in different plant tissues and additionally identified new BPM2 splice variants associated with plant embryogenesis. Compared to the canonical BPM2 protein, all alternatively spliced BPM2 isoforms retain an intact MATH domain but have a truncated BTB domain. The subcellular localization of the canonical and three possible BPM2 protein isoforms, and their colocalization with BPM-interacting partners WRI1, HB6 and MYC2, were analysed in *Nicotiana benthamiana* epidermal cells. Colocalization analysis indicated that the canonical BPM2 protein colocalized with targets in the nucleus, while BPM2 isoforms with a truncated C-terminal BTB domain altered the intracellular distribution of target proteins. This effect is most pronounced with the transcription factor WRI1, a key regulator of seed development, whose nuclear localization was altered by some BPM2 isoforms (Figure 1). These results suggest that alternative splicing of BPM2 may generate protein isoforms with distinct subcellular functions, potentially reshaping the localization and activity of BPM targets and providing an additional regulatory layer for BPM-mediated protein turnover.

References

1. L. Chen et al., Plant Cell 25 (2013) 2253–2264.
2. M. Juranić and T. Dresselhaus, Plant Signal. Behav. 9 (2014) e28242.

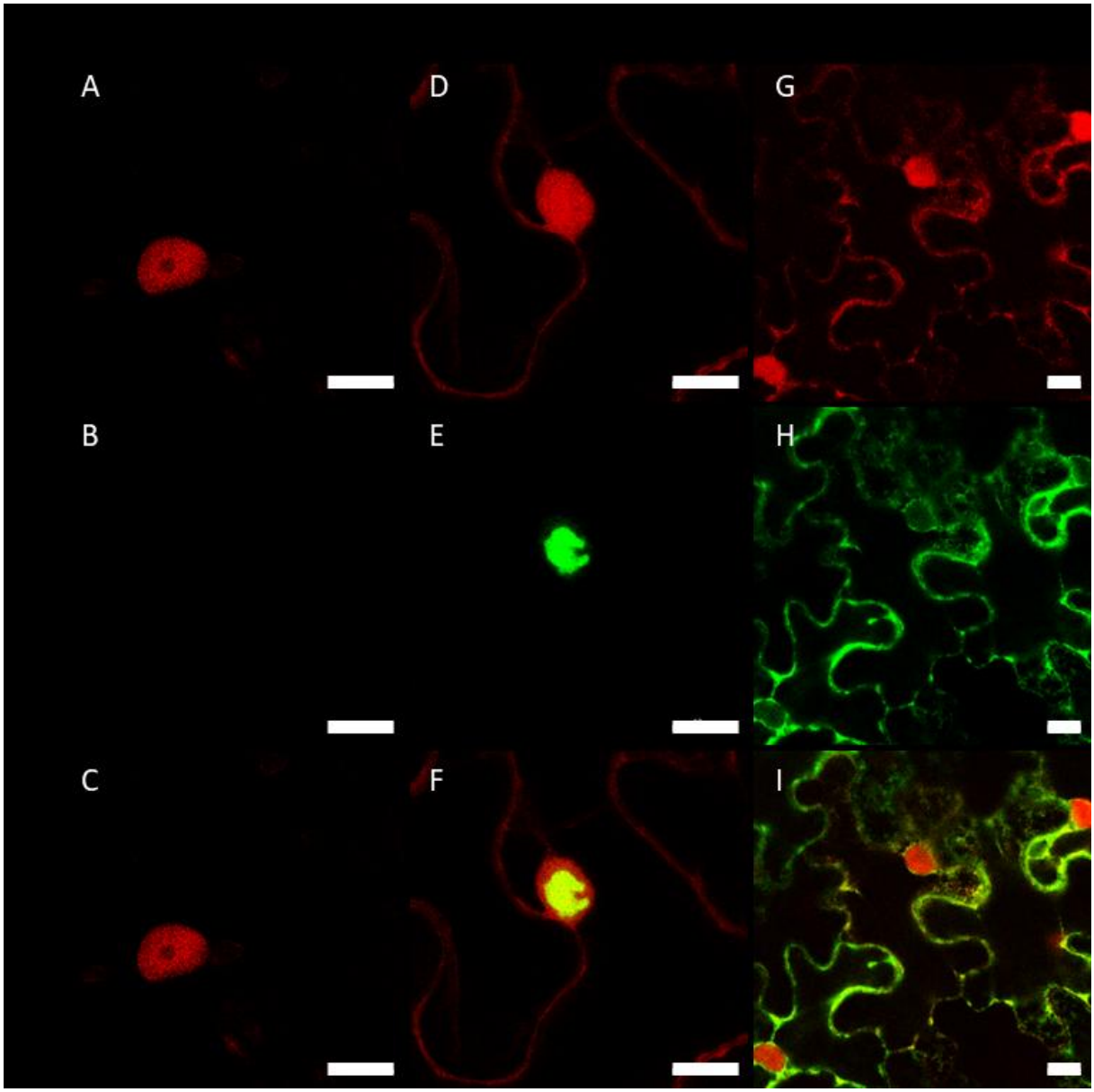

Figure 1. Subcellular colocalization of EGFP-tagged BPM2 protein isoforms with mRFP1-WRI1 in *Nicotiana benthamiana* epidermal leaf cells. WRI1 alone localized exclusively in the nucleus (A–C). The canonical BPM2.12 isoform and WRI1 colocalized in the nucleus (D–F), while the alternative BPM2.10 isoform retained WRI1 in the cytoplasm (G–I). Scale bar: 10 µm.

Towards Ultra-rapid TEM Sample Processing

Knapp Magdalena, Hobmayer Elio, Reberz Lena, Ladurner Peter, Seybold Anna
University of Innsbruck, Department of Zoology, Electron Microscopy, Technikerstraße 25, 6020 Innsbruck, Austria
Corresponding author: Magdalena.knapp@uibk.ac.at

Usually, several hours are needed for a chemical fixation process and additional days are needed to have a fully embedded sample ready to be cut into ultrathin slices to later be imaged with a transmission electron microscope. Although several scientists have tried to speed up these processes using various methods and devices in the past decades, today these long procedures are still the most widespread. Sample processing involves the fixation, dehydration, infiltration and polymerization with the goal for the samples to be as close as possible to their natural state. Why is it still common that each of these processes takes so long although there are faster methods that yield similar or even better results? The chemical reactions that occur while fixing the sample are usually extremely fast, so a faster diffusion of the fixing agents through the tissue would shorten the fixation process. Also, there are the beliefs that more viscous solutions like resin require a longer duration to diffuse through the sample and that an oven temperature higher than 60°C damages the sample and/or the resin. Here we show, using flatworms as a model system, that all major processing steps – fixation, dehydration, infiltration and polymerisation – can be substantially shortened while still yielding samples suitable for transmission electron microscopy.

Incidental Bile Duct Hamartoma (Von Meyenburg Complex) Identified During Forensic Autopsy

Mujkić Robert[a], Ugljarević Mladen[b], Čekić Nenad[c,d], Šnajder Mujkić Darija[d], Rožac Karla[a], Ilić Ivana[a]

[a]*Department of Anatomy, Histology, Embryology, Pathological Anatomy and Pathological Histology, Faculty of Dental Medicine and Health, Josip Juraj Strossmayer University of Osijek, Osijek, Croatia*

[b]*Department of Pathology and Cytology, National Memorial Hospital Vukovar, 32000 Vukovar, Croatia*

[c]*Department of Surgery, National Memorial Hospital Vukovar, 32000 Vukovar, Croatia*

[d]*Department of Anatomy and Neuroscience, Faculty of Medicine, Josip Juraj Strossmayer University of Osijek, Osijek, Croatia*

Corresponding author: rmujkic@fdmz.hr

Introduction: Bile duct hamartoma, also known as the von Meyenburg complex, represents a benign ductal plate malformation of intrahepatic bile ducts. These lesions may be associated with fibropolycystic diseases involving liver, kidneys, and other organs [1,2]. Macroscopically, bile duct hamartomas are typically small lesions, usually measuring up to 0.5 cm in diameter, with a gray-white appearance and irregular contours. Multifocal distribution is common. Histologically, they are characterized by numerous small to medium-sized bile ductules embedded within dense fibrous stroma. The ductules are often variably dilated compared with normal intrahepatic bile ducts and are predominantly located within or at the periphery of portal tracts. They are lined by cuboidal to flattened epithelial cells possessing round to oval nuclei without significant cytologic atypia. The lesions may contain irregularly shaped cystic spaces filled with eosinophilic material or inspissated bile. Case report: A 51-year-old male was found dead at the bus terminal in Vukovar. Following an order issued by the County State Attorney's Office, and after completion of the scene investigation and external postmortem examination, during which the exact cause of death could not be determined with certainty, the body was transferred to the Department of Pathology at National Memorial Hospital Vukovar for autopsy examination. Autopsy findings: The autopsy established sudden cardiac death due to occlusive coronary artery disease as the cause of death. Incidental findings included simple bilateral renal cysts, as well as a microscopic hepatic hamartoma (benign developmental tumor), together representing an entity known as the von Meyenburg complex. Conclusion: Von Meyenburg complex is a rare benign malformation of the intrahepatic bile ducts, most commonly detected incidentally during histopathological examination or autopsy. Although clinically insignificant in most cases and no specific treatment is required, recognition of its characteristic morphological features is important to avoid misinterpretation as metastatic or other cystic hepatic lesions.

References

1. D. Qirinxhi et al., J. Radiol. Clin. Imaging 8 (2025) 68–71.
2. N. Sadiya et al., Arch. Med. Health Sci. 4 (2016) 261–263.

Combined Effects of Nanoplastic Exposure and Salinity Stress on Marine Microalgal Physiology and Cell Surface Properties

Novosel Vlašić Nives[a], Vukosav Petra[a], Mišić Radić Tea[a], Komazec Bruno[b], Peharec Štefanić Petra[b]

[a]*Ruđer Bošković Institute, Bijenička cesta 54, 10 000 Zagreb, Croatia*

[b]*University of Zagreb Faculty of Science, Department of Biology, Division of Molecular Biology, Horvatovac 102a, 10000 Zagreb, Croatia*

Corresponding author: nnovosel@irb.hr

Climate change and increasing anthropogenic pressures are profoundly altering aquatic environments. Among these pressures, declining ocean salinity combined with the growing prevalence of nanoplastics as emerging pollutants poses significant threats to the structure and functioning of marine ecosystems. Marine microalgae inhabit the surface, well-illuminated layer of the water column, making them particularly vulnerable to these stressors, which can alter both the composition and abundance of microalgal communities and induce physiological and cellular-level responses. This study aimed to investigate the interactive effects of nanoplastic exposure and reduced salinity on physiological responses and cell surface characteristics of the marine model microalga *Dunaliella tertiolecta*. Responses were evaluated through analyses of growth dynamics, photosynthetic efficiency, and nanostructural and nanomechanical cell surface properties. Short-term exposure (4 days) to nanoplastics resulted in stronger growth inhibition at 30 ppt compared to 40 ppt, with lower EC_{50} values observed at lower salinity levels. Photosynthetic performance also decreased at both examined salinities with increasing nanoplastic concentrations. Atomic force microscopy revealed nanoparticle adhesion to algal cell surfaces under both conditions, with ongoing analyses examining the combined influence of salinity and nanoplastics on cell stiffness and adhesion properties. By investigating the interaction between nanoplastic exposure and salinity changes, this study contributes to a better understanding of how multiple environmental stressors influence marine microalgal physiology and surface properties. Understanding these responses is crucial for predicting the broader ecological implications of nanoplastic pollution under future climate change scenarios.

Acknowledgements

This work is supported by the Croatian Science Foundation Project “Nanoplastics and microalgae: Unraveling nanostructural, nanomechanical and physiological responses (AlgaNanoPlast)” (IP-2025-02-7932).

Variation in Petal Epidermal Cell Morphology in *Primula elatior* Cultivars with Different Flower Colours

Prebeg Tatjana, Seuček Paula, Dujmović Mia, Kušen Mihael, Kremer Dario and Šic Žlabur Jana
University of Zagreb, Faculty of Agriculture, Svetošimunska cesta 25, 10000 Zagreb, Croatia
Corresponding author: tprebeg@agr.hr

Flower colour is among the main factors shaping the decorative value and consumer appeal of ornamental plants. While this trait is primarily determined by pigment composition, the perceived colour is also influenced by the anatomical structure of petals, particularly the morphology of epidermal cells [1,2]. In this study, we investigated petal epidermal cell morphology in selected cultivars of *Primula elatior* Hill (Primulaceae) with different flower colours. Petal colour parameters were quantified using CIELAB colour space coordinates, and pigment contents were determined spectrophotometrically and by HPLC. To assess epidermal cell characteristics, cross-sections and epidermal peels from fresh petal tissue were examined by light microscopy. Pigment analyses revealed that yellow and orange flowers were primarily coloured by carotenoids, pink and blue flowers by anthocyanins, while red flowers contained both classes of pigments. Anatomical examination of petal tissue showed that both adaxial and abaxial epidermal cells were conical, while the mesophyll tissue was loosely structured with abundant intercellular spaces. The morphological characteristics of epidermal cells varied between flowers of different colours, showing differences in cell length and width, angle between outer walls, and cell tip radius. The morphology of epidermal cells also differed between the adaxial and abaxial sides of the petals, with abaxial epidermal cells generally having less steep side walls and wider tips compared with adaxial epidermal cells. The results of this study demonstrated significant variation in the morphology of petal epidermal cells among *Primula elatior* cultivars with different flower colours. As the morphological characteristics of epidermal cells influence their optical properties, integrating anatomical analysis may provide a more comprehensive understanding of the mechanisms underlying colour formation and the factors affecting the colour attributes of flower petals.

References

1. K.I. Noda et al., Nature 369 (1994) 661–664.
2. H.M. Whitney et al., Ann. Bot. 108 (2011) 609–616.

Potential of Dutch Elm Disease Fungus *Ophiostoma novo-ulmi* for Biosynthesis of Selenium Nanoparticles

Rušec Vedran[a], Katanić Zorana[a], Gvozdić Vlatka[b], Kovač-Andrić Elvira[b], Krstin Ljiljana[a], Suknović Dragica[c], Erceg Ina[d], Štolfa Čamagajevac Ivna[a]

[a]*Department of Biology, Josip Juraj Strossmayer University of Osijek, Ulica Cara Hadrijana 8/A, 31000 Osijek, Croatia*

[b]*Department of Chemistry, Josip Juraj Strossmayer University of Osijek, Ulica Cara Hadrijana 8/A, 31000 Osijek, Croatia*

[c]*University Hospital Centre Osijek, Clinical Institute of Nuclear Medicine and Radiation Protection, Josipa Huttlera 4, 31000 Osijek, Croatia*

[d]*Division of Physical Chemistry, Ruđer Bošković Institute, Bijenička 54, 10000 Zagreb, Croatia*

Corresponding author: zkatanic@biologija.unios.hr

Selenium is an essential trace element that plays a critical role in numerous biological processes and is indispensable for maintaining human health. In the form of selenium nanoparticles (SeNPs), it exhibits high biological activity but lower toxicity than other inorganic selenium compounds, making it potentially useful in a variety of biomedical, agricultural, and environmental applications. SeNPs can be synthesised using various methods, including physical, chemical, and biological approaches. Physical and chemical methods often require expensive equipment or hazardous chemicals, whereas biological synthesis is more environmentally friendly and cost-effective. Moreover, biological synthesis enables the production of nanoparticles with improved biocompatibility. Consequently, green chemistry approaches using biological materials have been extensively investigated for the production of numerous nanoparticles, including SeNPs. As biomolecules participate in synthesis as well as in stabilisation and capping, the resulting biosynthesised nanoparticles possess diverse and unique biological properties [1]. Within this approach, filamentous fungi are considered to have high potential, although not all species are equally effective [2]. The aim of this study was to evaluate the potential of using *Ophiostoma novo-ulmi*, an extremely virulent phytopathogenic fungus responsible for the Dutch elm disease (DED) pandemic [3], in fungal-mediated synthesis of SeNPs. An aqueous fungal extract was prepared from the mycelium of cultures grown under optimal conditions and mixed with sodium selenite in the presence of ascorbic acid to facilitate the reduction of selenite ions. After incubation for 24 h, the reaction mixture developed a characteristic red colour. The synthesised SeNPs were characterised using ultraviolet–visible (UV–Vis) spectroscopy, Fourier-transform infrared (FT-IR) spectroscopy, powder X-ray diffraction (PXRD), dynamic light scattering (DLS), electrophoretic light scattering (ELS), and transmission electron microscopy (TEM). The results confirmed the formation of predominantly spherical, amorphous SeNPs, with fungal biomolecules participating in their reduction and stabilisation (Figure 1). Overall, this study demonstrated the potential of *O. novo-ulmi* in the mycosynthesis of SeNPs. However, future research is needed to optimise the synthesis conditions and evaluate the biological activities of SeNPs synthesised using *O. novo-ulmi*.

References

1. E.O. Mikhailova, Molecules 28 (2023) 8125.
2. H.G. Hussein et al., AMB Express 12 (2022) 68.
3. A.M. Comeau et al., Genome Biol. Evol. 7 (2015) 410–430.

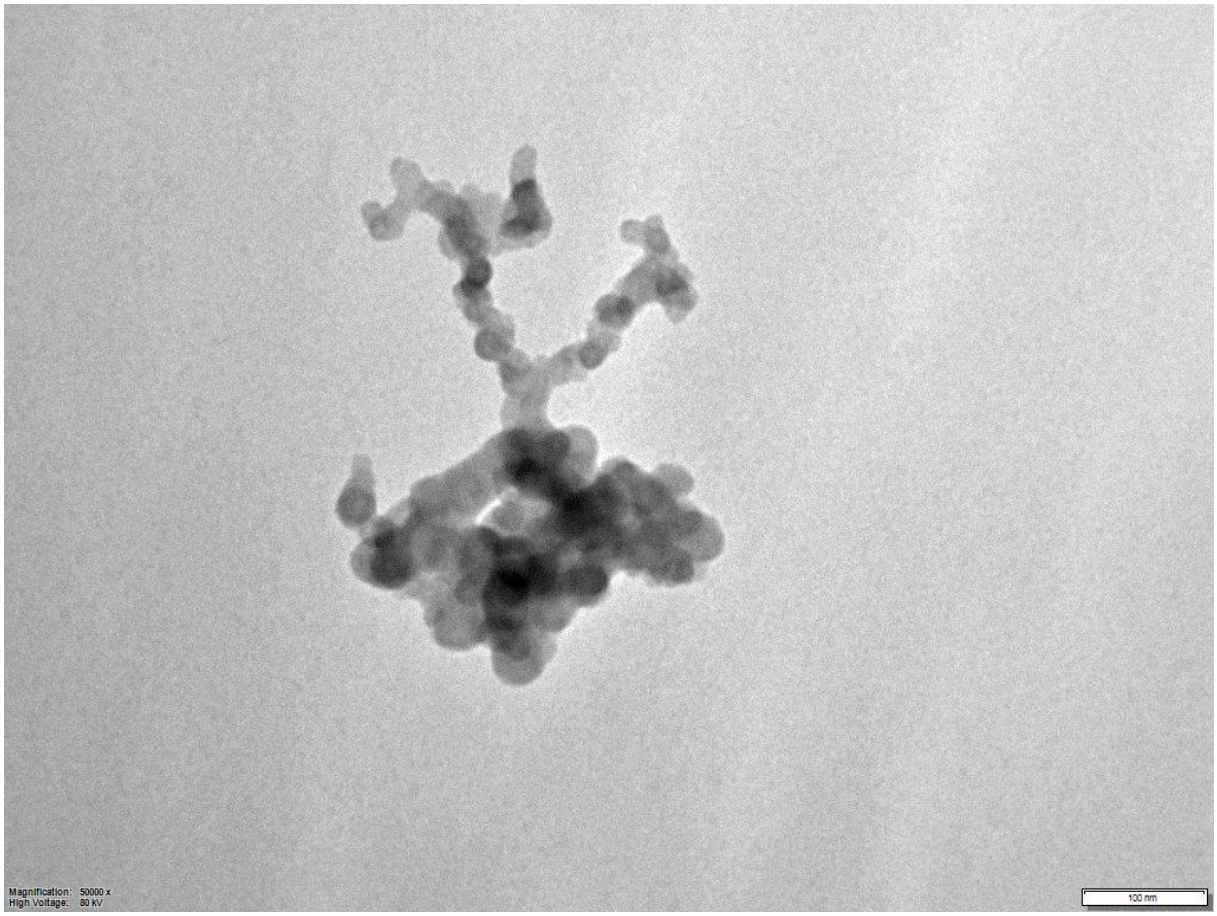

Figure 1. TEM image of the selenium nanoparticles (SeNPs) synthesized using phytopathogenic fungus *Ophiostoma novo-ulmi*.

From Ultrastructure to Volume EM: 3D Electron Microscopy Approaches in Invertebrate Systems

Knapp Magdalena[a], Reberz Lena[a], Rothbächer Ute[a], Hausen Harald[b], Seybold Anna[a]

[a]*Institute of Zoology and Center for Molecular Biosciences (CMBI), University of Innsbruck, Innsbruck, Austria*
[b]*Michael Sars Centre, University of Bergen, Bergen, Norway*

Corresponding author: anna.seybold@uibk.ac.at

Three-dimensional (3D) electron microscopy (EM) is changing our ability to understand complex biological organization at ultrastructural resolution. Here, we establish and apply a 3D EM workflow, including array tomography and serial block-face scanning electron microscopy (SBF-SEM) using a novel insertable system with high-resolution computational reconstruction. This integrative approach enables the visualization and analysis of cellular and tissue architecture across diverse biological systems. In invertebrates, it allows reconstruction of neural networks [1,2] and specialized tissues, providing insight into the organization, development, and functional adaptation of complex biological systems, including those with exceptional resilience. Overall, this work highlights the potential of 3D EM as a unifying platform to bridge scales from cells to tissues, enabling comparative and quantitative analysis of structure–function relationships across different biological systems.

References

1. A. Seybold et al., Front. Neurosci. 18 (2025) 1439897.
2. S. Kumar et al., bioRxiv (2026) 2026.02.04.703583.

Hepatic Collagen Deposition, Oxidative Status, and Lipid Metabolism Following Alendronate and Standardized Hop Extract Treatment in Ovariectomized Rats

Srb Nika[a], Rođak Edi[a], Grgac Robert[b], Debeljak Željko[a,b], Ilić Ivana[a,c], Oršolić Nada[d], Bijelić Nikola[a]

[a]*Department of Histology and Embryology, Faculty of Medicine Osijek, University of Osijek, J. Huttlera 4, 31000 Osijek, Croatia*

[b]*Department of Clinical Laboratory Diagnostics, University Hospital Centre Osijek, J. Huttlera 4, 31000 Osijek, Croatia*

[c]*Department of Anatomy, Histology, Embryology, Pathological Anatomy and Pathological Histology, Faculty of Dental Medicine and Health, University of Osijek, Crkvena 21, 31000 Osijek, Croatia*

[d]*Department of Animal Physiology, Faculty of Science Zagreb, University of Zagreb, Rooseveltov trg 6, 10000 Zagreb, Croatia*

Corresponding author: nsrb@mefos.hr

Estrogen deficiency is associated with metabolic disturbances extending beyond bone tissue and has been implicated in alterations of hepatic redox balance and lipid metabolism, which may precede structural tissue remodelling. This study evaluated the effects of alendronate, a standardized hop extract, and their combination on hepatic collagen deposition, oxidative status, and lipid metabolism in an ovariectomized rat model. Female rats underwent ovariectomy or sham surgery and received low- or high-dose alendronate, standardized hop extract, or their combination for two weeks. Hepatic collagen deposition was quantified by Picrosirius Red staining followed by morphometric image analysis (Figure 1). Biochemical analyses included hepatic catalase activity, malondialdehyde (MDA), protein carbonyls, total cholesterol, and triglycerides. Ovariectomy significantly reduced hepatic catalase activity compared with sham-operated animals. Alendronate significantly affected catalase activity, with a significant interaction between alendronate and hop extract, whereas hop extract alone had no significant effect. Increased catalase activity was observed following high-dose alendronate treatment and following combined treatment with low-dose alendronate and hop extract compared with untreated ovariectomized animals. Hepatic lipid peroxidation assessed by MDA and oxidative protein damage assessed by protein carbonyl content did not differ between groups. Likewise, hepatic collagen deposition and total cholesterol concentrations remained unchanged. In contrast, hepatic triglyceride concentrations were significantly affected by alendronate treatment, and this effect was modified by co-administration of hop extract. These findings indicate that estrogen deficiency selectively alters hepatic antioxidant defense, while alendronate modulates catalase activity and triglyceride homeostasis without evidence of increased oxidative damage or collagen accumulation during the experimental period. This work represents one component of a broader research project investigating the systemic effects of alendronate, standardized hop extract, and their combination in an ovariectomized rat model [1,2].

References

1. E. Rođak et al., Med. Sci. 14 (2026) 239.
2. E. Rođak et al., Nutrients 18 (2026) 1685.

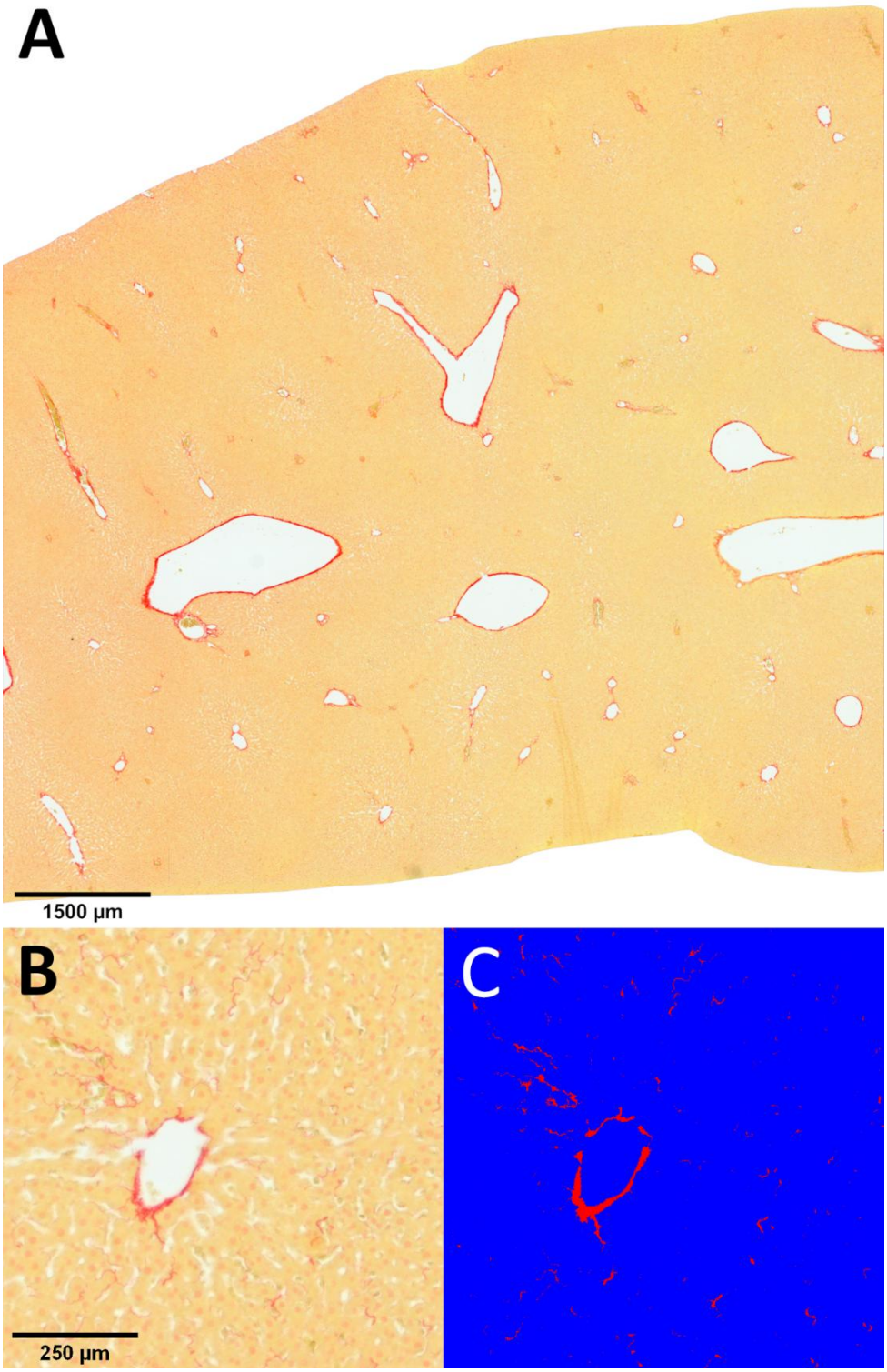

Figure 1. Analysis of collagen content in liver sections stained with picrosirius red. (A) Stitched image consisting of 10 x 10 grid imaged using 20× objective. (B) Magnified detail showing collagen fibers surrounding hepatocytes and central vein. (C) Image mask (derived from B) obtained using GIMP software showing segmented collagen fibers in red and total tissue area in blue. Scale bars: (A) 1500 µm and (B) 250 µm.

Microplastics Modulate the Toxicity of CTAB-Coated Silver Nanoparticles in *Chlorella vulgaris*: Evidence from Oxidative Stress and Ultrastructural Changes

Vuković Dona, Komazec Bruno, Peharec Štefanić Petra

University of Zagreb Faculty of Science, Department of Biology, Division of Molecular Biology, Horvatovac 102a, 10000 Zagreb, Croatia

Corresponding author: dona.vukovic@biol.pmf.unizg.hr

Silver nanoparticles (AgNPs) and microplastics (MPs) are emerging environmental pollutants that share similar pathways and can therefore encounter one another in aquatic environments, where their interactions may affect particle toxicity to aquatic organisms [1,2]. This study investigated whether polystyrene (MP-PS) and polymethyl methacrylate (MP-PMMA) microplastics influence the toxicity of cetyltrimethylammonium bromide-coated silver nanoparticles (AgNP-CTAB) in the freshwater green alga *Chlorella vulgaris*. Algal cultures were exposed for 72 h to 0.9 mg L^{-1} AgNP-CTAB and 50 mg L^{-1} and 150 mg L^{-1} MP-PS or MP-PMMA, applied individually and in combination. Cell viability was determined by propidium iodide staining and flow cytometry, reactive oxygen species (ROS) were quantified using the H_2DCFDA and DHE fluorescent probes, lipid peroxidation was assessed by malondialdehyde (MDA) content, and transmission electron microscopy (TEM) was used to examine ultrastructural changes in the algal cells. Exposure to AgNP-CTAB alone caused the highest increase in ROS and superoxide anion production and lipid peroxidation, accompanied by the strongest reduction in cell viability (30%). Co-exposure of AgNP-CTAB with both concentrations of MP-PS and MP-PMMA significantly improved cell viability compared with AgNP-CTAB alone, with the strongest protective effect observed for MP-PS. Individual treatments with MPs did not significantly affect cell viability. ROS and superoxide anion levels and MDA content were significantly decreased after all combined treatments, as well as in all individual MP treatments compared with AgNP-CTAB alone. In addition to AgNP-CTAB alone, exposure to 50 mg L^{-1} MP-PMMA also increased ROS levels compared with the control, whereas all combined treatments showed higher DHE probe intensity. Furthermore, the combined treatment of AgNP-CTAB and 50 mg L^{-1} MP-PMMA resulted in elevated MDA content. TEM analysis revealed that AgNP-CTAB alone caused plasmolysis. Exposure to 50 mg L^{-1} MP-PS and MP-PMMA alone did not significantly affect the ultrastructure of the alga compared with the control whereas after exposure to 150 mg L^{-1} MP-PS and MP-PMMA alone, the cell wall was deformed and the algal cells were in plasmolysis. All combined treatments of AgNP-CTAB and MPs caused plasmolysis of algal cells and deformation of the cell wall (Figure 1). Overall, the results demonstrate that MPs can mitigate AgNP-CTAB-induced oxidative stress and cytotoxicity in *Chlorella vulgaris*, although ultrastructural damage remains evident. These findings highlight that interactions between these particles can substantially modify the biological effects of AgNPs.

References

1. P. Li et al., Sci. Total Environ. 805 (2022) 150315.
2. P. Li et al., J. Hazard. Mater. 385 (2020) 121601.

Acknowledgements

This work was supported by the Croatian Science Foundation projects MINION (IP-2022-10-3824) and DOK-2025-02.

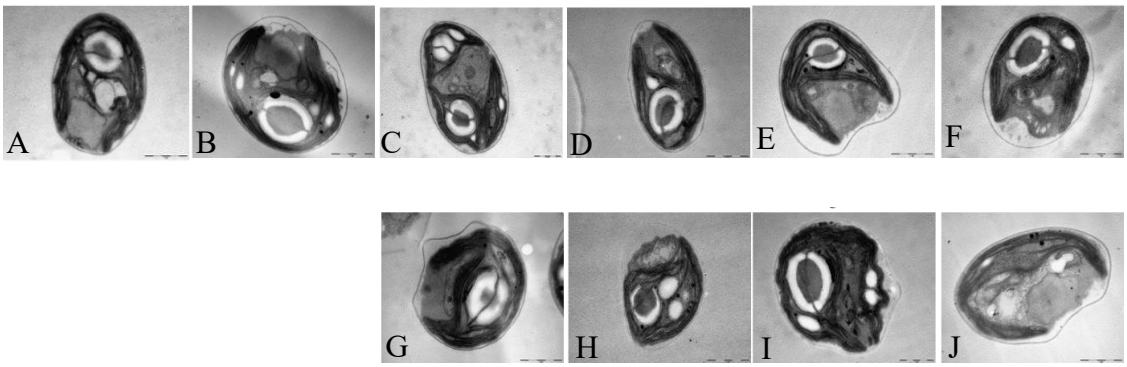

Figure 1. TEM micrographs of *Chlorella vulgaris* control cells (A) and cells after 72 h exposure to 0.9 mg L^{-1} AgNP-CTAB (B), 50 mg L^{-1} MP-PS (C), 50 mg L^{-1} MP-PMMA (D), 0.9 mg L^{-1} AgNP-CTAB and 50 mg L^{-1} MP-PS (E), 0.9 mg L^{-1} AgNP-CTAB and 50 mg L^{-1} MP-PMMA (F), 150 mg L^{-1} MP-PS (G), 150 mg L^{-1} MP-PMMA (H), 0.9 mg L^{-1} AgNP-CTAB and 150 mg L^{-1} MP-PS (I), 0.9 mg L^{-1} AgNP-CTAB and 150 mg L^{-1} MP-PMMA (J). Scale bars = 1 μm

Microplastics Modulate Silver Nanoparticle-Induced Oxidative Stress in *Chlorella vulgaris*: TEM Insights into Particle-Cell Interactions

Komazec Bruno, Furlić Anamarija, Peharec Štefanić Petra

University of Zagreb Faculty of Science, Department of Biology, Division of Molecular Biology, Horvatovac 102a, 10000 Zagreb, Croatia

Corresponding author: bruno.komazec@biol.pmf.unizg.hr

Microplastics (MPs) and silver nanoparticles (AgNPs) commonly co-occur in aquatic ecosystems, where their interactions may alter particle bioavailability and toxicity to primary producers [1,2]. This study investigated whether polystyrene (MP-PS) and polymethyl methacrylate (MP-PMMA) microplastics modulate the toxic effects of polyvinylpyrrolidone-stabilized AgNPs (AgNP-PVP) in the freshwater green alga *Chlorella vulgaris*. Algal cultures were exposed for 72 h to 0.110 mg L^{-1} AgNP-PVP and 100 mg L^{-1} MP-PS or MP-PMMA, applied individually and in combination with AgNPs. Cell viability was assessed using propidium iodide staining, total reactive oxygen species (ROS) were determined using the H_2DCFDA fluorescent probe, lipid peroxidation was estimated as malondialdehyde (MDA) content, and transmission electron microscopy (TEM) was used to visualize particle morphology, heteroaggregation and interactions with algal cells. Among the tested treatments, AgNP-PVP exhibited the highest phytotoxicity, as reflected by the strongest reduction in cell viability (22% cell death) and a significant increase in total ROS levels. In contrast, individual MP-PS and MP-PMMA treatments did not reduce viability or induce lipid peroxidation. Moreover, all MP-containing treatments generally showed lower ROS levels than the control, with significant decreases observed after individual treatment with MP-PMMA and combined treatment with AgNP-PVP and MP-PS. MDA content increased significantly after AgNP-PVP exposure and after both combined treatments with MPs, indicating membrane lipid damage, whereas individual MP treatments remained comparable to the control. Co-exposure to AgNP-PVP with MP-PS or MP-PMMA reduced cell death to 15% and 16%, respectively, relative to AgNP-PVP alone, suggesting that MPs partly mitigated AgNP-PVP toxicity. TEM confirmed adsorption of AgNP-PVP and both types of MPs onto the cell wall (Figure 1). TEM also revealed the formation of AgNP-PVP–MP complexes and heteroaggregates in the growth medium, supporting the hypothesis that adsorption of AgNP-PVP onto MPs reduces nanoparticle and/or Ag^+ bioavailability. Overall, the results indicate that polymer type and particle interactions can substantially modulate AgNP toxicity in freshwater microalgae, suggesting that microplastic–nanoparticle interactions may alter the environmental risk of silver nanoparticles in freshwater ecosystems by reducing their bioavailability to primary producers.

References

1. P. Li et al., Sci. Total Environ. 805 (2022) 150315.
2. B. Huang et al., Environ. Sci. Technol. 53 (2019) 3871–3879.

Acknowledgements

This work was supported by the Croatian Science Foundation project MINION (HRZZ IP-2022-10-3824).

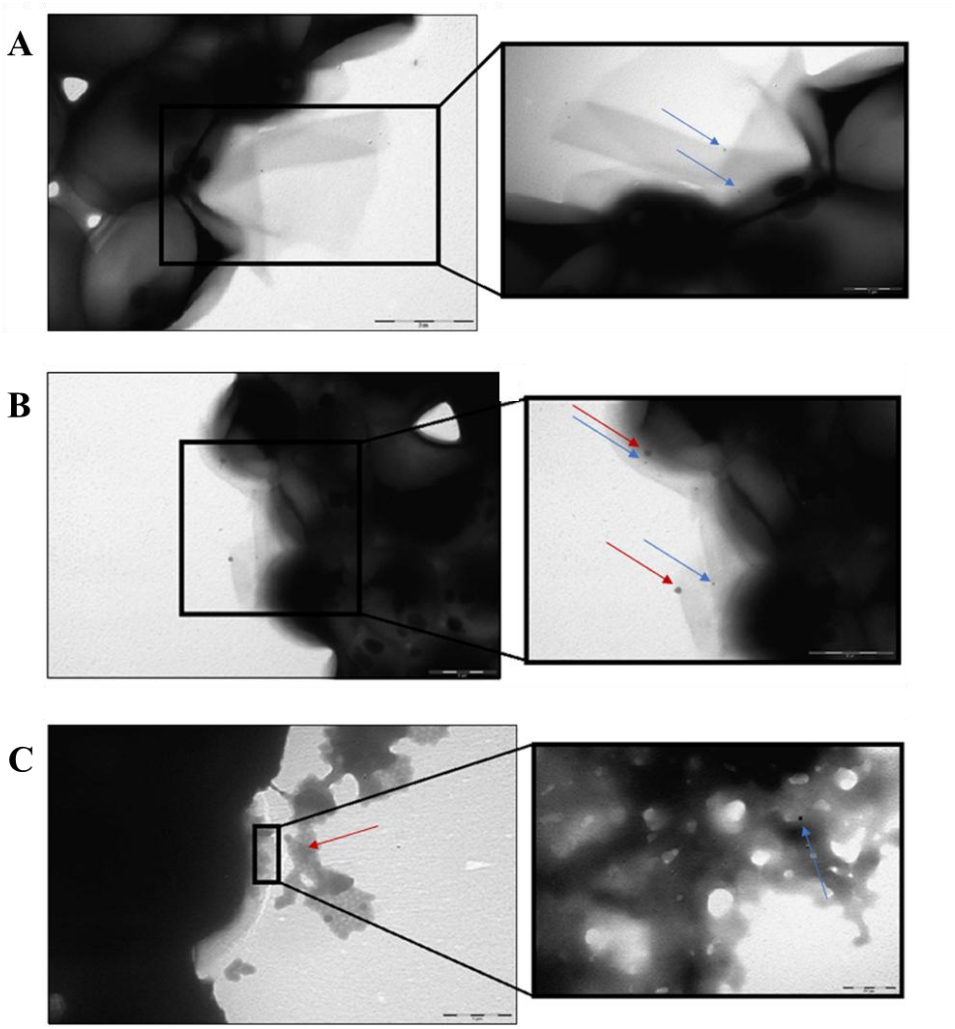

Figure 1. TEM micrographs of *Chlorella vulgaris* cells after 72 h exposure to (A) AgNP-PVP, (B) AgNP-PVP in combination with MP-PS, and (C) AgNP-PVP in combination with MP-PMMA. Enlarged areas show adsorption of particles on the algal cell surface and/or their mutual interaction. Blue arrows indicate AgNP-PVP, while red arrows indicate microplastic particles: MP-PS in panel B and MP-PMMA in panel C.

POSTER PRESENTATIONS

MATERIAL SCIENCE

Development of Hybrid TiO_2 Nanoplates-Based Antimicrobial Coatings for Stainless Steel Surfaces

Ivanišević Irena, Erceg Ina, Strasser Vida, Dutour Sikirić Maja

Ruđer Bošković Institute, Division of Physical Chemistry, Laboratory for Biocolloids and Surface Chemistry, Bijenička cesta 54, Zagreb, Croatia

Corresponding author: sikiric@irb.hr

High-touch surfaces made of stainless steel (SS) are widely used in public and clinical environments because they are durable, corrosion-resistant, and easy to clean [1]. Applying TiO_2-based photocatalytic coatings onto SS surfaces introduces self-disinfecting activity, as under the exposure of sunlight TiO_2 generates reactive oxygen species (ROS) that inhibit bacterial biofilm formation [2]. However, effective SS surface pretreatment is essential to improve the adhesion, uniformity, and long-term stability of functional TiO_2 coatings. In addition, careful adjustment of the colloidal chemistry is key requirement to control dispersibility and to prevent particle agglomeration [3]. In this work, TiO_2 nanoplates (TiNPls) (0.1 wt%) were used as a functional material for the preparation of a stable ethanol-based dispersion. To adjust the dispersion's chemistry and processability, Pluronic F-127 (PLU) (1 wt%) was used as a nanograin stabilizer, while poly(vinyl butyral) (PVB) resin (4 wt%) was added to promote the adhesion of the polymeric coating onto the metallic SS substrate. Prior to coating fabrication, the SS plates were acid-etched to enhance roughness. The stability and viscosity of the prepared colloidal dispersion were fine-tuned to enable smooth preparation of the PVB/PLU/TiNPls coatings by dip-coating, drop-casting, and airbrush techniques (Figure 1). In addition, the number of deposited layers was also optimized with three layers providing the best homogeneity of TiNPls per unit area. Detailed material characterization of the synthesized nanomaterial, and its colloidal dispersion, was conducted by diverse methods, highlighting the usage of scanning electron microscopy (SEM) as an indispensable tool for precise monitoring of each step of the fabrication process.

References

1. C. Duarte Bernardino et al., ACS Appl. Mater. Interfaces 17 (2025) 12507–12519.
2. V. Kumaravel et al., Chem. Eng. J. 416 (2021) 129071.
3. Lj. Spasojević et al., RSC Adv. 15 (2025) 21341–21368.

Acknowledgements

This research has been financed by the EU Horizon Europe Programme (STOP project, Grant Agreement 101057961).

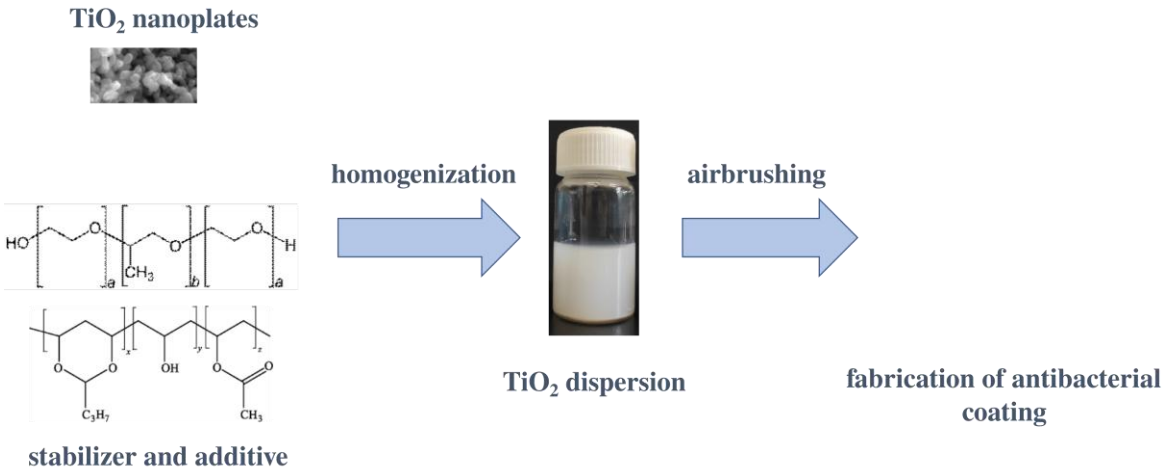

Figure 1. Schematic presentation of fabrication of antibacterial coating by airbrushing TiO_2-based colloidal dispersion.

From Silica to Apple Skin: AFM Insights into Roughness and Smoothing Effect of Polyelectrolyte Multilayer

Jerin Katarina, Klačić Tin, Kovačević Davor
University of Zagreb Faculty of Science, Department of Chemistry, Horvatovac 102A, 10000 Zagreb, Croatia
Corresponding author: kjerin@chem.pmf.hr

Preserving fresh produce and modifying their surfaces to prolong shelf life has gained significant interest due to climate-oriented policies. Biocompatible polyelectrolyte multilayers (PEM) have been shown to provide effective moisture and antimicrobial barriers while also improving the appearance of the produce [1]. While there is extensive research on the ability of PEMs to preserve food, as well as on their fundamental properties on metal, silica, and similar model substrates [2], much remains to be learned about their properties when applied directly to fruit skin. This study investigates the morphological properties of edible PEM coatings prepared via the layer-by-layer method directly onto both apple skin and a model substrate. The primary focus is placed on how the underlying surface topography influences the evolution of the film's final roughness. Using Atomic Force Microscopy (AFM), an evaluation of the thickness and surface roughness of chitosan and carboxymethylcellulose films at different pH was conducted (Figure 1). The main focus of this study is the comparison between PEM surface roughness on apple skin versus a flat silica substrate. Interestingly, the AFM data revealed opposite roughness trends between the two surfaces. On the flat silica surface, PEM deposition increases nanometer-scale roughness, with thicker films leading to higher roughness values. On the other hand, on the inherently rough and irregular apple cuticle, a thicker PEM film results in a smoother surface. Our findings [3] demonstrate that while thin PEM films cannot completely mask the large surface irregularities of the apple skin, thicker films progressively fill these micro-cavities, leading to a significant smoothing effect. This AFM study highlights that the final morphology of PEM coatings is heavily substrate-driven rather than being an intrinsic property of the polymer film itself. Understanding this substrate-dependent smoothing effect is crucial for optimizing the antimicrobial efficacy of edible protective films on agricultural products such as apples.

References

1. X. Liu et al., Colloids Surf. A 529 (2017) 1016–1023.
2. J. Nikolić et al., ACS Omega 8 (2023) 20031–20041.
3. K. Jerin et al., ACS Food Sci. Technol. 5 (2025) 1156–1165.

Acknowledgements

This research was supported by the Croatian Science Foundation under the bilateral Slovenian-Croatian APPLPEMs project (IPS-2020-01-6126) and by the European Union - NextGenerationEU through the National Recovery and Resilience Plan 2021-2026. Institutional grant of University of Zagreb Faculty of Science (PMF-CROFUND).

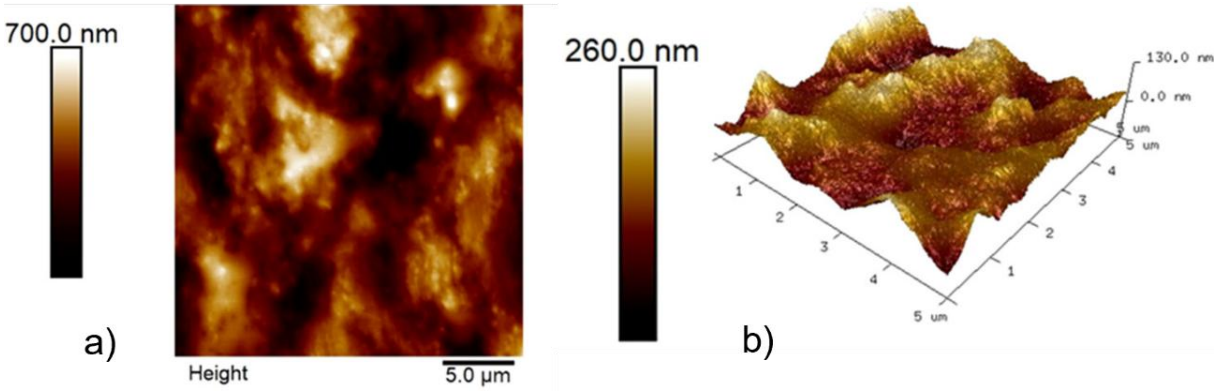

Figure 1. (a) 25 µm × 25 µm AFM image of apple skin; (b) corresponding 5 µm × 5 µm 3D image.

Morphology and Charge Transport of TiO_2 Electron Transport Bilayers Modified with Transition Metal Dichalcogenide Nanotubes

Klobučar Lucija[a,b], Kojić Vedran[a], Dolić Stjepan[a,b], Juraić Krunoslav[a], Zak Alla[c], Laikhtman Alexander[c], Gajović Andreja[a]

[a]*Ruđer Bošković Institute, Bijenička cesta 54, 10000 Zagreb, Croatia*
[b]*Department of Chemistry, Faculty of Science, University of Zagreb, Horvatovac 102a, 10000 Zagreb, Croatia*
[c]*Physics Department, Faculty of Sciences, Holon Institute of Technology, Ya'akov Fichman St 18, Holon, 5810201, Israel*

Corresponding author: Stjepan.Dolic@irb.hr

Titanium dioxide nanomaterials are commonly used as photoanodes in photoelectrochemical devices and solar cells due to their chemical stability, non-hazardous nature, low cost and ease of fabrication. The main obstacles for the application of TiO_2 photoanode nanomaterials are their wide band gap and low electron mobility, both of which limit solar radiation absorption and negatively affect charge separation. A popular strategy for enhancing charge transport and improving visible light absorption in TiO_2 materials is the preparation of composite or heterojunction structures. Various reports on TiO_2-based composites used as electrodes or photoelectrodes showcased improved charge collection compared to pure TiO_2 [1]. Transition metal dichalcogenides, such as MoS_2 or WS_2, exhibit a narrower band gap than TiO_2, as well as a favourable energy level alignment with TiO_2. Additionally, the electron mobilities of WS_2 and MoS_2 showed significantly higher values compared to TiO_2. The combination of these properties makes transition metal dichalcogenides particularly suitable for TiO_2-based composite and heterojunction applications in photoelectrochemical devices and solar cells, as they could enhance charge transfer and improve the photogenerated charge carrier separation of TiO_2 [2]. In this work, we have synthesised WS_2 and MoS_2 nanotubes using a high-temperature vapor-gas-solid one-pot reaction. We have prepared TiO_2 thin-film bilayers, comprised of a thin compact TiO_2 layer topped with a mesoporous TiO_2 layer, both deposited by spin coating. We have examined and compared the effects of infiltrating WS_2 and MoS_2 nanotubes in both the compact and the mesoporous TiO_2 layers by analysing the structural, optical, electrochemical and photoelectrical properties of the resulting composite layers. Scanning electron microscopy images of WS_2 and MoS_2 nanotubes incorporated in the compact TiO_2 layer reveal that the nanotubes are poorly distributed within the compact matrix, while the WS_2 nanotubes incorporated in the mesoporous TiO_2 layer appear uniformly dispersed and well-integrated (Figure 1). This is reflected in the XRD measurements of the thin films, as the reflections characteristic for WS_2 and MoS_2 are present only for samples with nanotubes incorporated in the mesoporous TiO_2 layer. Electrochemical characterisation reveals that embedding WS_2 or MoS_2 nanotubes in the compact layer strongly enhances anodic currents but suppresses the distinction between dark and illuminated responses, consistent with improved conductivity and efficient interfacial charge transfer. When WS_2 nanotubes are placed in the mesoporous overlayer, cyclic voltammetry and transients indicate a heterojunction that promotes interfacial charge separation and enhances photocurrent at positive bias [3]. These findings demonstrate a significant potential for the improvement of TiO_2 bilayer electron transport layers and, consequently, photoelectrochemical and solar cells.

References

1. P.S. Ramaripa et al., Int. J. Electrochem. Sci. 19 (2024) 100444.
2. S.S. Sinha et al., J. Phys. Chem. C 125 (2021) 6324–6340.
3. H.M. Hill et al., Nano Lett. 16 (2016) 4831–4837.

Acknowledgements

The presented results were obtained within the framework of cooperation between the Government of the Republic of Croatia and the Government of the State of Israel with co-financing from the Ministry of Science, Education and Youth Croatia and Ministry of Science and Technology of Israel through the project Novel perovskite solar cells with enhanced performance based on hybrid halide perovskite/transition-metal disulphides nanocomposites (Sol-HP-TMD-NanoComp) and the Croatian Science Foundation programme Young researchers' Career Development Project - Training New Doctoral Students (DOK-2025-02) and financially supported by the European Regional Development Fund for the project 'Materials for clean energy, advanced sensors and quantum technologies' (Grant No. PK.1.1.10.0002).

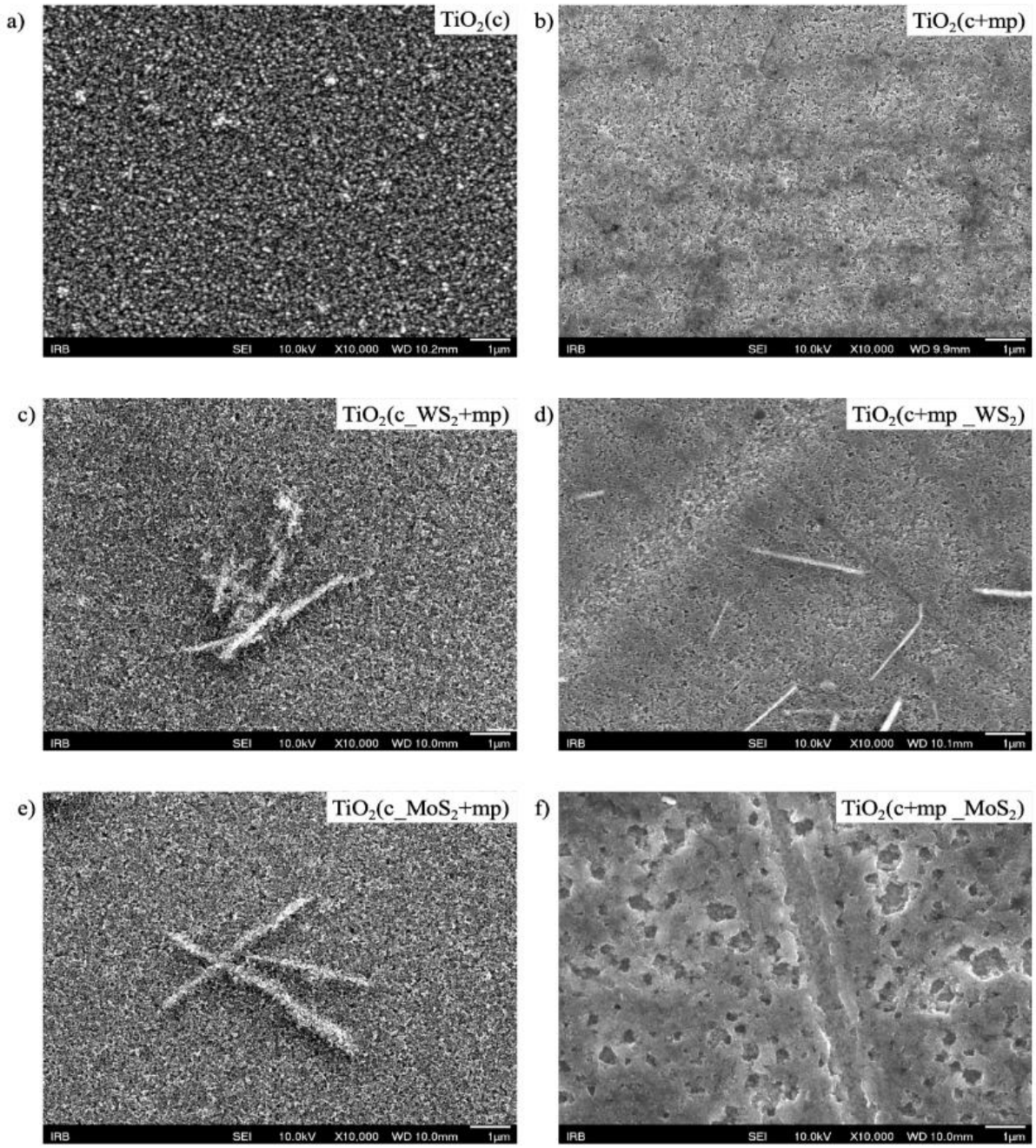

Figure 1. SEM images of pure TiO_2 thin films: (a) compact layer (TiO_2(c)) and (b) compact plus mesoporous layer (TiO_2(c+mp)); and TiO_2 films with WS_2 nanotubes incorporated into the compact (c) or mesoporous (f) layer; and TiO_2 films with MoS_2 nanotubes incorporated into the compact (d) or mesoporous (e) layer.

Correlating Microstructure and Magnetic Domain Evolution in NdFeB Micromagnets Using Lorentz TEM

Ražnjević Sergej, Sršan Vinko, Gračanin Nika, Šturm Sašo

Department for Nanostructured Materials, Jožef Stefan Institute, Jamova cesta 39, 1000 Ljubljana, Slovenia

Corresponding author: Sergej.Raznjevic@ijs.si

Understanding the relationship between microstructure and magnetic behaviour is essential for optimizing the performance of NdFeB permanent magnets, particularly at the microscale. In this work, magnetic domain configurations and magnetization processes in a focused ion beam (FIB)-prepared NdFeB micromagnet were investigated by transmission electron microscopy (TEM), with emphasis on Lorentz (Fresnel) imaging. A TEM lamella (10 µm × 10 µm × 100 nm) was prepared from bulk NdFeB with an average grain size of ~300 nm. Lorentz TEM was performed under low-field conditions to preserve the intrinsic magnetic state. Magnetic domains were visualized through Fresnel contrast generated by defocused imaging (Figure 1). Three domain morphologies were identified: lamellar, finger-like, and vortex/spaghetti domains. Lamellar domains, commonly associated with high coercivity and alignment along the crystallographic easy (c-) axis, were rare. Instead, finger-like and vortex domains dominated, indicating locally disturbed magnetic anisotropy, grain misorientation, and reduced coercivity. *In situ* magnetization experiments were carried out by applying magnetic fields with the objective lens, calibrated using a Hall probe. The field was varied from the virgin state to ±0.8 T. Increasing field strength progressively transformed the multidomain structure into nearly single-domain regions, while field reversal enabled direct observation of domain-wall motion and magnetization reversal. High-angle annular dark-field (HAADF) imaging confirmed the high crystallinity of the grains, and diffraction-based orientation mapping revealed local crystallographic misalignment. Chemical analysis identified Nd-rich, Fe-poor triple junctions and minor carbon inclusions, but these features showed no measurable influence on the observed magnetic domain structures. The combination of Lorentz TEM and *in situ* magnetic field application enables direct correlation of magnetic configurations with structural features at the nanoscale. The results indicate that magnetic behaviour in NdFeB micromagnets is governed primarily by specimen geometry and domain complexity rather than chemistry or crystallinity alone, providing valuable insight for the optimization of advanced permanent magnetic materials.

Acknowledgements

This work is supported by the Slovenian Research Agency (ARIS) under grant number P2-0084 and the European Union's Horizon Europe research and innovation program GREENE (grant agreement no. 101129888).

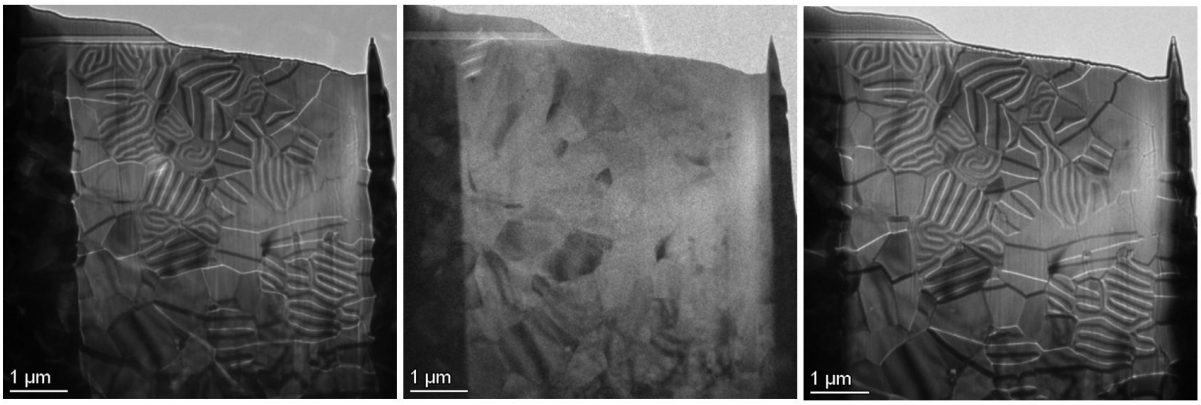

Figure 1. Principle of Fresnel (Lorentz) TEM imaging. No magnetic contrast is observed in focus (df = 0). Defocusing reveals domain walls through Lorentz beam deflection: over-focus (df > 0) produces dark contrast, whereas under-focus (df < 0) results in bright contrast.

SEM–EDS Characterization of Ottoman Gold Coins

Salčinović Fetić Amra, Hrvat Kerima
University of Sarajevo, Faculty of Science, Zmaja od Bosne 35, 71000 Sarajevo, Bosnia and Herzegovina
Corresponding author: amra.s@pmf.unsa.ba

Scanning Electron Microscopy coupled with Energy-Dispersive X-ray Spectroscopy (SEM–EDS) is a powerful tool for verifying the authenticity of coins through precise determination of their elemental composition. An important advantage of this technique is that it is non-destructive, allowing valuable numismatic specimens to be analyzed without causing damage [1]. Furthermore, the elemental composition of historical coins can provide valuable insights into the political and economic conditions prevailing at the time of their minting [2]. In this paper, we present the results of an investigation of Ottoman gold coins, commonly known as Mahmudian ducats, minted during the reign of Sultan Mahmud II. A total of five coins from a private collection were examined: three minted in 1829 and one each from 1830 and 1831. The analyses were carried out using a JEOL JSM IT 200A scanning electron microscope. No prior surface preparation or cleaning was performed before examination. Two SEM–EDS measurements were conducted on the reverse side of each coin (Figure 1). As expected, the results confirmed that the coins are primarily composed of gold, with smaller and varying proportions of silver and copper. These elements were found to be homogeneously distributed. In addition, the microhardness of the coins was measured using a DHV-1000Z microhardness tester equipped with a 128° diamond pyramid indenter. Five measurements were performed on the reverse side of each coin using a load of 0.0981 N and a dwell time of 10 s. The hardness results correlate well with the elemental composition of the coins.

References

1. M. Rodrigues et al., Appl. Phys. A 99 (2010) 351–356.
2. E. Taş et al., Mediterr. Archaeol. Archaeom. 22 (2022) 35–50.

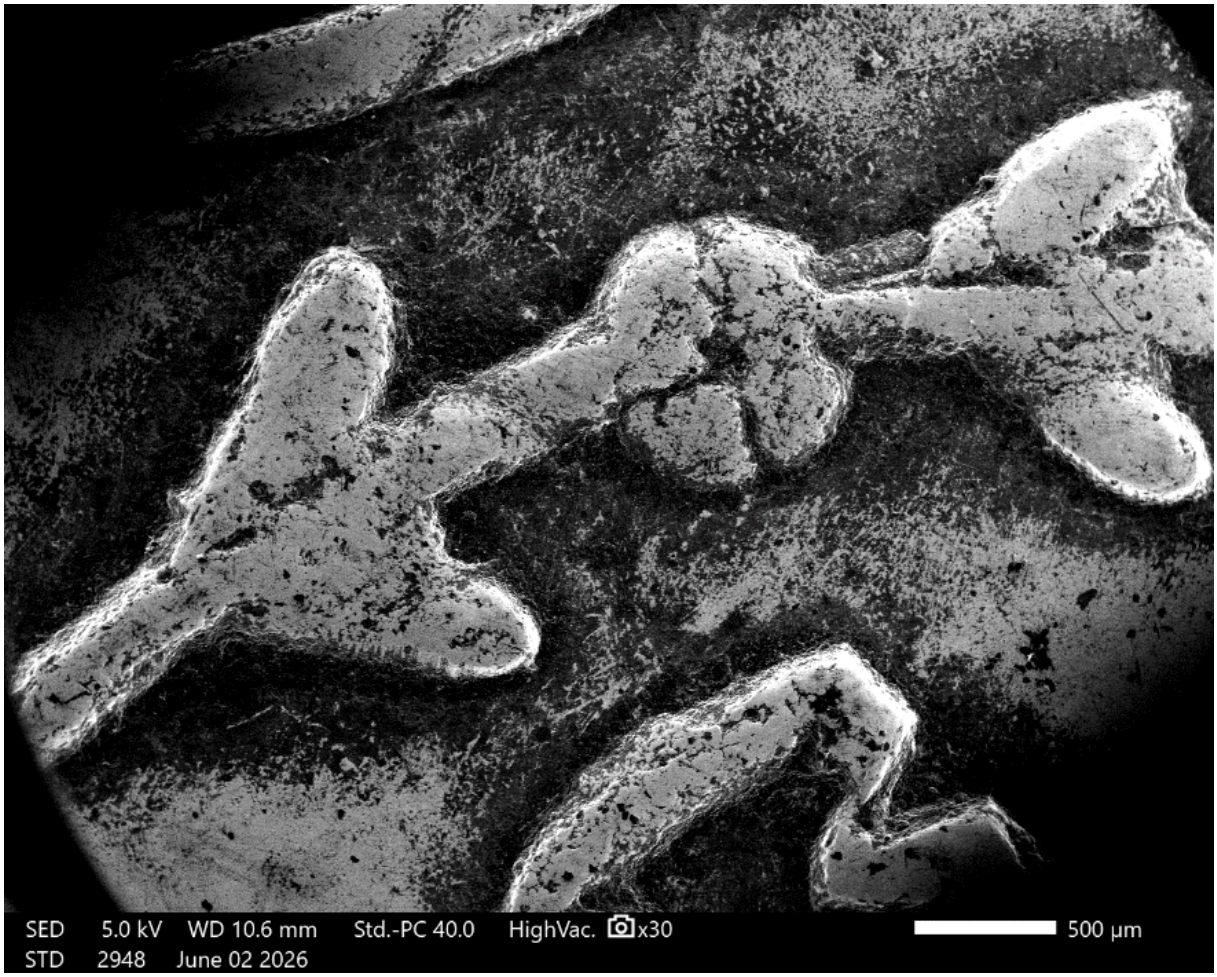

Figure 1. SEM image of a detail on the reverse side of the 1822 Ottoman gold coin.

Bio-Based Tannic Acid and Phytic Acid Coatings for Multifunctional Textiles

Vojtkuf Karlo, Biljanić Helena, Kosanović Jelena, Marušić Katarina, Matijaković Mlinarić Nives
Ruđer Bošković Institute, Bijenička cesta 54, Zagreb, Croatia
Corresponding author: kavojtkuf@irb.hr

The growing demand for sustainable protective textiles has encouraged the development of bio-based surface treatments that provide multiple functions while reducing reliance on conventional additives. Tannic acid (TA) and phytic acid (PA) are attractive bio-based compounds with complementary functionalities. TA interacts with textile fibres and contributes to char formation, UV absorption, and antimicrobial activity, whereas the high phosphorus content of PA promotes dehydration and carbonisation during thermal exposure [1,2]. Cotton, nylon, polyester and nylon-cotton (NyCo) fabrics were functionalised with coatings based on TA coordinated with iron ions and PA. Two pretreatment strategies, gamma irradiation at different doses and atmospheric conditions and copper-ion coordination, were compared with layer-by-layer (LbL) and one-pot deposition. Colour change and washing durability were assessed by colorimetric measurements, while surface morphology, coating uniformity, and elemental composition and distribution before and after washing were examined using scanning electron microscopy coupled with energy-dispersive X-ray spectroscopy (SEM-EDS). UV protection was assessed through ultraviolet protection factor (UPF) and UVA/UVB transmission, while surface wettability and charge were examined by water contact angle and zeta-potential measurements. Textile composition, pretreatment and deposition method influenced coating performance and retention after washing. Cotton exhibited the greatest improvement in UV protection, particularly after copper-ion pretreatment followed by LbL deposition, with markedly reduced UVA and UVB transmission. NyCo also showed enhanced protection, while nylon achieved its best performance after LbL deposition following irradiation at 15 kGy; polyester showed only modest changes. Cotton and polyester generally became more hydrophobic, whereas nylon and NyCo showed treatment-dependent behaviour. All fabrics exhibited negative zeta potentials, with the most pronounced treatment-related changes observed for polyester and nylon. Elemental analysis confirmed the presence and distribution of phosphorus- and iron-containing species. Overall, deposition of tannic acid coordinated with iron ions and phytic acid provides a versatile and environmentally favourable approach to the development of multifunctional protective textiles.

References

1. S. Kulkarni et al., ACS Appl. Mater. Interfaces 13 (2021) 61620–61628.
2. A. Bifulco and G. Malucelli, Polymers 18 (2026) 671.

nanosurf



Zoom into the Future

Discuss your application with our experts and explore
cutting-edge technology for nanoscale surface characterization.

Nanosurf AG | Gräubernstr. 12-14 | 4410 Liestal | Switzerland | www.nanosurf.com | info@nanosurf.com

See while you mill.

New ZEISS Crossbeam 750 with Gemini 4

ZEISS



ZEISS Crossbeam 750
High-end FIB/SEM system with Gemini 4 column for the most challenging imaging and milling tasks

Gemini 4 delivers enhanced clarity at tilt with minimal magnetic interference at the sample.
It provides a larger undistorted field of view and exceptional stability for live imaging during milling, enabling confident endpoint control even in the most challenging low kV tasks.

www.zeiss.com

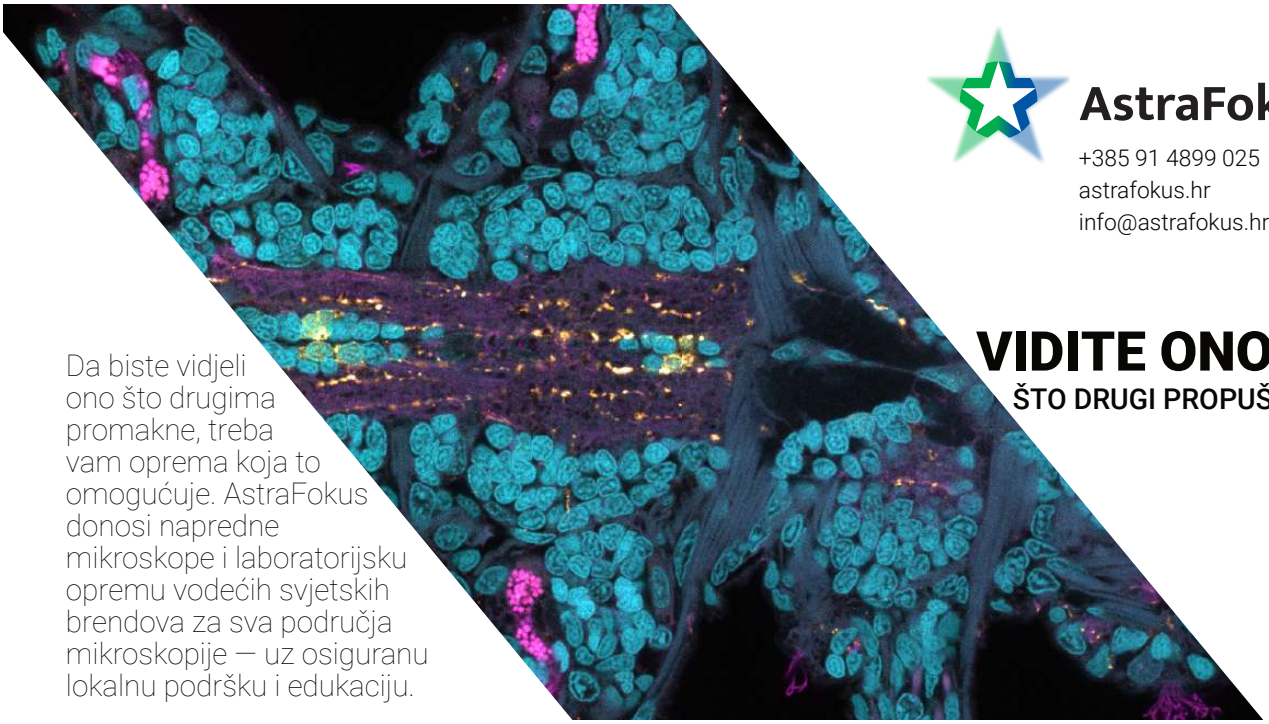

AstraFokus
+385 91 4899 025
astrafokus.hr
info@astrafokus.hr

VIDITE ONO
ŠTO DRUGI PROPUŠTAJU

Da biste vidjeli ono što drugima promakne, treba vam oprema koja to omogućuje. AstraFokus donosi napredne mikroskope i laboratorijsku opremu vodećih svjetskih brendova za sva područja mikroskopije — uz osiguranu lokalnu podršku i edukaciju.

ZEISS abberior telight NIREOS KFBIO technology for health. CoolLED Simply Better Control
HAMAMATSU PHOTON IS OUR BUSINESS DeltaPix - Discover the Details LIEDER MADE IN GERMANY IPI Inland Polymer Industries GmbH iolight

AUTHOR INDEX

Authors and coauthors · numbers refer to the first page of each abstract

B

Balog Marta 29
Bauer Nataša 51
Berger Frédéric 51
Bijelić Nikola 60
Biljanić Helena 77
Bischof Sandra 6
Blažanović Angela 23
Bočina Ivana 13, 48
Bojanić Krunoslav 39

C

Caput Mihalić Katarina 33
Cerovski Sara 49
Christiansen Silke 39
Cvjetko Petra 33

Č

Čeh Miran 37
Čekić Nenad 54
Čižmar Tihana 36, 40
Čurila Viktoria 29

D

Daneu Nina 18
Debeljak Željko 60
Delaš Aždajić Marija 31
Dolić Stjepan 36, 71
Dragojević Andreja 42
Drev Sandra 37
Dujmović Mia 56
Dunatov Toni 37
Dutour Sikirić Maja 39, 67

E

Erceg Ina 39, 57, 67
Eržić Ema 29

F

Fernandez Godoy María 13
Filić Vedrana 32, 49
Fredotović Željana 48
Frlin Marta 51
Furlić Anamarija 64

G

Gajović Andreja 36, 37, 71
Gračanin Nika 73
Grgac Robert 60
Gudlin Lovro 27
Gunde Miha 37
Gvozdić Vlatka 57

H

Hausen Harald 59
Heffer Marija 29
Herak Bosnar Maja 27

H

Hmelina Karla 23
Hobmayer Elio 53
Hrabar Jerko 13
Hrvat Kerima 75

I

Igrec Dunja 28
Ilić Ivana 31, 54, 60
Inkret Suzana 39
Ivanišević Irena 67

J

Jagić Mateja 51
Jastrzebski Sandra 15
Jazvinšćak Jembrek Maja 27
Jerin Katarina 69
Juraić Krunoslav 36, 71

K

Kalajzic Ivo 15
Kamenjarin Juraj 48
Karlić Rosa 51
Katanić Zorana 57
Keresteš Gaj 51
Kević Nives 13
Kittel Ágnes 11
Kitzberger František 4
Klačić Tin 22, 69
Klobučar Lucija 36, 71
Knapp Magdalena 53, 59
Kojić Vedran 36, 40, 71
Komazec Bruno 55, 62, 64
Kosanović Jelena 77
Kosec Tadeja 23
Kovačević Davor 69
Kovačević Zorana 6
Kovač-Andrić Elvira 57
Kremer Dario 56
Krstin Ljiljana 57
Kušen Mihael 56

L

Ladurner Peter 53
Laikhtman Alexander 71
Leljak-Levanić Dunja 51
Lorenzo Joseph 15
Lorković Zdravko 51

M

Macan Jelena 42
Maček Kržmanc Marjeta 18
Marušić Katarina 77
Matić Anita 28
Matić Mario 37

AUTHOR INDEX

02

Authors and coauthors · numbers refer to the first page of each abstract

M

Matijaković Mlinarić Nives 77
Mihajlović Lovro 29
Mikić Dajana 23
Mišić Radić Tea 55
Miškec Karlo 51
Močnik Petra 23
Modrušan Vanja 33
Mujkić Robert 31, 54

N

Novak Sanja 15
Novosel Vlašić Nives 55

O

Oršolić Nada 60
Otmačić Ćurković Helena 23
Ovčar Juraj 37

P

Pavić Valentina 29
Pavin Nenad 32
Peharec Štefanić Petra 55, 62, 64
Petrović Marin 20
Poljuha Danijela 33
Popović Jasminka 37
Prebeg Tatjana 56
Proust Bastien 27

R

Radetić Lucija 40
Radman Sanja 48
Ražnjević Sergej 73
Reberz Lena 53, 59
Restović Ivana 13
Rođak Edi 15, 60
Rooj Subhashis 18
Rothbächer Ute 59
Rožac Karla 54
Rudan Marina Dimlić 13
Rušec Vedran 57

S

Salčinović Fetić Amra 75
Seuček Paula 56
Seybold Anna 53, 59
Skelin Ilić Josipa 40
Skoko Željko 37
Sladonja Barbara 33
Spreitzer Matjaž 18
Srb Nika 60
Sršan Vinko 73
Stepinac Emma 51
Strasser Vida 67
Strnad Martin 4

S

Suknović Dragica 57

Š

Šic Žlabur Jana 56
Šimić Marija 49
Škrobot Vidaček Nikolina 27
Šnajder Mujkić Darija 54
Šoštar Marko 32
Štancl Paula 51
Štimac Valentina 27
Štolfa Čamagajevac Ivna 57
Šturm Sašo 8, 73
Šutić Maja 27

T

Tadić Tonči 37
Tolić Iva 2, 27
Tomić Luketić Kristina 37
Týč Jiří 4

U

Ugljarević Mladen 54
Ugrin Marina 13
Uzelac Božac Mirela 33

V

Vancová Marie 4
Vidaković-Cifrek Željka 51
Viljetić Barbara 29
Vinicki Krunoslav 16
Vitko Sandra 51
Vojtkuf Karlo 77
Vrbančić Lea 27
Vukosav Petra 55
Vuković Dona 62
Vuković Popović Ana 28
Vuko Elma 48
Vyšanská Monika 44

Z

Zak Alla 71

W

Weber Igor 32, 49